BMEiCON 2026

Biomedical Engineering International Conference

Innovations in Medical Technology
for a Healthier Tomorrow

Fukuoka, Japan

October 10–13, 2026

CONFERENCE BOOKLET

CONNECT • COLLABORATE • INNOVATE

Organized by

ThaiBME.org

FIT
Fukuoka Institute of Technology

Supported Organizations

IEEJ

IFMBE

Technical Sponsors

IEEE Fukuoka Section 福岡支部

IEEE EMB Thailand Chapter

IEEE Advancing Technology for Humanity

IEEE EMBS West Japan Chapter

BMEi2026 Booklet

Message from the General Chair

It is my great pleasure to welcome you to the **18th Biomedical Engineering International Conference (BMEiCON 2026)**, taking place from **October 10–13, 2026, in Fukuoka, Japan**.

I am particularly delighted to welcome the BMEiCON community back to Fukuoka. Bringing this international conference to Japan once again provides a valuable opportunity to strengthen the long-standing academic cooperation between Thailand and Japan while expanding connections with researchers and institutions from across the world.

BMEiCON has established itself as an important international forum for researchers, engineers, healthcare professionals, educators, and students to present their latest work and exchange perspectives on advances in biomedical engineering. The interdisciplinary nature of our field makes such interaction especially important, as many of today's healthcare challenges require collaboration across engineering, medicine, biological sciences, information technology, and related disciplines.

This year's conference offers a comprehensive technical program covering a broad range of biomedical engineering topics. In addition to the technical sessions, we are honored to welcome our distinguished invited speakers:

Associate Professor Somyot Kaitwanidvilai
Dean, School of Engineering
King Mongkut's Institute of Technology Ladkrabang, Thailand

Professor Nobuhiko Kojima
Graduate School of Nanobioscience
Yokohama City University, Japan

Professor Kuo-Yung Hung
Department of Mechanical Engineering
Ming Chi University of Technology, Taiwan

Yoshihiro Tange
Department of Advanced Medical Sciences, Faculty of Medicine
Oita University, Japan

Manuel H. Luque Casanave
Faculty of Mechanical Engineering
Universidad Nacional de Ingeniería, Lima, Peru

Their participation brings valuable expertise and diverse perspectives to BMEiCON 2026, and I am confident that their presentations will stimulate new ideas and meaningful discussions among our participants.

Organizing an international conference of this scale requires the commitment and cooperation of many people. I would like to express my sincere gratitude to the organizing committee, Technical Program Committee, reviewers, session chairs, and support staff for their tremendous efforts in preparing the conference. I also extend my appreciation to our collaborating organizations and institutions for their continued support of BMEiCON.

Above all, I would like to thank our authors and participants. Your research contributions, active participation, and willingness to exchange ideas are at the heart of this conference. I encourage everyone to take full advantage of the technical sessions and networking opportunities to meet colleagues, establish new partnerships, and explore possibilities for future collaboration.

I hope that **BMEiCON 2026** will be both professionally rewarding and personally memorable. While you are here, I also encourage you to experience Fukuoka—a welcoming city that combines modern innovation with rich culture, excellent cuisine, and warm hospitality.

On behalf of the organizing committee, I warmly welcome you to **BMEiCON 2026 in Fukuoka** and wish you a productive, enjoyable, and successful conference.

Warm regards,

Prof. Tadayuki Akagi
General Chair, BMEiCON 2026
Fukuoka Institute of Technology, Japan

Email: t-akagi@fit.ac.jp

Welcome Message

Technical program chair

On behalf of the organizing committee, it is my great pleasure to welcome all participants to the **18th Biomedical Engineering International Conference (BMEiCON 2026)**, held in **Fukuoka, Japan, from October 10–13, 2026**.

BMEiCON has long served as an international forum where researchers, engineers, healthcare professionals, academics, and students come together to share new ideas and advances in biomedical engineering. We are especially delighted to return to Fukuoka for the third time and to continue strengthening the academic and professional connections between our communities in Thailand, Japan, and countries around the world.

The strong response to BMEiCON 2026 reflects the continued growth and vitality of our field. This year, we received **195 paper submissions**, from which **162 papers** were selected for presentation following a rigorous peer-review process. The technical program comprises **24 sessions**, providing a broad platform for participants to present their research, exchange perspectives, and explore emerging developments across biomedical engineering and related disciplines.

An important highlight of this year's conference is our distinguished group of invited speakers. We are privileged to welcome:

Associate Professor Somyot Kaitwanidvilai
Dean, School of Engineering
King Mongkut's Institute of Technology Ladkrabang, Thailand

Professor Nobuhiko Kojima
Graduate School of Nanobioscience
Yokohama City University, Japan

Professor Kuo-Yung Hung
Department of Mechanical Engineering
Ming Chi University of Technology, Taiwan

Yoshihiro Tange
Department of Advanced Medical Sciences, Faculty of Medicine
Oita University, Japan

Manuel H. Luque Casanave
Faculty of Mechanical Engineering
Universidad Nacional de Ingeniería, Lima, Peru

We sincerely appreciate their participation and look forward to the knowledge, perspectives, and inspiration they will bring to our conference.

BMEiCON 2026 would not be possible without the commitment of many individuals working behind the scenes. I would like to express my sincere appreciation to all members of the Technical Program Committee and our reviewers for their careful evaluation of the submitted papers and their contribution to maintaining the academic quality of the conference.

My special appreciation goes to **Dr. Adisorn Leelasantithum, Publication Chair**, for coordinating the publication process; **Professor Tadayuki Akagi, General Chair**, for his leadership and support; **Dr. Sarinporn Visitsattapongse, Financial Chair**, for her dedicated work; **Keiko Yoshii, Publicity Chair**, for promoting the conference; and **Satoshi Makita, General Secretary**, for his invaluable coordination. I am equally grateful to the entire organizing and local committees, whose commitment and teamwork have made this conference possible.

Beyond the presentations and technical discussions, I hope BMEiCON 2026 will provide opportunities to renew friendships, establish new collaborations, and generate ideas that extend well beyond these four days. Our networking activities are intended to encourage these connections and strengthen the international biomedical engineering community.

I wish all participants a productive and memorable conference. May you enjoy stimulating discussions, meaningful collaborations, and the opportunity to experience the unique hospitality and atmosphere of **Fukuoka**.

Welcome to **BMEiCON 2026**, and I look forward to meeting you throughout the conference.

Warm regards,
Chuchart Pintavirooj
Technical Program Committee
BMEiCON 2026
Email: chuchart.pi@kmitl.ac.th

Message from the President of ThaiBME

It is my great honor and pleasure to welcome all participants to the **18th Biomedical Engineering International Conference (BMEiCON 2026)**, to be held from **October 10–13, 2026, in Fukuoka, Japan**.

Over the years, BMEiCON has grown into an important international platform for researchers, engineers, healthcare professionals, educators, and students to share knowledge and explore new developments in biomedical engineering. This year, we are delighted to return to Fukuoka and to continue our close collaboration with our Japanese and international partners.

Biomedical engineering plays an increasingly important role in addressing the challenges of modern healthcare. Rapid advances in medical technologies, artificial intelligence, biomedical instrumentation, medical imaging, rehabilitation engineering, biosensors, digital health, and other emerging fields are creating new opportunities to improve healthcare and quality of life. At the same time, these developments remind us of the importance of bringing together expertise from engineering, medicine, science, and technology.

The **Thai Society of Biomedical Engineering (ThaiBME)** is committed to advancing biomedical engineering through research, education, professional development, and international cooperation. BMEiCON represents an important part of this mission by providing a forum where new research can be presented, ideas can be openly exchanged, and collaborations can be established across institutions, disciplines, and national boundaries.

On behalf of ThaiBME, I would like to express my sincere appreciation to our co-organizers and collaborating organizations, as well as the General Chair,

Technical Program Committee, organizing committee, reviewers, keynote speakers, session chairs, authors, and volunteers. Their dedication and collective efforts have made BMEiCON 2026 possible.

Most importantly, I would like to thank all participants for joining us. Your contributions, discussions, and exchange of ideas are what give this conference its true value. I hope BMEiCON 2026 will not only provide opportunities to learn about the latest advances in biomedical engineering but also inspire new ideas, strengthen existing partnerships, and create new friendships and collaborations for the future.

I wish everyone a successful and rewarding conference and hope that you will also enjoy the culture, hospitality, and memorable experiences that **Fukuoka** has to offer.

It is my pleasure to welcome you to **BMEiCON 2026**.

Warm regards,

Somkiat Watanasirichaigoon

President
Thai Society of Biomedical Engineering (ThaiBME)

Email: somkiat.wat@mahidol.edu

Keynote

Professor Dr. Somyot Kaitwanidvilai

Dean of School of Engineering, King Mongkut's Intstiture of Technology Ladkrabang

Engineering the Future of Healthcare: AI, Intelligent Systems, and the Next Generation of Biomedical Innovation

Abstract

Healthcare is entering a new era in which biomedical engineering is increasingly driven by the convergence of artificial intelligence (AI), intelligent systems, advanced sensing, robotics, connectivity, and data science. Around the world, the focus is shifting from conventional medical devices and isolated diagnostic tools toward connected, adaptive, and patient-centered systems that can continuously understand physiological conditions, support clinical decisions, and personalize healthcare interventions.

Several emerging directions are shaping this transformation. AI-assisted medical imaging is improving the detection, segmentation, and interpretation of abnormalities in radiology, pathology, ophthalmology, and other image-based specialties. Wearable and Internet of Medical Things technologies are enabling continuous monitoring of physiological signals outside traditional hospital environments, creating opportunities for early detection and preventive healthcare. Meanwhile, AI-based predictive models are increasingly being explored for risk stratification, disease progression, treatment response, and personalized medicine.

Another important frontier is the integration of AI with biomedical robotics and intelligent therapeutic systems. Surgical and rehabilitation robots, assistive

technologies, smart prostheses, and precision robotic systems are becoming increasingly capable of adapting to patients and clinical environments. Digital twins and computational physiological models offer another promising direction by creating virtual representations of patients or organs that may support treatment planning, simulation, and individualized therapy. At the same time, multimodal and generative AI are opening new possibilities for integrating medical images, biosignals, clinical information, and other heterogeneous data into more comprehensive decision-support systems.

An example from our recent work demonstrates this transition from AI prediction toward intelligent therapeutic systems. We developed an AIoT-based Adaptive Neuro-Fuzzy Inference System for high-flow oxygen therapy, integrating SpO_2 and respiratory-rate information with a cloud-based intelligent model to recommend adjustments in oxygen flow and FiO_2. Simulation-based closed-loop evaluation demonstrated the potential of continuous intelligent adjustment compared with less frequent manual titration, while bench testing verified the accuracy of the oxygen-delivery hardware. This study also highlights an important lesson: an accurate AI prediction model is not automatically an effective controller; biomedical AI must be designed as part of a complete feedback, safety, and clinical-supervision architecture.

Looking forward, the greatest impact of AI in biomedical engineering may therefore come not from replacing clinicians, but from creating intelligent partnerships between humans, machines, and data. The next generation of biomedical innovation must combine technical performance with interpretability, safety, cybersecurity, clinical validation, ethical responsibility, and human-centered design. Ultimately, the challenge for biomedical engineers is to transform AI from an algorithm into a trustworthy healthcare system—connecting sensing to intelligence, intelligence to action, and engineering innovation to better patient outcomes.

Curriculum Vitae

Associate Professor Dr. Somyot Kaitwanidvilai is an academic and researcher at King Mongkut's Institute of Technology Ladkrabang (KMITL), Thailand, with extensive experience in intelligent control systems, robotics, artificial intelligence, machine vision, optimization, and advanced engineering applications. His multidisciplinary research provides a strong foundation for applications in biomedical engineering, particularly in precision robotics, intelligent sensing, medical automation, and AI-assisted systems.

He received his doctoral degree from the Industrial Systems Engineering (ISE) Program at the Asian Institute of Technology (AIT) under a Royal Thai

Government full scholarship. He also holds Master's and Bachelor's degrees in Electrical Engineering from KMITL. His academic and professional background spans electrical engineering, automation, industrial systems, intelligent control, and applied artificial intelligence.

A major area of his research is the development of robust and intelligent control techniques for complex dynamic systems. His work includes optimization-based control, adaptive control, fuzzy systems, neural networks, particle swarm optimization, machine learning, and computer vision. These technologies are highly relevant to biomedical engineering applications requiring accurate motion control, real-time decision making, intelligent monitoring, and human–machine interaction.

His research has also addressed robotic manipulation and high-precision control. Recent work includes the development of robust control approaches for MIMO microsurgical manipulation systems, demonstrating the applicability of advanced control methodologies to precision medical and biomedical robotic systems. His broader experience in robotic arms, force and impedance control, autonomous systems, sensor fusion, and intelligent visual inspection further supports interdisciplinary research between engineering, robotics, and healthcare technologies.

Dr. Kaitwanidvilai has published extensively in international journals indexed in Web of Science and Scopus. His research covers robust control, robotics, artificial intelligence, machine learning, computer vision, smart manufacturing, intelligent surveillance, and sensing technologies. His work emphasizes translating theoretical engineering methods into practical systems capable of operating reliably in complex real-world environments.

In addition to research and teaching, he has served as a reviewer for international journals, a technical committee member and session chair for international conferences, and an external examiner for graduate programs at several universities.

His current interests include AI-enabled intelligent systems, precision robotics, advanced sensing and image analysis, adaptive and robust control, and the integration of engineering technologies into biomedical and healthcare applications. His interdisciplinary perspective aims to bridge control engineering, artificial intelligence, robotics, and biomedical engineering toward safer, smarter, and more effective technologies.

Email: somyot.ka@kmitl.ac.th

Keynote

Distinguished Professor Kuo-Yung Hung
Dean, College of Engineering
Director, Research Center for Intelligent Medical Devices (RCIMD)
Distinguished Professor, Department of Mechanical Engineering
Ming Chi University of Technology, Taiwan

From Laboratory Innovation to Commercialized Biomedical Technologies: A Journey Across Medical Devices, Biomaterials, Medical Robotic, and Sustainable Healthcare Products

Abstract

Translating academic research into real-world products is one of the most challenging yet impactful missions in biomedical engineering. This keynote speech will present a series of successful technology commercialization experiences spanning biomaterials, medical devices, and sustainable healthcare products. The presentation will highlight how interdisciplinary engineering research can evolve from laboratory-scale innovation into clinically applicable and commercially viable products through collaboration among universities, hospitals, research institutes, and industrial partners.

The first part of the keynote introduces the development of surface-modified dental implants and artificial dental root technologies developed in collaboration with Chang Gung Memorial Hospital and Chang Gung Medical Technology in Taiwan. The project successfully achieved Taiwan TFDA approval and U.S. FDA 510(k) clearance, demonstrating the importance of integrating materials science, biomedical engineering, and industrial manufacturing capabilities.

The second part focuses on biodegradable biomedical membranes, including anti-adhesion membranes and periodontal regeneration membranes developed together with Nanya Plastics Corporation. These technologies combine electrospinning, biodegradable polymers, and tissue engineering concepts to improve wound healing, reduce post-surgical adhesion, and

promote bone regeneration. I will discuss the pathway from material formulation and animal testing to pilot-scale manufacturing and regulatory preparation.

The keynote will also present the development of a portable intelligent chest drainage system designed for clinical respiratory care applications. The device integrates sensing, pressure monitoring, and intelligent control technologies to provide a compact and user-friendly solution for thoracic drainage management. The project demonstrates how engineering integration and industry collaboration can accelerate medical device prototyping and product realization.

In addition, environmentally sustainable healthcare materials will be introduced through the development of highly oil-absorbent biodegradable facial masks fabricated using eco-friendly nanofiber technologies. The research integrates bamboo-derived carbon nanoparticles and biodegradable polymeric materials to achieve enhanced skincare functionality while reducing environmental impact.

Finally, the presentation will discuss critical factors influencing successful technology transfer and commercialization, including interdisciplinary collaboration, intellectual property strategy, clinical validation, regulatory approval, manufacturing scalability, and industry-academia partnership models. I hope this keynote can provide valuable insights for researchers and young engineers seeking to bridge the gap between academic innovation and industrial application in the biomedical engineering field.

<table>
<tr><td> 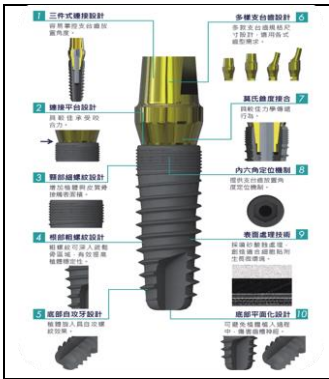 </td><td> 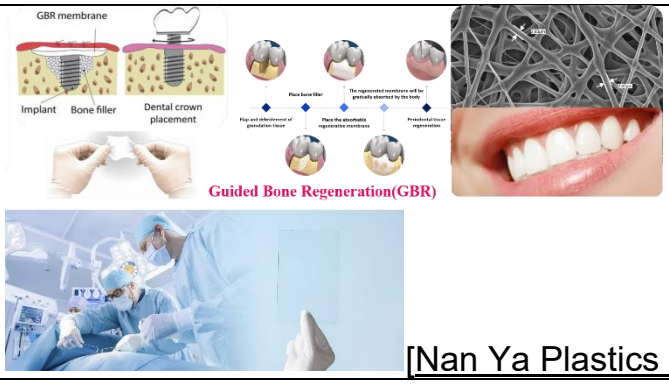

[Nan Ya Plastics Corp.]</td></tr>
<tr><td>Dental implant</td><td>Biodegradable biomedical membranes, including anti-adhesion membranes and periodontal regeneration membranes</td></tr>
<tr><td> 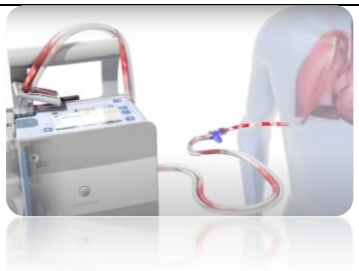 </td><td> 
[Promedicol Company]</td></tr>
<tr><td colspan="2">Portable intelligent chest drainage system designed for clinical respiratory care applications</td></tr>
<tr><td></td><td></td></tr>
</table>

Steam thermal vest [Formosa Biomedical Technology Corp.]	Oil-absorbent biodegradable facial mask

Curriculum Vitae

Professor Kuo-Yung Hung is Dean of the College of Engineering, Director of the Research Center for Intelligent Medical Devices (RCIMD), and Distinguished Professor in the Department of Mechanical Engineering at Ming Chi University of Technology (MCUT), Taiwan. He received his Ph.D. in Engineering and Systems Science from National Tsing Hua University in 2004 and previously served as a senior engineer at AU Optronics.

Over the past two decades, Professor Hung has established an interdisciplinary research platform bridging engineering innovation, biomedical technology, intelligent automation, and industrial implementation. His current research is strategically focused on three major areas: advanced implantable medical devices, critical component technologies for semiconductor equipment, and intelligent medical robotic systems.

1. Advanced Implantable Medical Devices

Professor Hung has extensive experience in the development, validation, and commercialization of implantable and regenerative medical technologies. His research on titanium surface modification and hydroxyapatite coating for artificial dental implants contributed to commercial products that obtained Taiwan medical device approval and U.S. FDA 510(k) clearance. His team has also developed a biodegradable periodontal regeneration membrane, recognized by the 21st National Innovation Award, as well as a biodegradable anti-adhesion membrane that obtained TFDA approval in 2025 and was successfully commercialized in 2026.

His research emphasizes the complete translational pathway from biomaterial design, surface engineering, biological validation, and animal testing to regulatory approval, technology transfer, and industrial production, establishing a strong platform for next-generation implantable and regenerative medical devices.

2. Critical Component Technologies for Semiconductor Equipment

Professor Hung also leads industry-oriented research on critical materials, component reliability, failure analysis, and advanced manufacturing

technologies for semiconductor equipment. Through long-term collaboration with industrial partners, his team has developed analytical and verification methods for key equipment materials and components, helping manufacturers solve critical reliability and production issues in advanced semiconductor processing systems.

His work on enabling component technologies for advanced semiconductor packaging equipment received the 2026 TSIA Semiconductor Equipment Innovation Award, recognizing its successful industrial implementation and commercialization. The 2026 TSIA Semiconductor Equipment Innovation Award is selected by distinguished industry experts and scholars representing Taiwan's semiconductor sector. With only three winning teams selected in 2026, the award is highly competitive and demands strong technological innovation and practical industrial impact. Professor Kuo-Yung Hung's team developed a high-performance solution for a critical component in CoWos advanced packaging bonding processes, significantly improving equipment stability. The achievement directly addresses a key technological bottleneck in advanced semiconductor packaging equipment and demonstrates substantial value in technological innovation, industrial implementation, and strengthening the autonomy and resilience of the semiconductor equipment supply chain. This research direction strengthens the linkage between university research and Taiwan's advanced semiconductor equipment supply chain, particularly in technologies supporting next-generation packaging and high-precision manufacturing.

3. Intelligent Medical Robotic Systems

A third major research focus is the development of intelligent medical and elderly-care robotic systems based on autonomous mobile robot (AMR) platforms. Professor Hung's team has established proprietary AMR technologies integrating autonomous navigation, multimodal sensing, intelligent control, human–machine interaction, and modular application interfaces.

These platforms are being developed for hospitals, long-term care institutions, elderly-care environments, and industrial applications, including medication and material delivery, environmental monitoring, patrol assistance, and interactive healthcare services. His current research further integrates AI, multimodal perception, voice interaction, and human-centered service functions to develop next-generation autonomous healthcare robots for aging societies.

Academic and Industrial Impact

During the past three years, Professor Hung has secured more than $2 million in industry–academia collaborative research funding and generated more than $0.4 million in technology transfer revenue. He holds more than 30 invention patents in Taiwan, the United States, and China.

His selected honors include the 2026 TSIA Semiconductor Equipment Innovation Award, the 19th and 21st National Innovation Awards, the Outstanding Young Engineering Professor Award from the Chinese Society of Mechanical Engineers, and the HIWIN Mechanical Thesis Awards in 2011 and 2015.

As Dean of the College of Engineering and Director of RCIMD, Professor Hung continues to integrate academic research, clinical needs, and industrial resources. His long-term vision is to establish internationally competitive technology platforms in advanced implantable medical devices, semiconductor equipment technologies, and intelligent medical robotics, transforming university research into high-impact technologies with measurable clinical, industrial, and societal value.

Email: kuoyung@mail.mcut.edu.tw

Keynote

Yoshihiro Tange, Ph.D.

Department of Advanced Medical Sciences,

Faculty of Medicine, Oita University, Japan

“Recent Advancements in Biomedical Engineering:Development of Artificial Kidneys and International Transfer of Supporting Biomedical Engineering Technologies”

Abstract

Chronic kidney disease (CKD) affects nearly 10% of the global population and represents a growing public health challenge worldwide. The number of patients requiring hemodialysis is projected to reach approximately 5.4 million by 2030, underscoring the urgent need for further technological innovations in renal replacement therapy.

Hemodialyzers play a central role in blood purification; however, their performance is often compromised by membrane fouling, a phenomenon caused by the adsorption and accumulation of blood proteins on membrane surfaces during treatment. Fouling increases mass transfer resistance and reduces the efficiency of uremic toxin removal. Therefore, understanding and mitigating fouling remains a critical issue in the advancement of artificial kidney technologies.

In this lecture, recent findings on membrane fouling and dialysis membrane performance will be presented from a biomedical engineering perspective. Particular attention will be given to the relationship between membrane fouling, biocompatibility, and the quality of dialysis fluid. Although hemodialyzers are strictly regulated as single-use medical devices in Japan, reuse practices continue in some countries and regions. The lecture will discuss how ultrapure dialysis fluid contributes to patient safety, treatment efficacy, and the long-term sustainability of dialysis therapy.

In addition to technological developments in artificial kidneys, the latter part of the lecture will highlight biomedical engineering education initiatives conducted

through a long-standing academic partnership between Japan and Thailand. Over the past fifteen years, these collaborative activities have promoted capacity building, knowledge exchange, and human resource development in biomedical engineering across the Asia-Pacific region.

By integrating advances in artificial kidney technology with international educational collaboration, this keynote lecture aims to demonstrate how biomedical engineering can contribute not only to innovative healthcare solutions but also to the cultivation of the next generation of biomedical engineers. It is hoped that this presentation will further strengthen academic partnerships between Japan and Thailand and promote future international collaboration in biomedical engineering.

Curriculum Vitae

Dr. Yoshihiro Tange is a Lecturer in the Department of Advanced Medical Sciences, Faculty of Medicine, Oita University, Japan. He earned extensive clinical experience as a Clinical Engineer before transitioning to academia, where his work has focused on renal replacement therapies, dialysis engineering, medical device technology, and biomedical engineering education.

Professional Experience

- **2022-Present**
  Lecturer, Department of Advanced Medical Sciences, Faculty of Medicine, Oita University, Japan
- **2008-2022**
  Faculty Member, Department of Medical Engineering, Kyushu University of Health and Welfare, Miyazaki, Japan
- **2002-2008**
  Clinical Engineer, Nagoya Memorial Foundation (Nagoya, Japan) and Seiyoukai Hemodialysis Clinic (Okayama, Japan)

Research Interests

- Artificial kidney technologies and renal replacement therapies
- Hemodialysis membrane performance and biocompatibility
- Dialysis fluid purification systems
- Clinical engineering and medical device management
- Biomedical engineering education and international collaboration

Keynote

Nobuhiko Kojima, Ph.D.
Professor, Laboratory of Regenerative Biology,
Department of Life and Environmental System Science,
Graduate School of Nanobioscience, Yokohama City University, Japan

Does Engineering an Organ Mean Reproducing the Real Organ?

Abstract

I have pursued the engineering of organs for nearly three decades. In tissue engineering, considerable effort has been devoted to reproducing the structures and functions of biological organs. This raises a fundamental question: does engineering an organ necessarily require faithfully reproducing its natural counterpart? Depending on the purpose, it may be more appropriate to redesign tissue architecture and composition according to the functions to be achieved.

My research has focused on three-dimensional tissue engineering based on cell aggregates, initially with the aim of reproducing tissue architecture and the microenvironment as faithfully as possible (Reproduce). I have developed heterogeneous spheroids composed of hepatocytes and vascular endothelial cells, hepatocyte spheroids incorporating hydrogel beads to enhance mass transport, and spheroids incorporating extracellular matrix (ECM) to reproduce cell–ECM interactions and cellular polarity.

As my research progressed, I began to modify these components according to specific purposes. Hydrogel beads were incorporated to

create tissue architectures suitable for xenogeneic islet transplantation, while changes in ECM composition were used to develop islet disease models. I have also explored hydrogel-bead incorporation to improve spheroid transparency for image-based analysis. These studies represent different forms of tissue redesign, in which tissue architecture and composition are intentionally modified to achieve specific functions or purposes (Redesign).

This perspective has also led to the development of a “liquid liver,” in which liver-associated functions are reconstructed using cells, biomaterials, and functional components without reproducing the anatomical structure of the liver itself. Rather than asking “How should we build a liver?”, the focus shifts to “How can we achieve the functions that are needed?”

In this talk, I will introduce the ideas and fabrication approaches that have shaped my work on spheroid design, together with examples of tissue redesign. I hope this perspective will provide young researchers in cell-based engineering with both practical insights and a different way of thinking about how to design their research.

Curriculum Vitae

Dr. Nobuhiko Kojima is a Professor at Yokohama City University. His research focuses on three-dimensional cell culture, tissue engineering, regenerative medicine, and microphysiological systems (MPS), with particular emphasis on the design and control of cellular microenvironments.

Education

1996 Bachelor of Engineering, Osaka University
1998 Master of Engineering, Osaka University
2001 Ph.D. in Biochemistry, The University of Tokyo

Professional Experience

2001–2003 Research Scientist, Kanagawa Academy of Science and Technology
2003–2006 Research Associate, The University of Tokyo
2007–2009 Senior Researcher, UCLA and VAGLA Healthcare System
2009–2013 Project Assistant Professor, The University of Tokyo
2013–2024 Associate Professor, Yokohama City University
2022–2025 Chief Technology Officer (CTO), Ecocell Inc.

2024–present Professor, Yokohama City University
2024–present Director, Career Support Center, Yokohama City University
2024–present Assistant to the President, Yokohama City University

Research Interests
Three-dimensional cell culture and tissue engineering
Spheroids and organoids
Microphysiological systems (MPS)
Regenerative medicine
Physical microenvironment and cellular engineering

Email: nobuhiko@yokohama-cu.ac.jp

Keynote

Manuel Luque Casanave, Research-professor,
Faculty of Mechanical Engineering,
Universidad Nacional de Ingenieria, Lima, Peru

New approaches in biomedical engineering applied to improve the human living conditions on the Moon and on Mars

Abstract

Human long-term habitation on extraterrestrial environments such as Mars and the Moon requires the development of disruptive biomedical engineering technologies, capable of compensating for atmospheric incompatibility and reduced-gravity physiological alterations. This work presents an integrated biomedical-technological proposal focused on two critical challenges for future planetary colonization: autonomous individual respiration support on Mars and adaptive hemodynamic regulation of the lower extremities under hypogravity conditions. The first proposal introduces an innovative photonic respiration-assist system designed to generate breathable oxygen directly from the carbon dioxide-rich Martian atmosphere. The concept is based on the application of high-energy ultraviolet photonic dissociation using specialized laser emitters operating near the 160-167 nm wavelength range. These ultraviolet photons possess sufficient quantum energy to induce molecular bond cleavage in CO_2, enabling photodissociation into oxygen-containing species without dependence on conventional catalytic reactors or high-mass electrolysis systems. The proposed mechanism leverages solar photon energy amplification and ultraviolet photochemistry to reduce energy

consumption and system complexity compared with traditional oxygen extraction technologies. This approach may provide a lightweight, scalable, and wearable oxygen-generation platform suitable for extravehicular activities and distributed habitat life-support systems

The second proposal addresses cardiovascular deconditioning and impaired peripheral circulation caused by prolonged exposure to reduced gravity on Mars. A biomedical nanofluidic circulation-enhancement system is proposed to maintain physiological perfusion in the lower limbs equivalent to terrestrial hemodynamic conditions. The system integrates implantable or wearable nanopumps with a closed-loop proportional–integral–derivative (PID) control architecture. Real-time arterial Doppler flow sensors continuously monitor blood velocity and volumetric flow in the lower extremities. These measurements are processed by a nanocontroller that compares the detected hemodynamic parameters against predefined Earth-equivalent perfusion setpoints. Wireless adaptive control signals are then transmitted to the nanopump network to dynamically accelerate or decelerate microcirculatory assistance, thereby stabilizing peripheral perfusion and minimizing venous stasis, muscle atrophy, and orthostatic intolerance. The proposed framework combines photonic engineering, nanobiomedical systems, physiological control theory, and extraterrestrial medicine into a unified strategy for sustaining human health beyond Earth. These concepts may contribute to the next generation of biomedical support technologies for future lunar and Martian missions, offering potential pathways toward autonomous life-support, improved astronaut mobility, and enhanced long-duration planetary survival.

Curriculum Vitae

Manuel Luque Casanave Graduated as a Mechanical-Electrical Engineer from the Universidad Nacional de Ingeniería (UNI). Experienced in the formulation and implementation of biomedical projects in Peru, Brazil, Colombia, Guatemala, Switzerland, Italy, Sweden, England. Graduated as a Systems Analyst from the Pontificia Universidad Católica de Peru Awarded a British Council scholarship for postgraduate studies in control

systems at the University of Surrey (UK, 1985–1986); received a USAID/IEE scholarship for an international diploma in energy at TVA/University of Tennessee at Chattanooga (USA, 1988). Awarded a Fulbright Commission scholarship for environmental research, serving as a researcher and visiting professor at the University of Pittsburgh (USA, 1992); received a Swedish government scholarship for technologies regarding environmental protection and prevention in industrial processes under the SIDA/Norköping University agreement (Sweden, 1997).

Professor and researcher at the Universidad Nacional de Ingeniería (UNI). Focuses on designs incorporating innovation and emerging, disruptive technologies. Proposed innovative technologies to NASA aimed at ensuring human survival on the Moon and Mars. Served as the UNI project lead for the NASA HERC design competitions in Huntsville, Alabama (USA) in 2019, 2020, and 2023, securing first place for UNI while competing against over 120 universities worldwide.

Developed an innovative procedure applying Boolean models to address discrete control automation problems known as the Jeans-Luque Method. This innovation was developed in the UK in 1986 in collaboration with Professor Jeans during a scholarship awarded by the British government. It holds two invention patents and one utility design as well as three intellectual property rights.

Presentations featuring innovative engineering proposals at over 150 national and international conferences. Authorship of more than 600 technical articles, papers, essays, and technological proposals published by institutions such as the Universidad Nacional de Ingeniería (Peru), Universidad Federico Santa María (Chile), the University of Pittsburgh (USA), the University of Texas (USA), the University of Comahue (Argentina), the University of the Andes (Venezuela), and the Universidad San Carlos de Borromeo (Guatemala). In newspapers including *El Comercio* (Peru), *La República* (Peru), *El Mercurio* (Chile), the *Surrey Mirror* (UK), and *Södermanlands Nyheter* (Sweden); and in magazines such as *World Leather* (UK), *Stakeholders* (Peru), *Energía y Mecánica* (Peru), *FONAM* (Peru), and *Visión*, as well as publications by the College of Engineers of Peru, the College of Engineers

of Guatemala, the National University of Engineering (Peru), and the Society of Engineers of Peru.

“Hypothesis regarding the “Effects of Electromagnetic Fields on Human Beings” in the international journal *Consumidores y Desarrollo* (Consumers and Development), Year XIX/No. 1/January–April 2004, Chile; ISSN 0717-2680. Publication of the hypothesis regarding the interaction between mobile phones and tumors in the international journal *Consumidores y Desarrollo*, Year XIX/No. 3/September–December 2004, Chile; ISSN 0717-2680. https://www.academia.edu/80216344/Radiaciones_electromagn%C3%A9ticas_y_l a_salud

“Optimized Design of a Spinal Prosthesis using Finite Element Structural Analysis” in the journal *Ciencia e Ingeniería* (Science and Engineering), Faculty of Engineering – Universidad de los Andes (ULA), Mérida, Venezuela, Vol. 23, March 2002, No. 1; ISSN 1316-7081. https://alicia.concytec.gob.pe/vufind/Record/UUNI_7f115df5455891483ed4035074 abdcef/Details http://erevistas.saber.ula.ve/index.php/index/search/authors/view?firstName=M.&middleName=H.&lastName=Luque&affiliation=Universidad%20Nacional%20de%20I ngenier%C3%ADa&country=PE

Proposal to the international scientific community of the “Thermomagnetic Hypothesis” regarding the interpretation of the origin of the energy potentially used by Unidentified Flying Objects (UFOs). Argentina / USA 2013 Facebook_: https://www.facebook.com/209412885905003/posts/ufo-variable hypotheses-thermomagneticmanuel-luque-casanave-the-first-scientist /209422015904090/

Youtube: https://www.youtube.com/watch?v=kzMHROJhA7g “Development of an electric wheelchair prototype able to climb steps and controlled by inertial sensors" presented at the 2019 12th Biomedical Engineering International Conference (BMEiCON) by Manuel Luque Casanave and co-authors from the Universidad Nacional de Ingeniería

(UNI). https://www.researchgate.net/publication/339255772_Development_of_an_electric_wheelchair_prototype_able_to_climb_steps_and_controlled_by_inertial_sensors

Email: mluquec@uni.edu.pe

BMEiCON 2026 Floor Plan

Campus Map

Fukuoka Institute of Technology

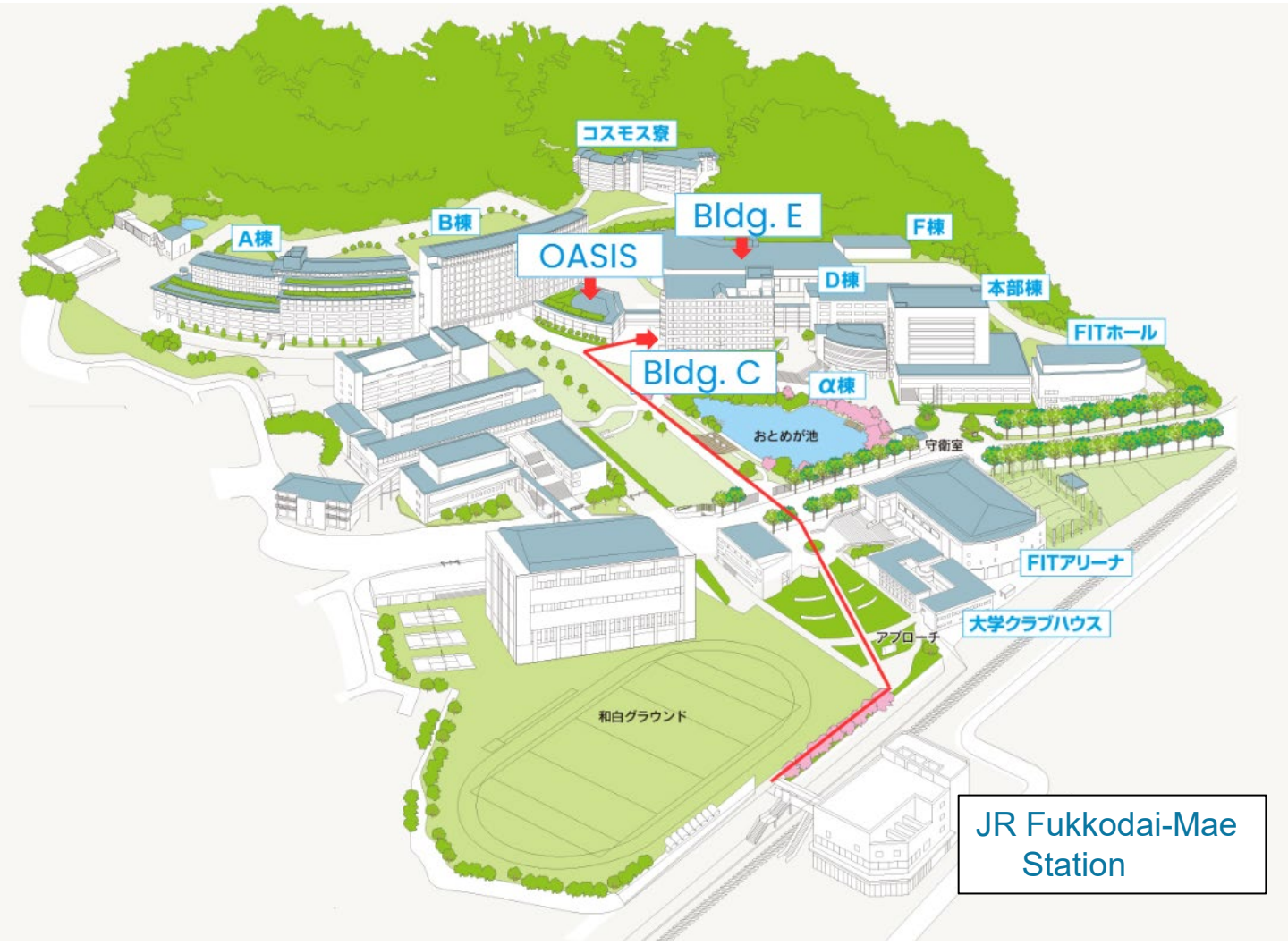

Building C: Registration, Main Hall (Room 1), Coffee Break
Building E: Room 2–4, Exhibition Hall
OASIS: Welcome Party Venue

Building C:　Registration, Main Hall (Room 1), Coffee Break

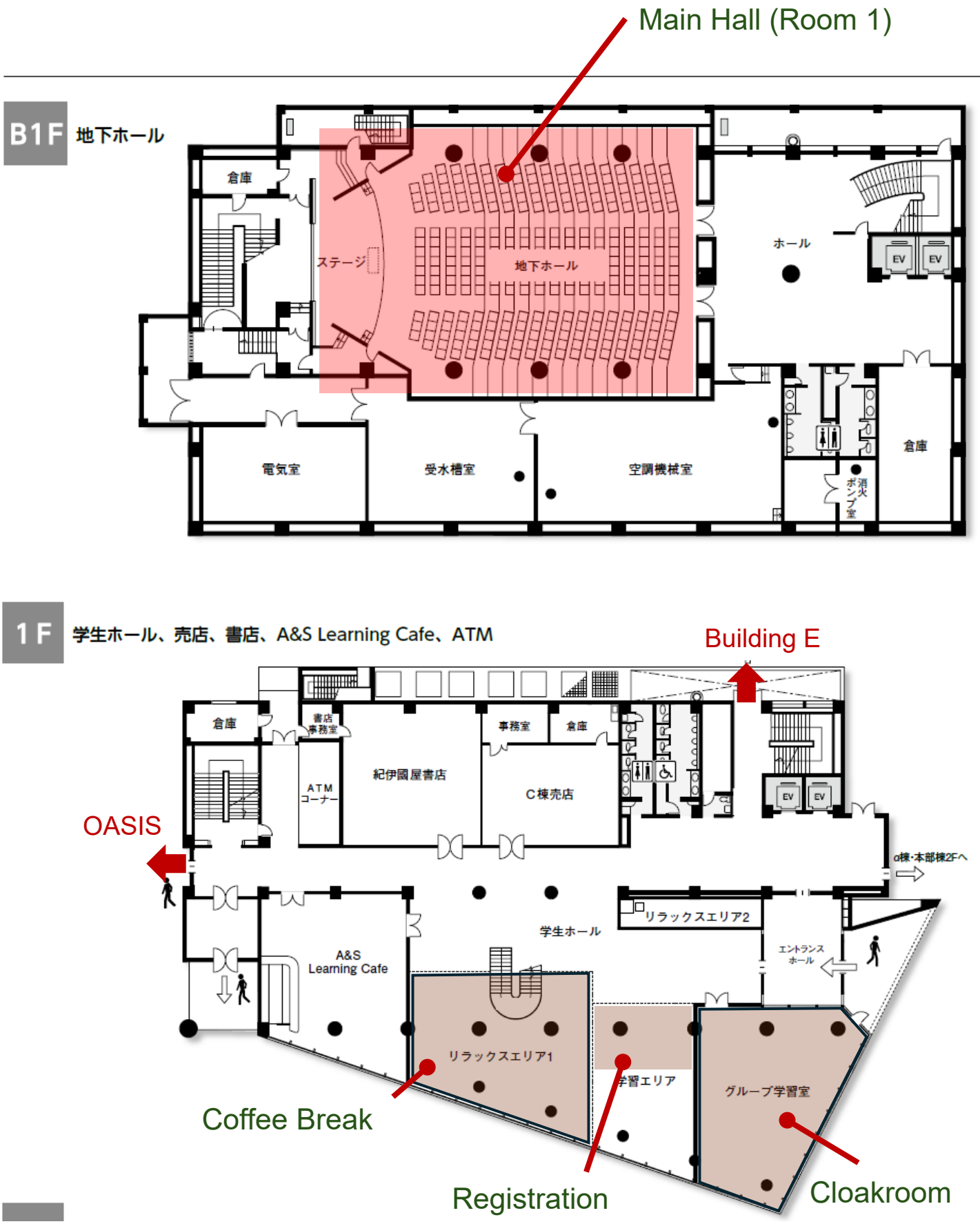

Building E:　Room 2–4, Exhibition Hall

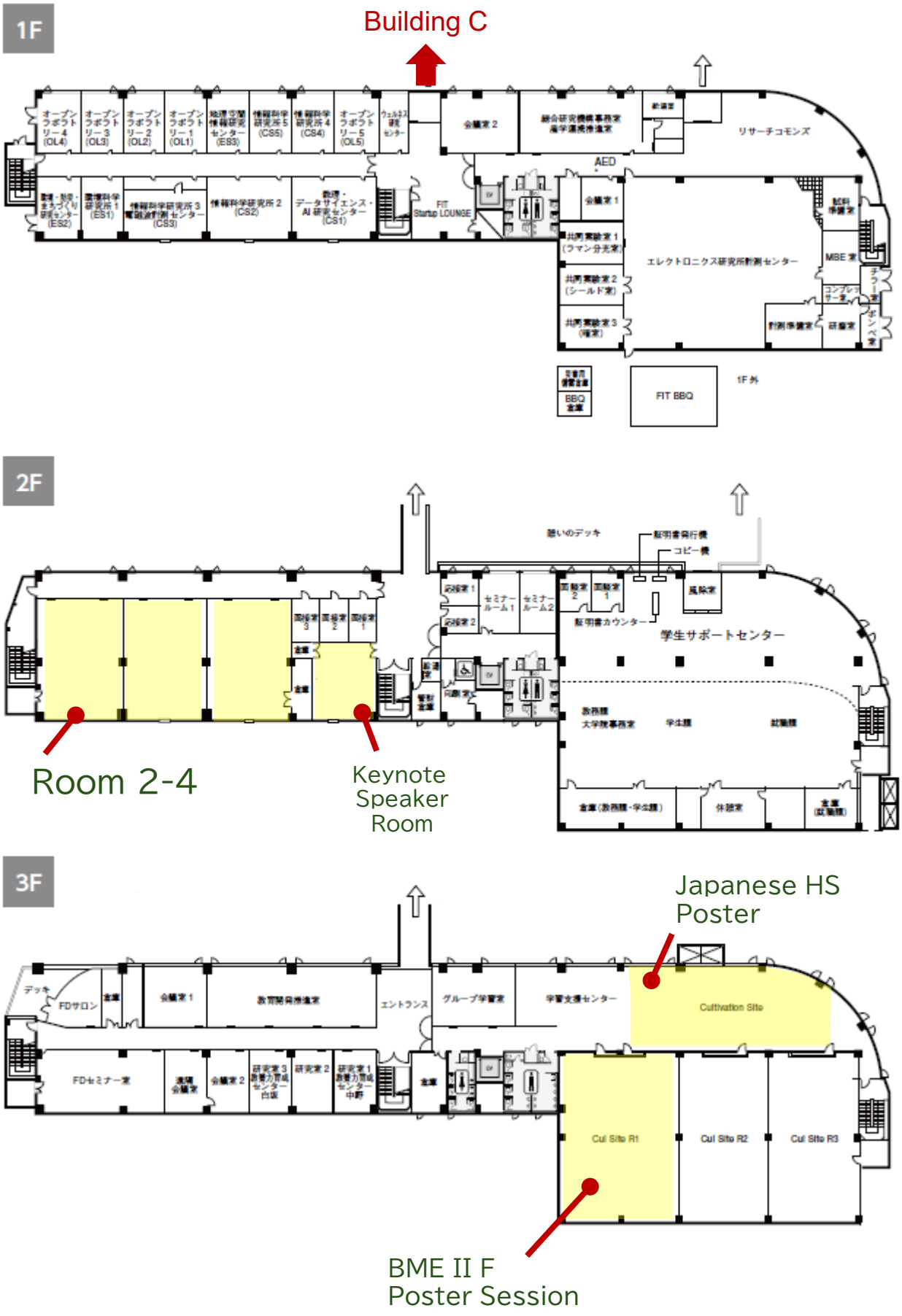

OASIS:　Welcome Party Venue

1F
学生ラウンジ（セブンイレブン）
アドバンス
レストランOASIS、FITCafe

お手洗い　EV エレベーター

ラーニングコーナー、ラーニングスペースは、
勉学のための場所です。大声で話したりゲーム等をすることは禁止です。

Welcome Party

BMEiCON 2026 Program

BMEiCON2026 Program								
Day 1: October 10, 2026								
11:00-13:00	Registration							
13:00-13:30	Openning Ceremony							
	General chair message, President of ThaiBME Message, Technical Program Chair Message							
13:30-13:45	Keynote I: Prof. Somyot Kaitwanidvilai							
13:45-14:30	Keynote II: Prof. Kuo-Yung Hung							
14:30-15:00	Coffee Break							
Session Room	Room1		Room 2		Room 3		Room 4	
Online Link	Click here >>							
Session Topic	D1R1AL- Medical Image Processing I		D1R2AL- Biomedical Signal Processing I		D1R3AL- Healthcare information I		D1R4AL- Bioinstrumentation / Technology, industry and education	
Session Chair	*Theerasak C. / Suchada T.*		*Tomohiko Igasaki*		*Suejit Pechprasarn*		*Thanate Angsuwatanakul*	
15:00-15:15	*1571314474*	*T. Wutthikulthanachai*	*1571314382*	*P. Uthansakul*	*20260007*	*P. Dilokworachot,*	*1571311854*	*Chien-Hsin Yao*
15:15-15:30	*1571315238*	*V. Diaz-Hernandez*	*1571315270*	*W. Rachatapan*	*20260008*	*L. Pholprasert,*	*1571313391*	*Abbrita Rahman*
15:30-15:45	*1571315273*	*Saksorn Thaijiam*	*1571315294*	*Punnut Sukkhun*	*1571323504*	*N. Bintee Rahman Peeya*	*1571316066*	*Pikari Fujii*
15:45-16:00	*1571315293*	*Hikari Saito*	*1571316462*	*Sayaka Suga*	*20260003*	*Chanakarn Sirirat*	*1571320700*	*Kawthar Usamah*
16:00-16:15	*1571316167*	*Wanida Kaewmunee*	*1571316804*	*Ping-Hung Hsieh*	*20260004*	*Nichapa Srisaranon*	*1571322950*	*Shuji Kikuchi*
16:15-16:30	*1571316870*	N. Naufal Rahman	*1571316852*	*Chun-Yi Liu*	*20260005*	*K. Thavornthammarit*	*1571314285*	*T. Angsuwatanakul*
16:30-16:45	*1571318175*	Teeranad Wanpradis	*1571318842*	*Suatmi Murnani*	*20260006*	*Mira Kantito*	*1571316788*	*Chayanis Daochai*
18:00-20:00	Welcome Party							
Day 2: October 11, 2026								
9:00-9:30	Registration							
9:30-10:15	Keynote III: Yoshihiro Tange							
10:15-10:45	Coffee Break							
Session Room	Room1		Room 2		Room 3		Room 4	
Online Link	Click here >>							
Session Topic	D2R1ML- Medical Image Processing II		D2R2ML- Biomedical Signal Processing II		D2R3ML- Healthcare information II / Biosensors I		D2R4ML- Healthcare information III	
Session Chair	*Timothy Gale*		*Limpiti Tulaya*		*Suzuki Seiichi*		*Yoshihiro Tange*	
10:45-11:00	*1571318846*	*Jidapa Prakobpol*	*1571322952*	*Yuxin Liu*	*1571315562*	*Suzuki Seiichi*	*1571304292*	*Hiranya Sritart*
11:00-11:15	*1571320378*	*V. Semshchikov*	*1571322973*	*Haruto Hamada*	*1571322306*	*Krittaphat Inparot*	*1571313298*	*Seonjae Yun*

11:15-11:30	*1571320520*	*Koki Ito*	*1571322994*	*Ayaka Choki*	*1571315325*	*Sadah Lahad*	*1571314771*	*W. Limpornchitwilai*
11:30-11:45	*1571321812*	*Kitsada Thadson*	*1571323336*	*Chotipong Sakorn*	*1571321238*	*C. Phiphattanaphiphop*	*1571314776*	*Wen-Jou Chang*
11:45-12:00	*1571321819*	*Jaturon Umken*	*1571323653*	*Ahmed Safari*	*1571315633*	*C. Shiraishi*	*1571316204*	*Warin Suttiron*
12:00-12:15	*1571321826*	*Thazin Bo Bo*	*1571323714*	*Ryunosuke Kirita*	*1571316058*	*Sung Soo Lee*	*1571318116*	*Si-Wei Yang*
12:15-12:30	*1571322071*	*Napat Naowarangsee*	*1571324679*	*Mehwish Moiz*	*1571316787*	*N. Vongmanee*	*1571323346*	*Prajat Paul*
12:30-13:45	Lunch							
Session Room	Room1		Room 2		Room 3		Room 4	
Online Link	Click here >>							
Session Topic	D2R1AE- Medical Image Processing III		D2R2AE- Biomedical Signal Processing III		D2R3AE- Biosensors II		D2R4AE- Bio-robotics and biomechanics I	
Session Chair	*Theekapun Charoenpong*		*Supan Tungjitkusolmun*		*Nobuhiko Kojima*		*Wongwit Senavongse*	
13:45-14:00	*1571305732*	*An Ta*	*1571319745*	*B. Rung-Ruang*	*1571317139*	*K. Pipatprasert*	*1571314260*	*Peter Berkelman*
14:00-14:15	*1571306251*	*V. Phanichraksaphong*	*1571321715*	*Cho Nandi Hlaing*	*1571318635*	*Mahalakshmi Kannan*	*1571315319*	*Itgel Megzer*
14:15-14:30	*1571306827*	*P. Amornprasertchai*	*1571321808*	*Wulin Xi*	*1571320051*	*Kroekchai Thongtae*	*1571319511*	*Michihiko Fukunaga*
14:30-14:45	*1571311836*	*P. Kamonvaranon*	*1571321871*	*Jun Akazawa*	*1571320836*	*Ajay Prasanth*	*1571321279*	*K. Boonyasurat*
14:45-15:00	*1571311914*	*Yu-Ti Tu*	*1571321950*	*Nicha Thachuen*	*1571322364*	*C. Phiphattanaphiphop*	*1571321925*	*S. Nakdhamabhorn*
15:00-15:15	*1571312635*	*Kitiyaporn Takham*	*1571322016*	*N. Jongnimitmongkol*	*1571322406*	*Kitsada Thadson*	*1571322829*	*John Minogue*
15:15-15:30	*1571313217*	*P. Paewpolsong*	*1571322289*	*Wei Li*	*20260009*	*Thitipa Rupprom*	*1571323450*	*S. Piyavannakul*
15:30:15:45	Coffee Break							
15:45-16:30	Keynote IV: Prof. Nobuhiko Kojima							
16:30-17:00	Photo Session							
17:00-18:00	Take off for banquet							
18:00-20:00	Banquet							
Day 3: October 12, 2026								
8:45-9:15	Registration							
9:15-10:00	Keynote V: Prof. Manuel Humberto Luque Casanave							
10:00-10:15	BMEiCON 2027 Announcement							
10:15-10:45	Coffee Break							
Session Room	Room1		Room 2		Room 3		Room 4	
Online Link	Click here >>							
Session Topic	D3R1ML- Medical Image Processing IV		D3R2ML- Bioinformatics I		D3R3ML- Cardiovascular and respiratory systems		D3R4ML- Biomedical Signal Processing IV	
Session Chair	*Che-Wei Lin*		*Ming-Long Yeh*		*Phornphop Naiyanetr*		*Tohru Yaki*	

10:45-11:00	1571322162	Gad Barash	1571314845	Watin Promfiy	1571303046	Tsubasa Tomii	1571299587	Ir. Dr. A. Azhim
11:00-11:15	1571322390	Thodsaporn Phansri	1571322328	Voraphop Vorapasit	1571314666	P. Naiyanetr	1571306249	V. Phanichraksaphong
11:15-11:30	1571322615	Arthit Buranasing	1571322686	Kunthida Srilasak	1571315983	Vasit Sirilapanan	1571306860	Saravanan M
11:30-11:45	1571322970	Riku Tanabe	1571322723	P. Kasembunyakorn	1571321186	Chiharu Kutsuzawa	1571306951	Yicong Xiao
11:45-12:00	1571323174	P. Putyuen	1571323513	Karnpitcha Meekul	1571322223	T. Wisitponchai	1571311730	Helen Mao
12:00-12:15	1571323454	Phichamon Intra	1571323790	M. Jobayer Chowdhury	1571322678	Akkarwin Li	1571312939	P. Tangkiatphaibun
12:15-12:30	1571323459	Phiengfah Upasen	1571322685	Jitpimon Siripanth	1571315222	Chieru Muta	1571313859	Yuchen Liu
12:30-13:45	Lunch							
Session Room	Room1		Room 2		Room 3		Room4	
Online Link	Click here >>							
Session Topic	D3R1AE- Biomedical Signal Processing V		D3R2AE- Medical Image Processing V / Bio-robotics and biomechanics II		D3R3AE- Biomaterials I		D3R4AE- Biomaterials II / Bioinformatics II	
Session Chair	Shin'ichiro Kanoh		Manuel Lique Casaneve		Tadayuki Akagi		Surapong Chatpun	
13:45-14:00	1571322290	Honoka Funatsuki	1571323738	P. Pathomnop	1571312342	Chawan Manaspon	1571322129	P. Reddy Budipalli
14:00-14:15	1571322638	N. Siribunyaphat	1571323766	Md Walid Hassan	1571314446	Patipat Kamdenlek	1571322606	C. Rattanapongvanich
14:15-14:30	1571322719	Arthit Buranasing	1571323767	S. Mannan Trisha	1571315027	Princess Joy Naig	1571323153	Pitcha Plaiplerd
14:30-14:45	1571322804	P. Panyachuai	1571325061	Diego Aedo	1571315412	Chonticha Annanon	1571323500	A. Puengprasert
14:45-15:00	1571322873	Yuki Jono	1571312150	Kodai Ochi	1571315574	Laphas Wijitpanya	1571323563	S. Limpijumnong
15:00-15:15	1571322900	Togi Kurata	1571312534	Yin Qing Tan	1571317637	T. Korpanitchkul	1571283038	S. Chokphoemphun
15:15-15:30	1571322912	Masato Kudo	1571313825	Mutsuki Hagiwara	1571319535	Arissara Suksap	1571310706	Vera Sa-ing
15:30-16:00	Coffee Break							
Session Room	Room1		Room 2		Room 3		R	
Online Link	Click here >>							
Session Topic	D3R1AL- Human machine/computer interface I		D3R2AL- Therapeutic and diagnostics systems		D3R3AL- Other Biomedical Engineering / Telemedicine		D3R4AL- Medical device design / Human machine-computer interface I	
Session Chair	Boonserm Kaewkamnerdpong		Arthon Sunpanich		Chanchai Thaijiam		Jeerawan Thanarat	
16:00-16:15	1571321520	Muhammad Asif	1571311812	Takeshi Joyashiki	1571323495	Bao Nguyen	1571316301	Jeerawan Thanarak
16:15-16:30	1571322020	K. Kaewkamnerdpong	1571314696	P. Sangong	1571323503	Chau Vo	1571314406	Pasin Thansuwat
16:30-16:45	1571322882	Konemany Kanlaya	1571322550	Annika Harnack	1571323324	T. Kraisarin	1571314367	Sakurako Yamamura
16:45-17:00	1571322850	Kiyotaka Fujii	1571323384	Geunho Shim	20260001	K. Piphounnok	1571319436	P. Chantayanee
17:00-17:15	1571322872	Alexander Woo	1571323749	T. Sopithikul	20260002	S. Usama Hussain Shah Bukhari	1571323758	Mathew Fujikami
17:15-17:30	1571322444	P. Orankichalearn	1571323805	Shriya Thakur	20260010	Somchat Taertulakarn	1571323146	Hiroki Ishii

17:30-18:00	Move to conference hall
18:00-18:30	Closing ceremony/ Best paper award
Day 4: October 13, 2026	
8:00-16:30	Research Networking Event

BMEiCON 2026 — Session Abstracts

The following sections reproduce the session assignments and the abstracts from the supplied BMEiCON 2026 draft program and abstract collection.

D1R1AL

Medical Image Processing I

Session Chair: Theerasak Chanwimalueng

Time	Paper ID	Presenter	Paper Title
15:45–16:00	1571314474	T. Wutthikulthanachai	Microwave Imaging for Liver Tumor Detection Using a GA-Optimized Equilateral-Triangular Antenna at 2.45 GHz
16:00–16:15	1571315238	V. Diaz-Hernandez	Vision Transformer with Adaptive LAB-CLAHE Preprocessing for Automated Classification of Retinopathy of Prematurity Stages in Wide-Field Digital Retinal Images
16:15–16:30	1571315273	Saksorn Thaijiam	An AI-Based Elephant Biometric Identification and Electronic Medical Record System for Veterinary Healthcare and Conservation Management
16:30–16:45	1571315293	Hikari Saito	Shared-Detector Multi-Distance Optode Configuration for Enhanced Spatial Resolution and Depth-Selective Signal Extraction in CW- fNIRS
16:45–17:00	1571316167	Wanida Kaewmunee	Automated Spinal Alignment Angle Estimation Using Color-Constrained Blob Detection: A Comparative Study with Expert Measurements
17:00–17:15	1571316870	N. Naufal Rahman	Hierarchical Consistency Decoder for 3D Brain Tumor Segmentation: Promoting Anatomical Consistency via Sequential Soft Conditioning
17:15–17:30	1571318175	Teeranad Wanpradis	T2-Weighted MRI Radiomics for Survival Prediction in Oropharyngeal Cancer Patients: HPV-Stratified Analysis

1571314474 — Microwave Imaging for Liver Tumor Detection Using a GA-Optimized Equilateral-Triangular Antenna at 2.45 GHz

Authors: Thanakorn Wutthikulthanachai, Pannathorn Paiboonkulwong and Weerapong Buranatep (Srinakharinwirot University, Thailand); Chanchai Thaijiam (SWU, Thailand); Rattanan Laorboot (Srinakharinwirot University, Thailand); Saksorn Thaijiam (Patumwan Demonstration School, Thailand); Suchada Tantisatirapong (Srinakharinwirot University, Thailand)

Abstract: Early detection of liver tumors is crucial for improving treatment outcomes and reducing mortality. This study presents a microwave imaging system for non-invasive liver tumor detection, using a compact equilateral-triangular microstrip antenna operating at the 2.45 GHz ISM band. We optimized the antenna geometry using a Genetic Algorithm (GA) via a co-simulation framework between CST Microwave Studio® and MATLAB®. This approach allowed the optimization to account for the dielectric loading effect of a realistic multilayer human torso phantom. The system's performance was evaluated across tumor sizes of 10, 20, and 30 mm at five distinct depth positions, using Differential S11 (ΔS11), Signal-to-Clutter Ratio (SCR), and Delay-and-Sum (DAS) image reconstruction. Simulation results indicate that tumor size primarily influences reflected signal intensity, while depth dictates localization accuracy. We observed maximum ΔS11 values of −0.561 dB and −0.582 dB for the 20 mm and 30 mm tumors, respectively. Furthermore, most cases achieved an SCR greater than 5 dB, confirming effective discrimination between the tumor response and background clutter. Reconstructed images show that deeper tumors are localized with greater accuracy, though tumors near the system's symmetry axis may generate ghost artifacts due to the inherent limitations of the monostatic DAS configuration. Ultimately, these findings suggest that the proposed GA-optimized antenna offers an effective, low-cost platform for early liver tumor detection, establishing a practical foundation for future systems with improved reconstruction algorithms.

1571315238 — Vision Transformer with Adaptive LAB-CLAHE Preprocessing for Automated Classification of Retinopathy of Prematurity Stages in Wide-Field Digital Retinal Images

Authors: Valeria A. Diaz-Hernandez and Abimael Guzman-Pando (Autonomous University of Chihuahua, Faculty of Medicine and Biomedical Sciences); Graciela Ramirez-Alonso (Autonomous University of Chihuahua, Faculty of Engineering); Natalia G. Samano-Lira (Autonomous University of Chihuahua, Faculty of Medicine and Biomedical Sciences); Luis C. Hinojos-Gallardo and Marianna Pacheco-Quintana (Autonomous University of Chihuahua, Mexico)

Abstract: Retinopathy of prematurity (ROP) is one of the leading causes of preventable childhood blindness worldwide. However, clinical diagnosis relies on specialist experience and presents significant interobserver variability, particularly in early stages. Therefore, this paper proposes an automated ROP classification system combining the ViT-Base/16 architecture with a LAB-CLAHE preprocessing pipeline, evaluated on a public dataset of wide-field digital retinal images (WFDRI) with five diagnostic categories: Normal, Stage 1, Stage 2,

Stage 3, and Laser scars. Class imbalance was addressed through weighted random sampling and Focal Loss strategies. We used stratified K=5 cross-validation and an independent sealed test set for evaluation. The proposed model achieved 90.30% accuracy, 85.57% macro F1- score, and 98.39% AUC, surpassing previously reported baselines, including ResNet50, vanilla ViT-B, ConvNeXt-T, and ResNet101. Our work demonstrates that LAB-CLAHE preprocessing and class-imbalance strategies yield an accuracy gain over the vanilla ViT-B baseline, supporting the representational capacity of Vision Transformers for ROP classification. Grad-CAM analysis showed clinically plausible activation patterns, and an inference time of 16.80 ms per image demonstrates real- time feasibility.

1571315273 — An AI-Based Elephant Biometric Identification and Electronic Medical Record System for Veterinary Healthcare and Conservation Management

Authors: Saksorn Thaijiam (Patumwan Demonstration School, Thailand); Panprima Srisanit (Srinakharinwirot University, Patumwan Demonstration School, Thailand); Vasita Wispaphaew (Srinakharinwirot University, Thailand); Nicha Tungdumnunsawad (Office of the Basic Education Commission, Thailand); Suchada Tantisatirapong and Theerasak Chanwimalueang (Srinakharinwirot University, Thailand)

Abstract: Accurate individual elephant identification is essential for veterinary healthcare, conservation management, ownership verification, and legal protection against illegal trafficking. Traditional identification methods rely on manual observation of physical characteristics and are often subjective, time-consuming, and prone to human error. This study proposed an AI-based elephant biometric identification framework integrated with an elephant electronic medical record web application to support veterinary services and long-term conservation management. The proposed system employed a transfer learning approach based on a pre-trained ResNet-50 convolutional neural network for the classification of individual elephants from digital images. Elephant photographs collected under varying environmental conditions were preprocessed, augmented, and used to fine-tune the ResNet-50 model. The network learned discriminative biometric features, including facial morphology, ear contours, ear vein patterns, tusk characteristics, skin wrinkle distributions, and visible scars, enabling reliable recognition of individual elephants. Experimental evaluation was conducted on two independent elephant groups. For Dataset A, the model achieved an accuracy of 86.67%, precision of 87.49%, recall of 86.67%, and F1-score of 86.67%. For Dataset B, the proposed model achieved an accuracy of 90.83%, precision of 91.15%, recall of 90.83%, and F1-score of 90.92%. Upon successful identification, the corresponding elephant medical record was automatically retrieved through the elephant electronic medical record platform, facilitating rapid access to historical clinical information and supporting evidence-based veterinary decision-making.

1571315293 — Shared-Detector Multi-Distance Optode Configuration for Enhanced Spatial Resolution and Depth-Selective Signal Extraction in CW- fNIRS

Authors: Hikari Saito and Yuto Matsumoto (Tokyo Metropolitan College of Industrial Technology, Japan); Shuhei Kamogawa, Yasukuni Shibata and Kazuki Sato (School of Systems Design Tokyo Metropolitan University, Japan); Keiko Fukuda (Tokyo Metropolitan College of Industrial Technology, Japan)

Abstract: Continuous-wave functional near-infrared spectroscopy (CW-fNIRS) is widely used to map human brain activity but suffers from two major limitations: limited spatial resolution caused by sparse channel spacing and contamination of deep cortical signals by superficial hemodynamic artifacts in the scalp. To address both challenges simultaneously with conventional equipment, this study proposes a novel "shared-detector" optode arrangement, in which an additional detector shared among multiple light sources yields three distinct source-detector distances (short, standard 1, and standard 2) with minimal hardware extension. A depth-selective filtering algorithm, based on a two-layer forward model and Tikhonov regularization, isolates deep cortical signals from superficial hemodynamic artifacts. The method's efficacy was evaluated through numerical simulations and tissue-equivalent phantom experiments using a commercial CW-fNIRS system, which successfully resolved closely spaced deep targets undetectable by conventional single-distance topography. Superficial hemodynamic artifacts were suppressed to within 10% across all channels, enabling accurate, localized mapping of deep tissue absorption changes.

1571316167 — Automated Spinal Alignment Angle Estimation Using Color-Constrained Blob Detection: A Comparative Study with Expert Measurements

Authors: Wanida Kaewmunee, Sirawee Chaovalit and Jermphiphut Jaruenpunyasak (Prince of Songkla University, Thailand); Surapong Chatpun (Prince of Songkla Universiy, Thailand)

Abstract: Manual assessment of spinal alignment from clinical images can be time-consuming and may introduce measurement variability. This study developed an automated marker-based image analysis method

to estimate C7 and S2 spinal alignment angles from prone-position images of children with cerebral palsy (CP). Seven children with CP were included, and 40 original images were retained after quality screening and augmented to generate 200 images for evaluation. Automated measurements were compared with expert measurements using mean absolute error (MAE), root mean squared error (RMSE), Pearson correlation coefficient, intraclass correlation coefficient (ICC), scatter plots, and point of maximum deviation (PMD) selection agreement. The C7 angle showed an MAE of 1.11°, an RMSE of 2.08°, and an ICC of 0.672, whereas the S2 angle showed an MAE of 0.56°, an RMSE of 0.83°, and an ICC of 0.923. The proposed method produced measurements close to expert measurements, with better agreement for the S2 angle. These findings suggest its potential as a supportive tool for quantitative spinal alignment assessment in young children with CP.

1571316870 — Hierarchical Consistency Decoder for 3D Brain Tumor Segmentation: Promoting Anatomical Consistency via Sequential Soft Conditioning

Authors: Nafis Naufal Rahman, Aditya Akbar and Muhammad Faris El Hakim (Universitas Brawijaya, Indonesia)

Abstract: Accurate delineation of brain tumor sub-regions from multimodal MRI is essential for treatment planning yet remains challenging due to ambiguous boundaries and severe class imbalance. A fundamental anatomical constraint (Enhancing Tumor within Tumor Core within Whole Tumor, ET⊂TC⊂WT) is routinely ignored by models that predict all three sub-regions independently with sigmoid activations, permitting anatomically impossible outputs. We propose the Hierarchical Consistency Decoder (HCD), a single end-to-end decoder that promotes anatomical nesting (ET within TC within WT) via sequential soft conditioning. WT is predicted first from a multi-scale Feature Pyramid Network; TC is predicted conditioned on the WT soft mask; and ET is conditioned on TC. A Squeeze-Excitation block recalibrates the fused pyramid features before prediction, and an auxiliary hierarchical consistency loss penalizes constraint violations during training. We introduce the Hierarchy Violation Rate (HVR) to measure post- inference anatomical consistency independently of ground truth. Ablation studies reveal that hierarchical conditioning and SE recalibration provide complementary effects on DSC and HVR.º

1571318175 — T2-Weighted MRI Radiomics for Survival Prediction in Oropharyngeal Cancer Patients: HPV-Stratified Analysis

Authors: Teeranad Wanpradis (Medical Physics Program, Department of Radiology, Faculty of Medicine, Chulalongkorn University, Bangkok, Thailand); Charinya Pengsawang and Banthita Nabandit (Department of Radiological Technology and Medical Physics, Chulalongkorn University, Bangkok, Thailand); Mananchaya Vimolnoch and Sarin Kitpanit (Division of Radiation Oncology, Department of Radiology, King Chulalongkorn Memorial Hospital, Bangkok, Thailand); Chakkapong Chakkabat and Chawalit Lertbutsayanukul (Division of Radiation Oncology, Department of Radiology, Faculty of Medicine, Chulalongkorn University, Bangkok,Thailand); Sira Sriswasdi (Research Affairs, Faculty of Medicine, Chulalongkorn University, Bangkok, Thailand); Danita Kannarunimit (Division of Radiation Oncology, Department of Radiology, Faculty of Medicine, Chulalongkorn University, Bangkok,Thailand); Sararas Khongwirotphan (Department of Radiological Technology and Medical Physics, Chulalongkorn University, Bangkok, Thailand); Anussara Prayongrat (Division of Radiation Oncology, Department of Radiology, King Chulalongkorn Memorial Hospital, Bangkok, Thailand); Yothin Rakvongthai (Division of Nuclear Medicine, Department of Radiology, Faculty of Medicine, Chulalongkorn University, Bangkok, Thailand)

Abstract: Patients with oropharyngeal carcinoma (OPC) may experience different outcomes despite similar clinical stage and human papillomavirus (HPV) status, suggesting that routine clinical factors may not fully capture individual tumor risk. This retrospective study evaluated whether pretreatment T2-weighted MRI radiomics could improve prediction of overall survival (OS), disease-free survival (DFS), and distant metastasis- free survival (DMFS) beyond selected clinical variables, and whether performance differed by HPV status. A total of 214 patients with OPC treated with chemoradiotherapy were analyzed. Primary gross tumor volumes were manually delineated on pretreatment T2-weighted MRI, and 1,288 radiomic features were extracted using PyRadiomics. Robust features were selected using intraclass correlation coefficient filtering and cross-validated recursive feature elimination. Clinical, radiomics, and combined (clinical + radiomics) logistic regression models were developed for 3-year OS, DFS, and DMFS prediction. Performance was assessed with repeated five-fold cross-validation. Combined clinical-radiomics models improved prediction beyond selected clinical variables alone for most outcomes. For OS, validation AUC increased from 0.690 ± 0.081 for the clinical model to 0.780 ± 0.068 for the radiomics model and 0.798 ± 0.070 for the combined model (all $p < 0.05$). For DFS, the combined model yielded the highest AUC of 0.734 ± 0.072 compared with the clinical and radiomics models ($p < 0.05$), while the radiomics and clinical models yielded comparable performance ($p = 0.617$). For DMFS, the radiomics and combined models achieved similar validation AUCs of 0.699 ± 0.106 and 0.698 ± 0.102, respectively, with no significant difference between them ($p = 0.107$). However, the combined model significantly outperformed the clinical model ($p < 0.05$).

HPV-stratified analysis suggested that performance differences between HPV-positive and HPV- negative patients varied by endpoint and model type. In conclusion, pretreatment T2- weighted MRI radiomics provided complementary prognostic information beyond routine clinical factors and supported HPV-stratified risk assessment. External validation is needed before clinical implementation.

D1R2AL

Biomedical Signal Processing I

Session Chair: Tomohiko Igasaki

Time	Paper ID	Presenter	Paper Title
15:45–16:00	1571314382	P. Uthansakul	A Machine Learning Approach for Contactless HRV Measurement via Smartphone rPPG: A Pilot Study
16:00–16:15	1571315270	W. Rachatapan	A Comparison of Traditional Acoustic Features and Wav2Vec2.0 Representation for Thai Speech Emotion and Emotion Intensity Classification
16:15–16:30	1571315294	Punnut Sukkhun	Automatic Squat Classification Using Electromyography and Inertial Measurement Unit in Patients With Knee Pathology
16:30–16:45	1571316462	Sayaka Suga	Pilot ERP Study Using a Mask-Free Olfactory Presentation System to Assess Warm Food Odor Acceptance and Difficult-to-Verbalize Odor Perception Across Cultural and Dietary Backgrounds
16:45–17:00	1571316804	Ping-Hung Hsieh	Self-Supervised Fall Detection from IMU Signals Using Masked Reconstruction and Forecasting
17:00–17:15	1571316852	Chun-Yi Liu	Motion Classification Using a 1D-Wavelet-CNN Model Based on IMU Signals
17:15–17:30	1571318842	Suatmi Murnani	A Directional-State Phase Approach to Characterizing Movement Organization in Handwriting Tracing

1571314382 — A Machine Learning Approach for Contactless HRV Measurement via Smartphone rPPG: A Pilot Study

Authors: Phakaruch Uthansakul, Narin Songsakulwong, Chirat Chundang and Pirapong Inthapong (Surawiwat School, Suranaree University of Technology, Thailand); Talit Jumphoo, Wongsathon Pathonsuwan and Porntip Nimkuntod (Suranaree University of Technology, Thailand)

Abstract: Heart Rate Variability (HRV) is a critical indicator of autonomic nervous system dynamics, yet traditional electrocardiogram (ECG) tracking suffers from physical contact and cost constraints. While smartphone-based remote photoplethysmography (rPPG) offers a contactless alternative, conventional statistical processing fails to accurately capture short-term HRV (RMSSD) metrics due to peripheral vascular filtering effects. To address this limitation, this paper proposes a novel machine learning-enhanced framework to map smartphone rPPG signals onto clinical-grade HRV metrics. Under the supervision of a cardiologist, synchronous reference ECG and 1080p facial videos were acquired from healthy volunteers. A 468-point MediaPipe FaceMesh model was deployed for real-time facial tracking, isolating the highly correlated green color channel within optimized regions of interest to mitigate motion artifacts. Although the baseline statistical rPPG pipeline achieved precise heart rate estimation, it yielded an unacceptable RMSSD error of 80.8 ms. Crucially, integrating machine learning regressors substantially reduced this temporal discrepancy. Among the evaluated algorithms (Random Forest, Gradient Boosting, Ridge, and Lasso), the Lasso linear regressor emerged as the optimal model, reducing the RMSSD Mean Absolute Error by 78% down. This study validates a low-cost, machine learning- augmented contactless infrastructure, offering a robust prototype for biomedical engineering education and preliminary health trend assessment.

1571315270 — A Comparison of Traditional Acoustic Features and Wav2Vec2.0 Representation for Thai Speech Emotion and Emotion Intensity Classification

Authors: Warachaya Rachatapan (Department of Biomedical Sciences and Biomedical Engineering, Faculty of Medicine, Prince of Songkla University); Jiramate Charoenkhwan (Department of Artificial Intelligence Engineering, Faculty of Engineering, Prince of Songkla University); Wanwara Thuptimdang (Department of Biomedical Sciences and Biomedical Engineering, Faculty of Medicine, Prince of Songkla University)

Abstract: This study examines Thai speech emotion and emotion intensity recognition using traditional acoustic features and Wav2Vec2.0 representations. We considered two classification tasks: three-class emotion classification (Happy, Neutral, and Sad) and six-class emotion-intensity classification, in which each emotion was divided into normal and strong intensity levels. A multilayer perceptron (MLP) classifier was used for both classification tasks. The traditional acoustic feature set comprised of Mel- frequency cepstral coefficients (MFCCs), fundamental frequency (F0), and zero- crossing rate (ZCR), whereas the Wav2Vec2.0 features were extracted from pretrained speech representations. The results showed that Wav2Vec2.0 consistently outperformed the traditional acoustic features across two tasks. It achieved 87.2% accuracy for emotion classification and 58.5% accuracy for emotion-intensity classification, compared with 77.7% and

49.4%, respectively, for the traditional acoustic features. The findings indicate that pretrained speech representations are more effective for Thai speech emotion recognition, although accurate discrimination of emotion intensity remains challenging.

1571315294 — Automatic Squat Classification Using Electromyography and Inertial Measurement Unit in Patients With Knee Pathology

Authors: Punnut Sukkhun (Department of Biomedical Sciences and Biomedical Engineering, Faculty of Medicine, Prince of Songkla University); Suphansa Sriplot (Department of Physics, Faculty of Science, Prince of Songkla University); Wanwara Thuptimdang (Department of Biomedical Sciences and Biomedical Engineering, Faculty of Medicine, Prince of Songkla University)

Abstract: The squat is a key closed kinetic chain exercise for knee pathology rehabilitation, but unsupervised performance often leads to movement errors and exacerbated knee pain. This study investigated whether incorporating bilateral rectus femoris EMG alongside IMU measurements improves squat classification across 19 patients with knee pathology. Using a Random Forest classifier, we targeted three squat variations: correct squat, weight transfer to healthy leg, and injured leg placed in front. We evaluated performance across three configurations: EMG-only, IMU-only and multimodal fusion. The EMG+IMU fusion achieved moderate accuracy of 0.52 and sensitivity of 0.48, comparable to the IMU-only configuration, whereas the EMG-only demonstrated the lowest performance. Feature importance analysis showed a dominance of IMU features over EMG features. Furthermore, substantial inter-subject variability in sensitivity was observed, with performance ranging from 0.0 to 1.0. Consequently, integrating only rectus femoris EMG and IMU is insufficient for classifying compensatory squat postures in patients with knee pathology. Future research should employ multi-site sensor configurations incorporating agonist- antagonist muscle pairs to enhance clinical classification sensitivity.

1571316462 — Pilot ERP Study Using a Mask-Free Olfactory Presentation System to Assess Warm Food Odor Acceptance and Difficult-to-Verbalize Odor Perception Across Cultural and Dietary Backgrounds

Authors: Sayaka Suga (Mukogawa Women's University, Japan); Yuko Ohno (Osaka University, Japan); Zu Soh (Hiroshima University, Japan); Mitsuo Tonoike and Shinichi Yoshimura (The University of Osaka, Japan); Kaori Tamura (Kyushu Institute of Technology, Japan)

Abstract: Food odor perception is influenced by dietary experience, familiarity, and cultural background. Warm food odors are particularly relevant to the daily eating experience; however, conventional olfactory experiments often use odor containers or masks, complicating the presentation of odors under natural breathing conditions. In this pilot study, we examined whether event-related potentials (ERPs) recorded during a visual oddball task could capture subjective responses to warm food odors, including odor acceptance and difficult-to-verbalize odor perception. Five healthy adults participated in the study: three Japanese participants and two participants originally from Inner Mongolia who had lived in Japan for more than 8 and 13 years, respectively. Warm odor stimuli consisted of sea buckthorn juice and salted milk tea, which are familiar in Mongolia, and miso soup and yuzu tea, which are familiar in Japan. Using a mask-free olfactory presentation system, odors were presented as background olfactory contexts while participants performed a visual oddball task. Electroencephalogram responses and subjective evaluations of odor preference, familiarity, and positive or negative impressions were also evaluated. ERP waveforms for fruit-based beverage odors showed opposite tendencies between participant groups. Japanese participants exhibited a larger positive peak with shorter latency for yuzu tea than for sea buckthorn juice, whereas Inner Mongolian participants showed a clear late positive response to sea buckthorn juice and a smaller response to yuzu tea. Inner Mongolian participants did not show a distinct positive peak for salted milk tea, but rather a broad, low-amplitude late positive deflection at approximately 300-500 ms. Together with subjective reports indicating perception without discomfort but difficulty in verbal description, this pattern may suggest a difficult-to-verbalize olfactory state rather than weak or absent odor perception. These preliminary findings suggest that combining subjective odor evaluation with ERP measurements may help characterize diverse responses to warm food odors. This approach may be useful for future olfactory assessments, including the evaluation of olfactory dysfunction and treatment effects, without relying on strongly unpleasant stimuli.

1571316804 — Self-Supervised Fall Detection from IMU Signals Using Masked Reconstruction and Forecasting

Authors: Ping-Hung Hsieh (National Cheng Kong University, Taiwan); Chun-Yi Liu (National Cheng Kung University, Taiwan); Pi-Shan Sung (National Cheng Kung University Hospital, Taiwan); Chih-Lung Lin (National Cheng Kung University, Taiwan)

Abstract: Falls can cause severe physical injuries, psychological trauma, and even death. To mitigate these risks, many fall detection methods have been proposed to provide timely rescues. However, most existing approaches rely on supervised learning and require large amounts of labeled fall data. This work presents a self-supervised fall prediction approach using IMU signals. The proposed model learns normal motion patterns from activities of daily living (ADLs) and identifies fall-related motions using an anomaly score derived from prediction errors. Experimental results on the KFall dataset demonstrate that the proposed method achieves an accuracy of 98.4%, a sensitivity of 98.9%, and a false alarm rate of 1.0%. In cross-dataset evaluation, the proposed approach achieves an accuracy of 97.5%, a sensitivity of 94.2%, and a false alarm rate of 0.0%. These results demonstrate the effectiveness and generalization capability of the proposed self-supervised approach for wearable fall detection.

1571316852 — Motion Classification Using a 1D-Wavelet-CNN Model Based on IMU Signals

Authors: Chun-Yi Liu (National Cheng Kung University, Taiwan); Ping-Hung Hsieh (National Cheng Kong University, Taiwan); Peng-Ting Chen and Chih-Lung Lin (National Cheng Kung University, Taiwan)

Abstract: Falls are a major health risk for older adults and lead to severe injuries, reduced mobility, and loss of independence. Wearable devices incorporating IMUs provide a lightweight and portable solution for monitoring human motion. However, classifying IMU-based activity remains challenging because motion signals contain both short- term rapid changes and sustained temporal patterns. This work proposes a motion classification model based on a 1D-Wavelet-CNN using the KFall dataset. The proposed model integrates Haar wavelet decomposition with 1D convolutional feature extraction to preserve both low-frequency motion patterns and high-frequency transient variations. To evaluate the effectiveness of the proposed model, the model was compared with two baseline classification models. Experimental results show that the proposed model achieves an accuracy of 94.73% and a macro-F1 score of 94.29%, outperforming the other two models. In addition, the fall class achieves an F1-score of 99.71, indicating that the proposed model effectively distinguishes fall events from Activities of Daily Living (ADLs). These results indicate that the proposed 1D-wavelet- CNN provides an effective approach for IMU-based motion classification.

1571318842 — A Directional-State Phase Approach to Characterizing Movement Organization in Handwriting Tracing

Authors: Suatmi Murnani (Kumamoto University, Japan & Universitas Islam Indonesia, Indonesia); Kazuharu Hashitsume (Shimane University, Japan); Tomohiko Igasaki (Kumamoto University, Japan)

Abstract: Digital handwriting assessment increasingly utilizes spatiotemporal signals to support objective evaluation of handwriting performance. However, existing approaches primarily emphasize feature extraction and classification, providing limited insight into handwriting movement organization during execution. This study proposes a directional-state phase approach that represents handwriting movements using movement direction and directional change rate to characterize movement organization during handwriting tracing. The proposed approach was evaluated using an existing handwriting tracing dataset comprising 35 elementary school students performing uppercase English letter tracing tasks. Directional-state phase portraits were constructed from smoothed trajectories to quantify directional adjustment frequency and directional deviation severity. Linear mixed-effects models were used to examine differences across grade levels and stroke orientations. Representative examples showed that visually similar trajectories could exhibit distinct directional-state behaviors. Statistical analyses indicated that only directional deviation severity differed significantly across grade levels, whereas all proposed descriptors differed significantly across stroke orientations. These findings demonstrate the potential of directional-state phase portraits to complement trajectory-based handwriting assessment by characterizing endpoint-level directional-state behavior. Accordingly, the proposed descriptors should be interpreted as endpoint-level indicators of task-space movement organization rather than direct measures of upper-limb motor control.

D1R3AL

Healthcare information I

Session Chair: Suejit Pechprasarn

Time	Paper ID	Presenter	Paper Title
15:45–16:00	20260007	P. Dilokworachot,	Early Prediction of Alzheimer's Disease Using Machine Learning and Feature Selection
16:00–16:15	20260008	L. Pholprasert, N. Bintee Rahman	Machine Learning-Based Diabetes Classification Using a Reduced Set of Health Indicators
16:15–16:30	1571323504	Peeya	Kotha: A Conversational Clinical Scribe for Bengali Medical Documentation with Code-Switching Resilience
16:30–16:45	20260003	Chanakarn Sirirat	Machine Learning for Liver Cancer Prediction Using Clinical Data Collected Before and During the COVID-19 Pandemic
16:45–17:00	20260004	Nichapa Srisaranon	Automated Surgical Instrument Detection, Identification, and Counting Using YOLO
17:00–17:15	20260005	K. Thavornthammarit	Optimizing Hyperthyroidism Diagnosis Through Machine Learning and Feature Selection
17:15–17:30	20260006	Mira Kantito	Comparative Evaluation of Machine Learning Models for Brain Stroke Risk Prediction Using Feature Selection

20260007 — Early Prediction of Alzheimer's Disease Using Machine Learning and Feature Selection

Authors: Phuckwalun Dilokworachot, Salil Skulkiat ,Satriwithaya School, Bangkok Thailand;Suejit Pechprasarn College of Biomedical Engineering, Rangsit University, Thailand

Abstract: Alzheimer's disease (AD) is a progressive neurodegenerative disorder that affects memory, cognitive function, and daily activities. This study developed a machine learning framework for Alzheimer's disease classification, emphasizing reducing the number of predictor variables while maintaining classification performance. A publicly available clinical dataset obtained from Kaggle consisted of 2,149 instances and 35 attributes. After removing the PatientID and DoctorInCharge variables and balancing the diagnostic classes at a 1:1 ratio, 1,520 instances with 32 predictor variables and one target label (Diagnosis) were retained. A total of 36 machine learning models available in the MATLAB Classification Learner app (R2026a) were initially trained and evaluated using 5-fold cross-validation. The Boosted Trees Ensemble model achieved the best performance using all 32 predictors, with an accuracy of 93.34%, precision of 94.06%, recall of 92.54%, F1-score of 93.29%, and ROC-AUC of 0.936. Minimum Redundancy Maximum Relevance (MRMR) was subsequently applied to rank the predictors, and the best-performing classifier was progressively retrained using reduced feature subsets. The optimal subset consisted of five predictors: Activities of Daily Living (ADL), Functional Assessment, Mini-Mental State Examination (MMSE), Memory Complaints, and Behavioral Problems. Using these five predictors, validation accuracy increased from 93.34% to 93.80%, despite an 84.4% reduction in the number of predictor variables. These findings demonstrate that MRMR-based feature selection can substantially reduce model complexity while maintaining, and slightly improving, Alzheimer's disease classification performance.

20260008 — Machine Learning-Based Diabetes Classification Using a Reduced Set of Health Indicators

Authors: Lunnapratr Pholprasert and Napatr Simsiri , Satriwithaya School, Thailand; Suejit Pechprasarn College of Biomedical Engineering, Rangsit University, Thailand

Abstract: Diabetes is a major public health concern, and accessible methods for identifying individuals at risk may support timely screening and intervention. This study developed and evaluated machine learning models for binary diabetes classification using health indicators and investigated whether feature selection could reduce the number of predictor variables while maintaining classification performance. A publicly available dataset containing 253,681 observations and 21 health indicators was obtained from Kaggle. Prediabetic cases were excluded to construct a binary classification dataset comprising non-diabetic and diabetic individuals. The resulting balanced dataset was randomly split into 90% for training/validation and 10% for an independent test set. A total of 36 machine learning models were evaluated using 5-fold cross-validation on the training/validation set. The Narrow Neural Network and Coarse Gaussian SVM achieved the highest validation accuracy of 76.6%, followed by the Quadratic SVM at 76.5%. On the independent test set, both the Narrow Neural Network and Coarse Gaussian SVM achieved 77.1% accuracy. The Narrow Neural Network achieved a precision of 74.0%, a recall of 82.1%, and an F1-score of 77.8% and was selected for subsequent

feature-selection analysis. Feature selection reduced the predictor set from 21 to nine health indicators: General Health, Cholesterol Check, Age, Heavy Alcohol Consumption, Body Mass Index, High Cholesterol, High Blood Pressure, vegetable consumption, and history of Stroke. Using these nine predictors, the Narrow Neural Network achieved an accuracy of 76.5%, representing a 57.1% reduction in the number of predictors with only a 0.6 percentage-point decrease in accuracy compared with the full-predictor model. These findings demonstrate that a substantially reduced set of health indicators can retain comparable performance in diabetes classification, supporting the development of simpler, more practical machine learning-based approaches for diabetes risk screening.

1571323504 — Kotha: A Conversational Clinical Scribe for Bengali Medical Documentation with Code-Switching Resilience

Authors: Nadia Bintee Rahman Peeya (Techvify Japan, Japan & Researcher, Japan)

Abstract: Manual medical-history taking is a documented bottleneck in Bangladeshi primary care, where over 92% of physicians face overwhelming workloads and EHR adoption remains below 5%. We present Kotha (Bengali for "talk"), a conversational LLM agent that interviews patients in natural Bengali, performs zero-shot structured extraction at tempera- ture 0, and emits a FHIR R4 bundle enriched with ICD-10 codes. The agent is provider-agnostic, enabling direct comparison of GPT-4o-mini, Claude Sonnet 4.6, and Gemini 2.5 Flash under an identical prompt and pipeline. On 50 clean Bengali dialogues, all three models reach ≥0.98 field accuracy, with Gemini leading at 0.999. On 100 heavily code-switched Bengali-English dialogues, Gemini and GPT-4o-mini retain near-ceiling accuracy (0.988 and 0.982) while Claude shows a moderate dip (0.919), establishing that intra-sentential code-switching (pervasive in Bangladeshi clinical speech) is not, in general, the primary obstacle to automated Bengali EHR extraction. We report these scores as an explicit upper bound given an 89% verbatim-leakage benchmark, and identify real clinical data, ASR integration, and dialect-aware evaluation as next steps.

20260003 — Machine Learning for Liver Cancer Prediction Using Clinical Data Collected Before and During the COVID-19 Pandemic

Authors: Chanakarn Sirirat, Pondpavee Kiatpathomchai , Satriwithaya School, Bangkok Thailand;Suejit Pechprasarn* College of Biomedical Engineering, Rangsit University, Thailand

Abstract: The COVID-19 pandemic has significantly disrupted healthcare services worldwide, affecting the diagnosis, management, and treatment of patients with liver cancer. This study investigates the application of machine learning techniques to classify liver cancer cases using a publicly available clinical dataset collected before and during the COVID-19 pandemic. The dataset, obtained from Kaggle, was preprocessed and balanced before model development. Multiple supervised machine learning algorithms were trained and evaluated using 5-fold cross validation. Model performance was assessed using accuracy, precision, recall, and F1-score. To improve model interpretability and reduce complexity, feature selection methods, including MRMR, ANOVA, and Kruskal–Wallis, were applied to identify the most informative predictors. Bayes Among the evaluated models, tree-based classifiers and Naïve achieved the highest classification performance, with a maximum accuracy of 99.60%. Furthermore, comparable predictive performance was maintained after reducing the number of predictors, indicating that a compact set of clinical variables is sufficient for accurate classification. These findings demonstrate the potential of machine learning and feature selection techniques to support liver cancer prediction using clinical data collected during the COVID-19 pandemic while providing a more efficient and interpretable predictive model.

20260004 — Automated Surgical Instrument Detection, Identification, and Counting Using YOLO

Authors: Nichapa Srisaranon, Natchanon Rodthan, And Pimpawaree Thiensukon ,Satriwithaya School, Thailand; Suejit Pechprasarn College of Biomedical Engineering, Rangsit University, Thailand

Abstract: Retained surgical items (RSIs) pose significant risks to patient safety during surgical procedures, while manual counting places a substantial administrative burden on medical personnel. To mitigate these issues, this study proposes an automated surgical instrument detection, identification, and counting using YOLOv8n. A comprehensive dataset comprising 9,361 images acquired from the Roboflow Universe platform across 18 distinct classes of surgical tools was utilized. The dataset was partitioned into a training set (70%, 6,553 images), a validation set (20%, 1,872 images), and a testing set (10%, 936 images), with data augmentation to enhance model generalization. Experimental results on the test dataset demonstrated exceptional detection performance, achieving a mean Average Precision at IoU threshold 0.5 (mAP@50) of 99.9%, a Precision of 99.8%, a Recall of 99.8%, and an F1-score of 99.8%, with a validation Average Precision (AP) of 100%. For future deployment, this verified framework is planned to be integrated into a real-time

computer vision system that connects to live video feeds. The proposed model provides a highly accurate and reliable foundation for smart operating room management, helping prevent retained foreign bodies and significantly reducing healthcare professionals' workloads.

20260005 — Optimizing Hyperthyroidism Diagnosis Through Machine Learning and Feature Selection

Authors: Kanokpich Thavornthammarit , Satriwithaya School , Bangkok, Thailand; Kitsada Thadson, Suejit Pechprasarn, Center of Excellence in Artificial Intelligence & Supercomputing, Rangsit University, Thailand

Abstract: Hyperthyroidism is a common endocrine disorder that can cause severe complications if not diagnosed and treated promptly. Although machine learning (ML) has shown considerable promise in supporting clinical diagnosis, the optimal classification algorithm and minimal set of predictive features for hyperthyroidism detection remain unclear. This study systematically compared 22 supervised ML classifiers, including decision trees, support vector machines, logistic regression, neural networks, discriminant analysis, Naïve Bayes, and ensemble learning methods, to identify the most effective model for hyperthyroidism classification. Using the UCI hyperthyroid dataset comprising 3,772 patient records, four feature selection techniques—Minimum Redundancy Maximum Relevance, Chi2, Analysis of Variance (ANOVA), and Kruskal–Wallis—were employed to evaluate the importance of 21 clinical predictors. Model training was performed using 5-fold cross-validation, and performance was assessed on an independent test set using accuracy, precision, recall, F1-score, and area under the receiver operating characteristic curve. Among the evaluated classifiers, the Boosted Trees model achieved the best overall performance, attaining 99.71% accuracy, 100.00% precision, 99.43% recall, a 99.71% F1-score, and a 99.72% AUC. Feature selection consistently identified thyroid-stimulating hormone, free thyroxine index, total thyroxine, and triiodothyronine as the most informative predictors. Models developed using only these four hormonal biomarkers maintained high predictive performance while reducing model complexity and computational requirements. Furthermore, TSH was identified as the single most influential predictor, and predictor combinations including TSH consistently outperformed those without it. These findings demonstrate that combining the Boosted Trees classifier with four key hormonal biomarkers provides an accurate, robust, and computationally efficient framework for hyperthyroidism classification. The proposed approach has the potential to support computer-aided diagnosis by improving diagnostic accuracy, reducing unnecessary laboratory testing, and facilitating efficient clinical decision-making

20260006 — Comparative Evaluation of Machine Learning Models for Brain Stroke Risk Prediction Using Feature Selection

Authors: Mira Kantito , Pimpawaree Thiensukon , Satriwithaya School, Bangkok, Thailand; Suejit Pechprasarn College of Biomedical Engineering, Rangsit University, Thailand

Abstract: Stroke is a major cause of mortality and long-term disability worldwide, highlighting the importance of effective methods for early risk assessment. This study presents a comparative evaluation of machine learning models for brain stroke risk prediction and investigates whether feature selection can reduce model complexity while maintaining predictive performance. An open-source dataset containing 4,981 records and ten demographic and clinical predictors was used. To address class imbalance, the dataset was balanced to 496 observations, comprising equal numbers of stroke and non-stroke cases. Multiple classification algorithms, including decision trees, logistic regression, support vector machines, Naïve Bayes, ensemble methods, and neural networks, were evaluated using 5-fold cross validation. Feature selection methods, including MRMR, Chi square, ANOVA, and Kruskal–Wallis, were subsequently applied to rank the predictors and determine an effective reduced feature set. Among the models using all predictors, Linear SVM achieved the highest cross-validation accuracy of 80.49%. Feature selection demonstrated that a reduced model using only six predictors— age, gender, hypertension, heart disease, average glucose level, and ever-married status— achieved 80.7% validation accuracy and 81.6% test accuracy, providing comparable predictive performance with fewer input variables. Age was consistently identified as the most influential predictor across the feature selection methods. These findings demonstrate that feature selection can substantially reduce the number of variables required for stroke risk prediction without compromising predictive performance, yielding a simpler and more interpretable model and providing a basis for further investigation of simplified machine learning approaches for stroke risk assessment

D1R4AL

Bioinstrumentation / Technology, industry and education

Session Chair: Thanate Angsuwatanakul

Time	Paper ID	Presenter	Paper Title
15:45–16:00	1571311854	Chien-Hsin Yao	Minimum-Sensing, Maximum-Inference: A Sensor-Embedding Design Framework for AI-Driven Behavioral Monitoring in Elderly Day Care
16:00–16:15	1571313391	Abbrita Rahman	BrailleMate: Design and Development of a Low-Cost Interactive Braille Learning Device for Visually Impaired Students
16:15–16:30	1571316066	Pikari Fujii	Development of Soft Electrical Artificial Skin for Neonatal Models to Support Bonding Formation
16:30–16:45	1571320700	Kawthar Usamah	Towards Controllable Speech in Tracheoesophageal Prostheses Using Artificial Vocal Folds: Experimental and Computational Analysis
16:45–17:00	1571322950	Shuji Kikuchi	Development of Ion-Selective Hydrogel Droplets for a Composite Droplet Network Battery
17:00–17:15	1571314285	T. Angsuwatanakul	V.View: A Thai-Language Mobile Application with RT-DETR-Based Banknote Recognition for Users with Visual Impairments
17:15–17:30	1571316788	C. Sujimongkol	Mobile Connectivity and Telehealth Awareness: A Bayesian Cross- National Ecological Analysis

1571311854 — Minimum-Sensing, Maximum-Inference: A Sensor-Embedding Design Framework for AI-Driven Behavioral Monitoring in Elderly Day Care

Authors: Chien-Hsin Yao (Feng Chia University & Lumo Co., Ltd., Taiwan); Meng-Han Lee (Taiwan); Hsien- Wei Liao (Feng Chia University & Lumo Co., Ltd., Taiwan); Yu-Hsuan Tseng (National Yunlin University of Science and Technology, Taiwan); Chuan-Hsun Lin and Yue-Der Lin (Feng Chia University, Taiwan)

Abstract: Long-term care (LTC) day care facilities still rely predominantly on manual facilitator observation to document engagement in therapeutic activities, resulting in care records that lack the biomarker fidelity required for AI-assisted care planning. Recent advances in AI-driven behavioral inference-including large language model (LLM)-based reasoning over sparse sensor signals and foundation models trained on large-scale wearable datasets-motivate a different engineering objective: the minimum viable sensing configuration required to support clinically meaningful inference. This paper develops a sensor-embedding design framework grounded in this Minimum-Sensing, Maximum-Inference philosophy. The framework derives embedding requirements from three rehabilitation measurement needs (cognitive response speed, motor execution quality, and rhythmic synchronization), specifies four operational design principles (perceptual transparency, passive acquisition, clinical metric alignment, and environmental robustness), and presents a three-layer embedded-sensing architecture that interfaces with downstream AIoT health-informatics pipelines. A rhythm-based conceptual prototype illustrates the joint satisfiability of the proposed principles and develops the Minimal Viable Sensing Set argument: a single inertial measurement unit may be sufficient in this rehabilitation context. The paper is positioned as a framework- first contribution; prototype implementation and single-site deployment validation with an industry partner in Taiwan are identified as the next stage of empirical work.

1571313391 — BrailleMate: Design and Development of a Low-Cost Interactive Braille Learning Device for Visually Impaired Students

Authors: Abbrita Rahman (Military Institute of Science And Technology, Bangladesh); Jannatul Ferdous Hame, Sithwat Bin Billah Shahed, Saira Binte Awal, Mst Umme Nashitun Haque, Anisha Fairooz Borsha and Tahia Ifreet (Military Institute of Science and Technology, Bangladesh)

Abstract: BrailleMate is a low-cost interactive Braille learning device designed to support independent education for visually impaired learners through synchronized tactile and audio feedback. The system integrates an Arduino Uno, six SG90 servo motors, a DFPlayer Mini audio module, and tactile navigation buttons to generate Braille characters and corresponding audio pronunciations. Performance evaluation demonstrated 95% tactile output accuracy, an average response time of 1.20 ± 0.03 s, and successful independent operation by 75% of visually impaired participants. Developed at a cost of approximately 40 USD, BrailleMate provides an affordable, portable, and accessible solution for beginner-level Braille education.

1571316066 — Development of Soft Electrical Artificial Skin for Neonatal Models to Support Bonding Formation

Authors: Pikari Fujii (Tokyo Institute of Technology, Japan); Wataru Hijikata (Institute of Science Tokyo, Japan)

Abstract: Bonding disorder is a condition in which caregivers experience difficulties forming an attachment with their child, leading to emotional rejection, which in turn affects the child's mental health and increases the risk of abuse. To prevent bonding disorder, the formation of attachment during the perinatal period is considered crucial. In this study, we propose a stretchable artificial skin that can simultaneously measure a mother's stroking force and palm perspiration as a new tool to support bonding formation during the perinatal period. The skin consists of a thin-film sheet composed of a moisture sensitive film and shear force by measuring the voltage changes between electrodes caused by elastomer deformation due to contact, humidity changes due to perspiration, and the resulting changes in capacitance and resistance, A large-area artificial skin was fabricated to verify the principle, demonstrating that compressive force and shear force can be estimated.

1571320700 — Towards Controllable Speech in Tracheoesophageal Prostheses Using Artificial Vocal Folds: Experimental and Computational Analysis

Authors: Kawthar Usamah (Iraq)

Abstract: Total laryngectomy results in the complete removal of the vocal folds. Current tracheoesophageal prostheses (TEPs) lack integrated vocal folds and rely on the passive vibration of the esophageal wall, producing a low-frequency monotonic sound that is often unsuitable, particularly for female users. This study presents a modified TEP design that integrates an artificial vocal fold (AVF) module directly into the prosthesis and evaluates it experimentally and numerically. In bench testing, the device produced a stable tone with a fundamental frequency (f0) ranging from 71 to 250 Hz and an amplitude of up to -14.1 dB. The AVFs were controlled using a pair of stretchable wires to enable basic pitch modulation. Adjustments in the wire tension resulted in frequency shifts of 19 Hz. Spectrogram analysis revealed harmonic patterns similar to those of natural phonation. A 2D fluid-structure interaction analysis performed in COMSOL Multiphysics was used to further characterize the airflow and vibration behavior. The model showed stable opening-closing cycles with AVF displacements of 1-2.6 mm and airflow velocities oscillating between 2.5 and 8.4 m/s. These findings indicate that integrating AVFs into TEPs is feasible and can generate speech like signal.

1571322950 — Development of Ion-Selective Hydrogel Droplets for a Composite Droplet Network Battery

Authors: Shuji Kikuchi and Zugui Peng (Institute of Science Tokyo, Japan); Kenta Shimba (The University of Tokyo, Japan); Yoshitaka Miyamoto (National Center for Child Health and Development, Japan); Tohru Yagi (Institute of Science Tokyo, Japan)

Abstract: Implantable bioelectronic devices require biocompatible power sources capable of long-term operation. To achieve higher power output, we are developing a composite droplet network battery that combines charge-selective hydrogels based on the Donnan exclusion effect with Droplet Interface Bilayers (DIB) incorporating membrane proteins. As a first step toward this goal, this study investigated the performance of the charge-selective hydrogel system. Polyelectrolyte-containing hydrogel droplets were assembled into battery units with either $CaCl_2$ or KCl concentration gradients, and their open-circuit voltages were measured. Electromotive force generation was confirmed in both systems; however, the voltage output and retention were lower than those reported previously. Furthermore, the $CaCl_2$-based battery exhibited superior voltage output and retention compared with the KCl-based battery, which is attributed to differences in ion transport, Donnan exclusion, and droplet interface conditions.

1571314285 — V.View: A Thai-Language Mobile Application with RT-DETR-Based Banknote Recognition for Users with Visual Impairments

Authors: Thanate Angsuwatanakul (Rangsit University, Thailand); Thapanee Khemanuwong (King Mongkut's Institute of Technology Ladkrabang, Thailand); Ekkapon Phairot (Songkhla Rajabhat University, Thailand); Thanaporn Wongbubpha and Puttaraporn Tananon (Rangsit University, Thailand); Pattanida Sodabun (King Mongkut's Institute of Technology Ladkrabang, Thailand)

Abstract: Visual impairment can substantially limit independent daily activities, particularly the identification and management of paper currency. In Thailand, visually impaired individuals often rely on family members, caregivers, or the public during financial transactions, potentially reducing privacy, confidence, and autonomy. Although assistive technologies are increasingly available, few are tailored to Thai-language users or designed to recognize Thai banknotes within an integrated mobile platform. This study presents V.View, a

Thai-language mobile assistive application that uses artificial intelligence-enabled computer vision to support visually impaired individuals. The application includes obstacle detection, banknote recognition, color identification, face recognition, and text reading. This paper focuses on the Thai Banknote Recognition Module, developed to promote independent financial management. The module applies the Real-Time Detection Transformer (RT-DETR) to detect and classify Thai banknotes captured through a smartphone camera. Recognized denominations are aggregated, and the total value is communicated through real-time Thai voice feedback. RT-DETR was selected for its end-to-end detection capability, absence of post-processing requirements such as Non-Maximum Suppression, and balance between detection accuracy and inference speed. The system was evaluated using five Thai banknote denominations: 20, 50, 100, 500, and 1,000 THB. It achieved 100% accuracy in classifying individual banknotes and 90% accuracy in calculating the total value of multiple banknotes. A preliminary usability evaluation with a visually impaired participant also indicated that the application was practical and accessible. These findings demonstrate the potential of Thai-language AI-powered assistive technologies to enhance financial autonomy, accessibility, and autonomous living while reducing reliance on external assistance.

1571316788 — Mobile Connectivity and Telehealth Awareness: A Bayesian Cross- National Ecological Analysis

Authors: Chinakorn Sujimongkol (Praboromarajchanok Institute, USA); Sukhontip Arunkamonphat (Praboromarajchanok Institute, Thailand)

Abstract: Background: Telehealth adoption depends not only on service availability but also on public awareness. Mobile connectivity may serve as a foundational infrastructure enabling population access to digital health information; however, its relationship with telehealth awareness across countries remains poorly characterized. Objective: To examine the association between national mobile connectivity and telehealth awareness using a Bayesian cross-national ecological framework. Methods: Country-level telehealth awareness estimates were assembled for twelve countries from seven population-based reports published between 2022 and 2024 across low-, middle-, and high-income countries. Mobile connectivity was measured using mobile cellular subscriptions per 100 population obtained from the World Bank World Development Indicators database. Telehealth awareness proportions were transformed to the logit scale, and country-specific measurement variances were derived from reported confidence intervals. Associations were evaluated using both frequentist weighted ecological regression and Bayesian ecological regression incorporating observation-level uncertainty. Results: Telehealth awareness ranged from 2.2% to 78.0%, whereas mobile connectivity ranged from 80.6 to 173.2 subscriptions per 100 population. Pearson correlation analysis demonstrated a moderate positive association between mobile connectivity and telehealth awareness ((r = 0.553), (p = 0.062)). In the weighted ecological regression model, mobile connectivity was positively associated with telehealth awareness after adjustment for income classification ((β = 1.127), 95% CI: 0.346-1.908, (p = 0.010)). Bayesian ecological regression yielded a posterior mean effect of 0.768 (95% CrI: 0.137-1.367). OR = 2.26 (95% CrI: 1.15-3.93). Income classification did not demonstrate a consistent independent association with telehealth awareness. Conclusions: Higher mobile connectivity was consistently associated with greater telehealth awareness across countries. These findings suggest that telecommunications infrastructure may contribute to population-level digital health readiness, although infrastructure alone is unlikely to be sufficient for telehealth adoption. Future research using larger country samples and individual-level data is warranted.

D2R1ML

Medical Image Processing II

Session Chair: Timothy Gale

Time	Paper ID	Presenter	Paper Title
10:45–11:00	1571318846	Jidapa Prakobpol	Spine X-Ray Image Analysis for Scoliosis Severity Detection Using YOLO
11:00–11:15	1571320378	V. Semshchikov	Intervention-Aware Hand Landmark Analysis for Reliable Video-Based Respiratory Monitoring of Preterm Infants
11:15–11:30	1571320520	Koki Ito	A Numerical Study of Novel X-ray CT Reconstruction using Scattered-Photon Information
11:30–11:45	1571321812	Kitsada Thadson	Chest X-Ray Image Analysis of Lung Segmentation using YOLO
11:45–12:00	1571321819	Jaturon Umken	Investigation of Microscopic Image Annotation Effects on Urinary Sediment Detection Using YOLO and Image Enhancement Techniques
12:00–12:15	1571321826	Thazin Bo Bo	A YOLOv8-OBB and Deep Learning Framework for Bone Mineral Density Estimation and Osteoporosis Screening from Lumbar Spine X-ray Images
12:15–12:30	1571322071	Napat Naowarangsee	Edge-Embedded LiDAR Point-Cloud Posture Classification toward Pressure Ulcer Prevention in Bedridden Patients

1571318846 — Spine X-Ray Image Analysis for Scoliosis Severity Detection Using YOLO

Authors: Jidapa Prakobpol (Satriwithaya school, Thailand); Jaruporn Rakkasikorn (Satriwithaya School, Thailand); Suejit Pechprasarn and Kitsada Thadson (Rangsit University, Thailand)

Abstract: Scoliosis is a spinal deformity characterized by an abnormal lateral curvature of the spine. Early diagnosis is crucial to prevent disease progression, but manual interpretation of spinal X-ray images is time-consuming and depends on clinical expertise. This study proposes an automated scoliosis severity detection approach using the You Only Look Once (YOLO) object detection framework. Three YOLO architectures (YOLOv8, YOLOv11, and YOLO26) with Nano (n) and Medium (m) variants were evaluated on a balanced four-class dataset (healthy, mild, moderate, and severe). The dataset was split into training (85%), validation (10%), and testing (5%), and all models were trained for 100 epochs under identical conditions. Performance was assessed using Precision, Recall, F1-score, mAP50, and mAP50-95. Results showed that YOLOv8n achieved the highest validation performance (mAP50: 79.99%, mAP50-95: 54.39%). On the test set, YOLO26m achieved the highest mAP50 (75.57%), while YOLOv8n obtained the highest mAP50-95 (47.77%) and Recall (84.53%). YOLO11m achieved the highest F1-score (73.61%), demonstrating the best balance between Precision and Recall. These results indicate that modern YOLO models provide reliable performance for automated scoliosis severity detection and show strong potential for computer-aided diagnosis in clinical practice.

1571320378 — Intervention-Aware Hand Landmark Analysis for Reliable Video-Based Respiratory Monitoring of Preterm Infants

Authors: Vladimir Semshchikov, Gale J Timothy and Peter Dargaville (University of Tasmania, Australia)

Abstract: Reliable respiration-from-video in the neonatal intensive care unit requires automatic rejection of intervals corrupted by caregiver handling. This paper presents a hand- centric intervention detector for long-duration video of preterm infants. MediaPipe hand landmarks are estimated from RGB and channel-swapped BGR views, converted into a Hand Skeleton Length descriptor, and adaptively separated into infant- and adult-sized detections using a two-component Gaussian mixture model. Frame-level detections, obtained on every tenth video frame, are post-processed into clinically interpretable care-event intervals by cutoff filtering and gap-based temporal merging. In an annotated subset of the PANDA (Prediction AND novel Detection of Apnoea in preterm infants) study, hand-presence detection achieved precision 0.93, recall 0.89, F1-score 0.91, and AUROC 0.95; size-based filtering achieved balanced accuracy 0.90 and reduced false intervention flags by 27% relative to a fixed-threshold baseline. The module provides an interpretable quality gate for neonatal vision-based respiratory monitoring.

1571320520 — A Numerical Study of Novel X-ray CT Reconstruction using Scattered-Photon Information

Authors: Koki Ito, Tatsuya Oshitani, Yoichi Yamazaki and Naohiro Toda (Aichi Prefectural University, Japan)

Abstract: In this study, we investigate the effectiveness of scattered-photon information on X-ray CT reconstruction based on a probabilistic photon-transport model that incorporates both crosstalk and photoelectric absorption. We first consider a previously established theorem showing that scattering-location-resolved photon counts can reduce the variance of attenuation-coefficient estimates under ideal measurement conditions. Then, we build an X-ray transport simulation for the two-dimensional measurement system assumed in the theoretical analysis, enabling evaluation of the effects of scattering, and use it to quantitatively analyze how various error factors expected in realistic measurement environments affect the estimation errors. The results suggest that scattered-photon information can significantly improve estimation accuracy under conditions of low crosstalk. Utilizing scattered-Xrays may present a new direction

1571321812 — Chest X-Ray Image Analysis of Lung Segmentation using YOLO

Authors: Kitsada Thadson (Rangsit University, Thailand); Kanokpich Thavornthammarit (Satriwithaya School, Thailand); Suejit Pechprasarn (Rangsit University, Thailand)

Abstract: Lung segmentation in X-Ray images plays an important role in supporting several diagnoses and clinical decisions. Advancements in state-of-the-art deep learning techniques significantly improve segmentation performance and reduce time consumption. You Only Look Once (YOLO), a full-pipeline object detection and segmentation framework developed by Ultralytics, has recently demonstrated its potential across various fields, including medical image analysis. This study proposed lung segmentation using various YOLO versions and sizes, evaluating both segmentation performance and computational efficiency. The results show that YOLOv8m achieved the highest segmentation performance among the investigated models, including YOLO11, the typical YOLO segmentation version, and YOLO26, the latest YOLO advancement with the promise of optimal computational requirements. Additionally, the shortest inference latency was achieved with the lightweight YOLO nano versions, at the cost of a slight decrease in performance. To summarize, all interest models perform outstandingly for lung segmentation in X-Ray images, with both performance and latency, at a small trade-off across different architecture scales.

1571321819 — Investigation of Microscopic Image Annotation Effects on Urinary Sediment Detection Using YOLO and Image Enhancement Techniques

Authors: Jaturon Umken, Sainaw Lin, Chanatip Khiewpanya, Suejit Pechprasarn and Kitsada Thadson (Rangsit University, Thailand)

Abstract: In automated urinary sediment analysis, deep learning models rely heavily on comprehensively annotated datasets. However, clinical datasets frequently suffer from under-annotation due to the sheer volume of micro-structures, such as erythrocytes and crystals, and the time constraints of human experts. This study investigates the hard performance limits imposed by incomplete ground-truth annotations on object detection models. We hypothesize that algorithmic precision is artificially capped by under-annotation, as valid morphological detections are penalized as false positives. To test this, models were trained on a deliberately under-annotated urinary sediment dataset and subjected to extensive image preprocessing and augmentation pipelines- including unsharp masking, adaptive thresholding, and grayscale conversion-designed to maximize feature visibility. Results indicate that, despite theoretical improvements in visual clarity, precision metrics did not improve. While preprocessing successfully amplified subtle particles, the absence of corresponding ground-truth references forced these valid predictions to be classified as errors. This study demonstrates that advanced preprocessing cannot rescue a fundamentally flawed ground truth, underscoring the need for exhaustive annotation validation before algorithmic optimization in medical computer vision.

1571321826 — A YOLOv8-OBB and Deep Learning Framework for Bone Mineral Density Estimation and Osteoporosis Screening from Lumbar Spine X-ray Images

Authors: Thazin Bo Bo, Aung Thein Htet, Aye Chan Myae, Suejit Pechprasarn and Kitsada Thadson (Rangsit University, Thailand)

Abstract: This study presents a framework for bone mineral density estimation and osteoporosis screening from lumbar spine X-ray images using YOLOv8n-You Only Look Once with oriented bounding box detection and deep learning-based regression. The proposed framework detects lumbar vertebrae L1-L4 and spinal implant regions, extracts vertebra-level and implant-related features, predicts bone mineral density using EfficientNet-B0, ResNet50, and DenseNet121, and converts the predicted bone mineral density into T-score-based osteoporosis categories. The YOLOv8n oriented bounding box detector achieved a mean average precision of 0.8611 at an intersection over union threshold of 0.5 and 0.7749 across thresholds from

0.5 to 0.95. During training, DenseNet121 achieved the best performance with a root mean squared error of 0.1329 and a coefficient of determination of 0.4847. EfficientNet-B0 achieved the best image-level performance with an accuracy of 82.72 percent and a macro- averaged F1 score of 0.8285, while ResNet50 achieved the best patient-level performance with an accuracy of 84.72 percent and a macro-averaged F1 score of 0.8501. These findings demonstrate that patient-level aggregation improves osteoporosis screening performance and that bone mineral density estimation provides an interpretable pathway from lumbar spine X-ray images to clinically meaningful score predictions.

1571322071 — Edge-Embedded LiDAR Point-Cloud Posture Classification toward Pressure Ulcer Prevention in Bedridden Patients

Authors: Napat Naowarangsee and Anak Khantachawana (King Mongkut's University of Technology Thonburi, Thailand); Sornkitja Boonprong (Faculy of Social Sciences, Thailand)

Abstract: Pressure ulcers affect an estimated 10 to 40 percent of bedridden elderly patients and impose a substantial healthcare burden. The established preventive measure, repositioning every two hours, is frequently missed under chronic caregiver shortages. Existing monitoring technologies remain inadequate: pressure-sensing mats require physical contact, RGB-D cameras depend on ambient light and raise privacy concerns, and vision-based skeleton estimation degrades substantially under blanket occlusion. A monitor that classifies lying posture directly from LiDAR depth point clouds runs entirely on a sub-USD-100 Raspberry Pi 5 edge device, with no network dependency; the approach is non-contact and privacy-preserving. A bedside solid-state LiDAR sensor (Intel RealSense L515), mounted obliquely, feeds a calibrated processing pipeline: empty-bed plane fitting, region-of-interest extraction, voxel downsampling, two-stage outlier removal, and subsampling to a fixed 1,024 points. The resulting point cloud is classified by a PointNet network into supine, left-lateral, and right-lateral postures. On a held-out test set of 300 samples drawn from the same two volunteers, the model attains a within-subject accuracy of 93.33 percent and a 0.932 macro- averaged F1-score, though right-lateral recall is the weakest at 0.80. An 8-bit quantized model executes in 15.6 ms per inference on the device. Raw color frames are never stored; only an abstract skeleton overlay is displayed, and an alert is raised when a posture persists for at least two hours. Active infrared illumination enables operation in complete darkness. These results demonstrate the feasibility of edge-deployed LiDAR posture monitoring for pressure ulcer prevention as a proof of concept.

D2R2ML

Biomedical Signal Processing II

Session Chair: Limpiti Tulaya

Time	Paper ID	Presenter	Paper Title
10:45–11:00	1571322952	Yuxin Liu	Behavioral Effects of Face-Mask Occlusion in a Six-Expression Recognition Task with Exploratory ROI-Based Evoked Potential Analysis
11:00–11:15	1571322973	Haruto Hamada	Decoding Speech Imagery via Listening-based Training for Speech BCIs
11:15–11:30	1571322994	Ayaka Choki	Relationship Between Structural Properties of the Visual Pathway and Motion-Onset Visual Evoked Potentials
11:30–11:45	1571323336	Chotipong Sakorn	Cross-Domain Generalization and Spectral Similarity Between Emotion and Odor-Evoked EEG
11:45–12:00	1571323653	Ahmed Safari	A Low-Cost SSVEP Brain-Computer Interface on Consumer EEG: Within-Subject Accuracy and a Cross-Session Transfer Case Study
12:00–12:15	1571323714	Ryunosuke Kirita	Conventional Band Power and Spectral Parameterization for Classifying Stroop and Analytical Tasks Across Participants
12:15–12:30	1571324679	Mehwish Moiz	Large-Scale Wrist-Worn Monitoring Reveals High Adherence and Diurnal Activity Fingerprints in People with Parkinson's Disease

1571322952 — Behavioral Effects of Face-Mask Occlusion in a Six-Expression Recognition Task with Exploratory ROI-Based Evoked Potential Analysis

Authors: Yuxin Liu, Baijun Song, Saori Nishikawa and Tomohiko Igasaki (Kumamoto University, Japan)

Abstract: This study investigated the effects of face-mask occlusion on facial expression recognition within the present stimulus set using behavioral measures and an exploratory region-of-interest (ROI)-based evoked-potential analysis. Fifteen healthy right-handed participants performed a six-expression recognition task under masked and unmasked conditions. Recognition accuracy was analyzed using a random- intercept binomial mixed model, whereas response times were analyzed using participant-level medians calculated from correct trials. Accuracy showed significant effects of Mask Condition and its interaction with Emotion, with Bonferroni-corrected reductions for sad and disgusted faces. Response time showed a significant effect of Mask Condition and a significant Mask Condition × Emotion interaction, with Bonferroni-corrected increases in response time for happy and sad faces. Neither the Mask Condition effects across the eight ROI/time-window measures nor the eight Mask Condition × Emotion interactions survived Benjamini-Hochberg correction. Preliminary sex-related comparisons also yielded no effects that survived correction for multiple comparisons. Thus, face-mask occlusion was associated with expression-dependent behavioral differences within the present stimulus set, whereas the evoked-potential findings remained exploratory.

1571322973 — Decoding Speech Imagery via Listening-based Training for Speech BCIs

Authors: Haruto Hamada (Institute of Science Tokyo, Japan); Zhuohao Zhang, Phurin Rangpong and Akima Connelly (Tokyo Institute of Technology, Japan); Zugui Peng and Tohru Yagi (Institute of Science Tokyo, Japan)

Abstract: In conventional speech BCIs, the speech imagery task required to acquire training data imposes a substantial burden on participants. In this study, we investigated the feasibility of decoding imagined speech by using EEG signals during listening, which impose a lower burden, as training data. EEG signals during listening and imagery were compared for the Japanese vowel syllable /a/ and consonant-vowel syllable /ka/ using ERSP-based topographic maps. We also constructed a machine learning model using FBCSP and SVM, compared the classification accuracy of a method using listening EEG as training data (L→I) with that of a conventional method using imagery EEG only (I→I), and explored electrode regions contributing to classification accuracy. The results showed that ERD was observed in the right frontal region in the 16-20 Hz band during /a/ imagery. In addition, several frequency bands showed no significant differences in brain activity between the listening and imagery tasks, suggesting the possible existence of features shared between the two tasks. Although classification accuracies using all 19 channels remained near chance level for both L→I and I→I, with no significant difference between them, the L→I condition tended to outperform the I→I condition in the right temporal region. These results suggest a certain potential for speech BCIs using listening EEG.

1571322994 — Relationship Between Structural Properties of the Visual Pathway and Motion-Onset Visual Evoked Potentials

Authors: Ayaka Choki, Masato Sugino, Hiroki Ishii, Kenta Shimba and Kiyoshi Kotani (The University of Tokyo, Japan); Shota Arakawa (The University of Tokyo Hospital, Japan); Kazuki Endo (Japan); Yuichi Suzuki (The University of Tokyo Hospital, Japan); Shiori Amemiya (Japan)

Abstract: While it is known that a positive correlation exists between neural fiber length within lesions and the latency of evoked potentials, it remains unclear whether structural transmission delays also occur in healthy human neural fibers. In this study, we combined diffusion MRI tractography with electrode-level analysis and source estimation of the motion-onset visual evoked potential (mVEP) to examine the relationship between fiber length, fiber density, and electrophysiological indices in the healthy visual pathway. The results showed a moderate correlation between N2 latency and fiber length, and a strong correlation between peak latency obtained from middle temporal (MT) source estimation and fiber length, indicating that transmission delay increases with fiber length. In addition, a strong negative correlation was observed between intracellular volume fraction (ICVF) and the P1-N2 amplitude difference, with a larger ICVF associated with a smaller amplitude difference. These findings demonstrate that, even in the healthy visual pathway, individual differences in anatomical fiber length and fiber density are reflected in the latency and amplitude of mVEP; in particular, the relationship between fiber length and transmission latency along the direct thalamus-MT pathway supports the presence of transmission delays in neural fibers. On the other hand, the interpretation of N2 latency and the relationship between ICVF and amplitude may involve more complex mechanisms, warranting further investigation.

1571323336 — Cross-Domain Generalization and Spectral Similarity Between Emotion and Odor-Evoked EEG

Authors: Chotipong Sakorn (KMITL, Thailand); Tulaya Limpiti (King Mongkut's Institute of Technology Ladkrabang, Thailand)

Abstract: Olfactory stimuli are often associated with distinct emotional responses that are measurable using EEG systems. However, research on olfactory EEG and emotional- state EEG are usually conducted separately; the inherent relationship between odor- evoked EEG and emotion EEG has not been studied directly. This study investigates a cross-domain framework between emotion-related and odor-evoked brain responses, treating emotion EEG as the source domain and odor-evoked EEG as the target domain. Four emotion classes (HVHA, HVLA, LVHA, LVLA) are analyzed alongside four odor conditions (Lemon, Rosewater, Smoke, Valerian). Relationships between the two domains are quantified using PSD-based Pearson correlation and STFT-based SSIM. The results confirm the predefined odor-emotion mappings, with predicted pairs exhibiting stronger similarity than non-corresponding pairs. Three classification strategies-SVM-RBF with late fusion, DANN, and Conformer-are evaluated via five-fold cross-validation on within-domain emotion EEG (98.0%, 94.1%, and 98.9% accuracy, respectively) and cross-domain testing on odor EEG. The cross- domain performance degrades to 83.0% for SVM and 85.0% for DANN, with Conformer achieving the best generalization at 93%. Since the two domains originate from independently acquired datasets, results are interpreted as evidence of transferable spectral characteristics under the predefined mapping rather than validated universal neurophysiological associations.

1571323653 — A Low-Cost SSVEP Brain-Computer Interface on Consumer EEG: Within-Subject Accuracy and a Cross-Session Transfer Case Study

Authors: Ahmed Safari (University of Doha for Science and Technology, Qatar); Oussama Djedidi (UDST, Qatar); Bekir S Çiftler (University of Doha for Science and Technology, Qatar); Rouaa Mohamed Naim (Hamad Bin Khalifa University, Qatar)

Abstract: Consumer-grade EEG headsets lower the cost of brain-computer interfaces (BCIs) enough to use them outside the clinic, but their real-world ceiling is rarely characterized beyond a single within-subject accuracy number. We build a low-cost, non-invasive Steady-State Visual Evoked Potential (SSVEP) BCI on the eight-channel Neurosity Crown and evaluate it under three increasingly strict protocols: per-subject cross-validation on 31 subjects (predictions pooled across subjects for reporting), leave-one- subject-out (LOSO), and a single held-out participant tested across three separate recording sessions. A systematic grid of seven feature representations and eight classifiers identifies filter-bank canonical correlation analysis with Riemannian tangent- space covariance features (FBCCA+Riemann) as the consistent winner, reaching about 74 % four-class accuracy ($\kappa \approx 0.65$, ITR $\approx$ 45 bpm) within subject under blocked, leakage-controlled cross-validation. The same pipeline collapses to 32.8 % under LOSO. For that held-out user, about 3 min of same-session calibration reaches within- subject-level accuracy (77.8 % on four test files), but it does not persist: a model calibrated in one session falls to chance days later, with a clean octave-flip error pattern,

while pooling sessions never beats same-session calibration. The practical consequence is a concrete deployment recipe: ship a pooled warm-start model, require a short per-session calibration block, and gate on signal quality. All processing runs in a modular web application with roughly 1.2 s end-to-end latency.

1571323714 — Conventional Band Power and Spectral Parameterization for Classifying Stroop and Analytical Tasks Across Participants

Authors: Ryunosuke Kirita (Kumamoto University, Japan); Swarubini PJ (IIT Hyderabad, India); Krushna Devkar (Indian Institute of Technology, Hyderabad, India); Nagarajan Ganapathy (IIT Hyderabad, India); Tomohiko Igasaki (Kumamoto University, Japan)

Abstract: EEG-based cognitive-state assessment has primarily focused on classifying workload intensity, although distinguishing task conditions that emphasize different cognitive demands may provide additional information for task-adaptive support. This study examined whether conventional, periodic, and aperiodic EEG spectral features could distinguish the Stroop and analytical task conditions in previously unseen participants. Nineteen-channel EEG was recorded from 30 healthy participants during 300-s task periods. Conventional log and relative band power, aperiodic offset and exponent, and periodic peak features were compared using within-participant statistics and repeated participant-grouped five-fold cross-validation. Stroop showed broadly higher alpha relative power, aperiodic offset, and aperiodic exponent, together with higher aperiodic-adjusted alpha and beta peak power. In contrast, conventional beta log and relative power were higher during the analytical task. Thus, the direction of the beta-band difference depended on whether the aperiodic spectral background was included in the power estimate. Conventional plus aperiodic features achieved the highest observed performance with a linear SVM (accuracy: 0.755 ± 0.041; F1: 0.753 ± 0.041; κ: 0.510 ± 0.082) but did not significantly outperform conventional power alone. Under the present fixed-order protocol, conventional power provided strong cross-validated predictive information, whereas periodic-aperiodic separation clarified the spectral components associated with the two task conditions.

1571324679 — Large-Scale Wrist-Worn Monitoring Reveals High Adherence and Diurnal Activity Fingerprints in People with Parkinson's Disease

Authors: Mehwish Moiz (University of New South Wales, Australia); Charlotte Lang (ETH Zurich - Institute for Biomechanics, Switzerland); Lloyd Chan (University of New South Wales, Australia); Yoshiro Okubo (Neuroscience Research Australia, Australia); Stephen Lord (Neuroscience Research Australia, Sydney, Australia); Ahmadreza Argha and Frederic Von Wegner (University of New South Wales, Australia); Deepak K. Ravi (ETH Zurich - Institute for Biomechanics, Switzerland); Matthew Brodie (University of New South Wales, Australia)

Abstract: Wrist-worn activity monitors provide opportunities for large-scale remote monitoring of Parkinson's disease (PD), but utility depends on participant adherence and sensitivity to disease and medication related changes that may fluctuate by time of day. This study investigated wear-time adherence, diurnal activity fingerprints, and active-hour thresholds using UK Biobank wrist accelerometry data. Wear-time adherence was higher in people with PD at Baseline [n=116] and Incident PD [n=343] as compared to Control participants [n=101,364] (mean 22.0 and 21.8 vs 19.6 hours/day, p=0.01). For activity analyses, the group with PD at Baseline were matched (1:10) with Controls for age, sex and wear time. Hourly step counts were used to generate weekday-hour fingerprint heatmaps, and linear mixed-effects models were used to assess group differences. Both groups exhibited bimodal profiles with primary activity peaks around 11AM and secondary peaks around 2PM. PD participants had reduced activity compared with Controls (228.5 vs 316.6 steps/hour) with significant Day, Hour-of-Day, and Group × Hour effects (all $p < 0.001$). Sensitivity analyses demonstrated that active- hour thresholds in the range of 15-100 steps/hour may reduce false-positive step detection during resting hours with minimal information loss. Collectively, these findings demonstrate that wrist-worn monitoring is highly acceptable to people with PD and can capture informative diurnal activity fingerprints at scale, providing a strong foundation for future development of wearable-derived digital biomarkers for remote disease monitoring and progression tracking.

D2R3ML

Healthcare information II / Biosensors I

Session Chair: Suzuki Seiichi

Time	Paper ID	Presenter	Paper Title
10:45–11:00	1571315562	Suzuki Seiichi	The Effect of Antibody Structure and BSA Coating of Coverslip on The Sensitivity of Fluorescence Anisotropy Immunosensor
11:00–11:15	1571322306	Krittaphat Inparot	Design and Optimization of the Fabrication Process for a Biomimetic Lung-on-a-Chip Structure with Microliter-Scale Flow Control
11:15–11:30	1571315325	Sadah Lahad	Design and Fabrication of a Hollow Microneedle Platform for Interstitial Fluid Collection Using Stereolithography 3D-printing
11:30–11:45	1571321238	C. Phiphattanaphiphop	Geometry-Dependent Bubble Suppression in SU-8/PDMS Micropillar Microchannels for Cell-Size-Compatible Culture Platforms
11:45–12:00	1571315633	C. Shiraishi	Three-Dimensional Printed Droplet Microfluidic System for Studying Kidney Stone Crystallization
12:00–12:15	1571316058	Sung Soo Lee	Restoring Tool-Tissue Force Awareness in Robotic Surgery: A Modeling-Driven Biaxial Capacitive Force Sensor for Surgical Haptics
12:15–12:30	1571316787	N. Vongmanee	Effect of Functional Monomers on Molecularly Imprinted Polymer- Based Detection of Serratia marcescens

1571315562 — The Effect of Antibody Structure and BSA Coating of Coverslip on The Sensitivity of Fluorescence Anisotropy Immunosensor

Authors: Suzuki Seiichi, Hao Konishi, Christine D.A.P. Wiyono, Motohiro Akashi and Shigeru Kato (Seikei University, Japan)

Abstract: In this study, sensitivity and detection limit of fluorescence anisotropy immunosensor (FAI) was investigated in relation with the characteristics of antibody molecule. The rapid expansion of air transportation has increased the risk of infectious diseases spreading over the world[1], and fast and simple diagnostic methods for multiple pathogen detection is desired. Conventional immuno-assay tests, such as ELISA or lateral flow tests, are reliable and easy enough for commercial use, but target pathogen is confined to one or some common diseases. On the other hand, immunosensors, such as surface plasmon resonance (SPR)[2] or ion sensitive field effect transistor (ISFET)[3] sensors are highly sensitive but not for multiple target detection. To attend this issue, we have proposed FAI, which detect the antigen binding by the molecular motion change[4]. Theoretically FAI sensor is robust to the surface adsorption of nonspecific molecule, which enables multiple pathogen target on single sensor substrate. We investigated the sensing response of antibody molecules derived from 3 different animal species. BSA coating of coverslip was also investigated to evaluate the adsorption of target antigen on the sensor surface.

1571322306 — Design and Optimization of the Fabrication Process for a Biomimetic Lung-on-a-Chip Structure with Microliter-Scale Flow Control

Authors: Krittaphat Inparot and Chalinee Phiphattanaphiphop (Chiang Mai University, Thailand); Rungrueang Phatthanakun (Synchrotron Light Research Institution (SLRI), Nakhon Ratchasima, Thailand)

Abstract: This paper presents the design, fabrication, and process optimization of a low-cost, biomimetic Lung-on-a-Chip platform for biomedical research. To minimize manufacturing costs and avoid the flow limitations of conventional rectangular channels, we developed a fabrication workflow using AZ P4620 thick-film positive photoresist on standard glass slides. A symmetrical, lung-inspired network with branched airways and bifurcated chambers was evaluated across small, medium, and large dimensional scales to determine the best configuration for lithographic development and operational stability. Experimental results showed that under a uniform UV exposure dose, the medium-scale design (900-µm channel width, 150-µm wall thickness) provided the fastest development kinetics, clearing residual photoresist within 2 minutes. However, fluid perfusion tests indicated that the small-scale architecture (750-µm channel width) delivered the highest mechanical integrity and hydrodynamic stability under continuous flow. Furthermore, 3D computational fluid dynamics (CFD) simulations confirmed that post-development thermal reflow successfully reshaped the rectangular channels into rounded semicircular profiles with horizontal partition barriers, eliminating fluid dead zones. Fluid analysis showed a stable laminar flow with a Reynolds number of 0.48. Although geometric constraints at narrow channel boundaries generated a localized peak wall shear stress of 1.32 Pa (13.2 dyn/cm^2), the shear stress across the main functional exchange interfaces remained well

within the safe physiological range of 1.9 to 2.4 dyn/cm^2. This optimized microfluidic platform serves as a practical and affordable tool for respiratory disease modeling and in vitro toxicological studies.

1571315325 — Design and Fabrication of a Hollow Microneedle Platform for Interstitial Fluid Collection Using Stereolithography 3D-printing

Authors: Sadah Lahad, Kewarin Phonklam and Tonghathai Phairatana (Department of Biomedical Sciences and Biomedical Engineering, Faculty of Medicine, Prince of Songkla University)

Abstract: Interstitial fluid (ISF) has emerged as a promising biofluid for minimally invasive monitoring owing to its rich biomarker content and strong correlation with blood composition. Hollow microneedles (HMNs) provide a direct fluidic pathway for ISF sampling while minimizing tissue damage. In this study, side-opening HMN arrays were fabricated using stereolithography (SLA)-based 3D printing for capillary-driven ISF collection. HMNs with a fixed height of 1500 µm and designed side-opening diameters of 300, 400, and 500 µm were fabricated and characterized by scanning electron microscopy. Surface wettability was further enhanced by polydopamine (PDA) coating, and its effect on fluid transport was evaluated. The results demonstrated that the side- opening diameter significantly affected fabrication quality. The 300 µm design exhibited complete lumen blockage, whereas the 400 and 500 µm designs produced unobstructed channels with dimensional deviations below 10%. Although the 500 µm design showed the highest fabrication fidelity, the 400 µm HMN provided the optimal balance between reliable channel formation and capillary-driven fluid transport. PDA coating significantly improved surface hydrophilicity, promoting spontaneous liquid uptake through the hollow channels. The optimized HMNs successfully extracted fluid from an agarose model and effectively penetrated an artificial skin model, demonstrating their potential for minimally invasive ISF sampling. These findings highlight the feasibility of PDA-coated, SLA-fabricated side-opening HMNs as a simple and cost-effective platform for future ISF collection and biomarker monitoring applications.

1571321238 — Geometry-Dependent Bubble Suppression in SU-8/PDMS Micropillar Microchannels for Cell-Size-Compatible Culture Platforms

Authors: Chalinee Phiphattanaphiphop (Chiang Mai University, Thailand); Tuntita Arrayatiraputtitorn (Chiangmai University, Thailand)

Abstract: Bubble formation presents a critical bottleneck in microfluidic platforms, particularly for long-term cell culture applications, where gas-liquid interfaces can induce detrimental shear stress, disturb the microenvironment, and cause cell death. To address this challenge, this study investigates the geometry-dependent bubble suppression efficiency of SU-8/PDMS microchannels embedded with various micropillar configurations. Microchannels featuring five distinct micropillar arrays (Patterns A-E) were designed and fabricated using UV-lithography and PDMS soft lithography. The fluid dynamic behavior and bubble trapping capabilities were evaluated under creeping-flow conditions (Re = 0.577) at a constant flow rate of 10 µL/min. Quantitative analysis revealed that geometric layout and structural spacing significantly influence bubble retention. Pattern C exhibited the highest vulnerability to bubble accumulation, yielding an average bubble area of 0.201 cm2 and a Sauter mean diameter (d32) of 5.063 mm. Pattern A showed moderate retention with an average area of 0.043 cm2 and a d32 of 2.337 mm. In contrast, Patterns B and D effectively mitigated bubble expansion, substantially reducing the d32 to 0.924 mm and 0.852 mm, respectively. Complete elimination of residual bubbles (d32= 0mm) was achieved in Pattern E due to its high-density pillar configuration. Considering cellular expansion requirements, while the confined geometry of Pattern E (100 µm channel width) is suitable for smaller cells, Pattern D offers the most viable compromise for larger cell cultures by providing sufficient spatial clearance while maintaining robust bubble suppression.

1571315633 — Three-Dimensional Printed Droplet Microfluidic System for Studying Kidney Stone Crystallization

Authors: Chutikarn Shiraishi (Chulalongkorn University, Thailand); Thammawit Suwannaphan (King Mongkut's University of Technology North Bangkok Bangkok, Thailand); Chanchai Boonla, Natcha Madared and Alongkorn Pimpin (Chulalongkorn University, Thailand)

Abstract: Kidney stone disease is a global health problem. The predominant type of kidney stone generally found in the form of calcium oxalate (CaOx) approximately 80% of all cases. CaOx occurs mainly as calcium oxalate monohydrate (COM) or dihydrate (COD). Detection of crystal at an early stage could help predict the risk of kidney stone formation before symptoms occur. This research developed a 3D-printed droplet microfluidic system to investigate CaOx crystallization. The devices were fabricated by stereolithography (SLA), using the Biomed Clear resin with channel cross section of 1 mm × 1 mm. Calcium chloride ($CaCl_2$) dissolved in artificial urine and sodium oxalate ($Na_2C_2O_4$) solutions were introduced through two separated inlets and merged in a continuous oil phase to form individual droplets. This study focused on the design of

the storage chamber using a buoyancy principle, comparing tapered chambers of 2, 4 and 6 mm to accumulate the precipitated crystals. Raman spectroscopy was used to detect the precipitate in the storage chamber. The results showed that the 6 mm chamber produced a greater amount of precipitate than the 2 and 4 mm chambers. In all cases, the wet precipitate was thinly distributed at the bottom of the chamber floor, and the amount of precipitate was not sufficient to be detected by Raman spectroscopy. For further investigation, when the collected samples were analyzed in the wet state solution, the Raman spectra exhibited inverted (negative) peaks resulting weak signal. On the other hand, drying the samples eliminated this inversion. This finding indicates that the collected crystals should be dried before Raman measurement to obtain correctly oriented characteristic peaks.

1571316058 — Restoring Tool-Tissue Force Awareness in Robotic Surgery: A Modeling-Driven Biaxial Capacitive Force Sensor for Surgical Haptics

Authors: Sung Soo Lee and Bardia Konh (University of Hawaii System, USA)

Abstract: Robotic-assisted minimally invasive surgery improves visualization, dexterity, and motion control, but the lack of direct tool-tissue force awareness remains a major limitation for safe tissue manipulation. This work presents a modeling-driven biaxial capacitive force sensor designed for surgical haptic feedback. The sensor detects normal and shear forces through capacitance changes in a compact Au-PDMS-Au architecture. Normal force is measured from compression-induced reduction of dielectric thickness, while shear force is measured from differential capacitance changes caused by lateral electrode displacement. Analytical models were derived to estimate the normal and shear capacitance-force relationships, and COMSOL Multiphysics simulations were performed to evaluate 3D deformation and electrostatic response. The normal-force analytical model and COMSOL simulation showed sensitivity of approximately 1.08 and 1.80 fF/N, respectively. The shear-force analytical model and COMSOL simulation showed sensitivity of approximately 0.067 and 2.439 fF/N, respectively. The higher simulated sensitivities are expected because the analytical model assumes idealized small-displacement sensing paths with constant dielectric thickness, whereas COMSOL captures the full three-dimensional multi- electrode geometry, nonuniform PDMS deformation, deformation-dependent electrode spacing, and fringing electric-field effects. These results demonstrate the feasibility of the proposed compact biaxial capacitive design and establish a foundation for future fabrication, calibration, and integration with robotic surgical instruments.

1571316787 — Effect of Functional Monomers on Molecularly Imprinted Polymer- Based Detection of Serratia marcescens

Authors: Naphatsawan Vongmanee (King Mongkut's University of Technology Thonburi, Thailand); Konsiri Arttakonsiripo (Track General Health Science, Learn Satit Pattana School, Bangkok, Thailand); Sarinporn Visitsattapongse (King Mongkut's Institute of Technology Ladkrabang, Thailand)

Abstract: Infections caused by Serratia marcescens pose a significant threat to immunocompromised patients due to its resistance to multiple antibiotics and ability to survive in nutrient-deficient environments. Conventional identification methods are often time-consuming and may lack specificity, resulting in delays in diagnosis and treatment. In this study, a molecularly imprinted polymer (MIP)-based biosensor was developed for the selective detection of S. marcescens. Three functional monomers, methacrylic acid, acrylamide and methacrylamide were investigated to evaluate their sensing performance. The methacrylic acid-based polymer exhibited the highest sensitivity, with a slope of 12.32 and an R^2 value of 0.9879. In addition, selectivity tests demonstrated a stronger response toward S. marcescens than toward Staphylococcus aureus, Pseudomonas aeruginosa, and the non-imprinted polymer (NIP). These findings suggest that the developed MIP-based biosensor has potential for the rapid and selective detection of S. marcescens in bacterial sensing applications.

D2R4ML

Healthcare information III

Session Chair: Yoshihiro Tange

Time	Paper ID	Presenter	Paper Title
10:45–11:00	1571304292	Hiranya Sritart	GIS-Based Obesity Surveillance and Risk Mapping: A Framework for Community Health Decision Support
11:00–11:15	1571313298	Seonjae Yun	Preliminary Agreement Between the Olfactory QUEST Protocol (O- QUEST) and the YSK-Threshold Reference for Olfactory Threshold Estimation
11:15–11:30	1571314771	W. Limpornchitwilai	Strategy-Based Behavioral Analytics in a Tablet Memory Game for Interpretable Cognitive Screening in Older Adults
11:30–11:45	1571314776	Wen-Jou Chang	A Digital Health Wallet for Verifiable Cross-Border Exchange of HL7 FHIR International Patient Summary
11:45–12:00	1571316204	Warin Suttiron	Personalized Healthcare Platform for Health Assessment and Lifestyle Management
12:00–12:15	1571318116	Si-Wei Yang	A Microservice-Oriented Cloud PACS for Unified Web and Traditional DICOM Imaging Workflows
12:15–12:30	1571323346	Prajat Paul	A Comparative Study of Prompt Engineering Strategies for Generative ASR Error Correction in Low-Resource Bangla Healthcare Speech

1571304292 — GIS-Based Obesity Surveillance and Risk Mapping: A Framework for Community Health Decision Support

Authors: Hiranya Sritart, Nattamon Niyomdecha and Somchat Taertulakarn (Thammasat University, Thailand); Kuson Tuntiwong (School of Dentistry King Mongkut's Institute of Technology Ladkrabang, Thailand); Sakiko Kanbara (Kobe City College of Nursing Kobe, Japan)

Abstract: Childhood and adolescent obesity is an increasing public health concern and is associated with long-term risks of noncommunicable diseases, disability, psychosocial consequences, and future healthcare burden. Conventional obesity surveillance often reports prevalence at broad administrative levels, which may be insufficient for identifying local clusters, contextual vulnerability, and area-specific intervention needs. This paper proposes a geospatial healthcare information framework to support area- based obesity surveillance and community health decision-making. The framework integrates health outcome data, population and socioeconomic context, environmental and built environment indicators, spatial analytics, and community decision-support outputs. It also presents an implementation workflow that includes problem definition, stakeholder identification, data acquisition, spatial linkage, indicator construction, spatial analysis, visualization, and translation of evidence risk maps, priority area maps, district risk profiles, and intervention planning outputs. Thailand is used as an illustrative context because childhood obesity is emerging alongside nutrition transition, urbanization, and regional socioeconomic diversity. The framework emphasizes that obesity should not be viewed only as an individual behavioral issue, but also as a spatially embedded public health problem shaped by local environments and social conditions.

1571313298 — Preliminary Agreement Between the Olfactory QUEST Protocol (O- QUEST) and the YSK-Threshold Reference for Olfactory Threshold Estimation

Authors: Seonjae Yun, Wonhoe Gu, YeongJin Son and Wooseop Kim (Neubreze Inc., Korea (South))

Abstract: Olfactory threshold testing is clinically relevant, but conventional staircase procedures can be burdensome for older adults. This preliminary validation study evaluated whether the Olfactory QUEST Protocol (O-QUEST), a QUEST-based adaptive threshold-estimation protocol using an in-house Phenyl-Ethyl Alcohol (PEA) odor kit, showed preliminary agreement with the YSK-threshold reference and shortened administration time. Twenty-seven older adults were analyzed after three invalid- response cases were excluded. Paired-difference agreement metrics showed a small positive mean bias (+0.704 points), non-parametric Limits of Agreement (LoA) from - 3.0 to +3.0 points, a median absolute difference of 1 point, 66.7% within-one-level agreement, 81.5% within-two-level agreement, quadratic weighted kappa of 0.723, and no significant proportional bias. Spearman correlation was treated separately as a secondary criterion-validity association and was significant (rho = 0.750, $p < .001$). Median administration time was 5 min for O-QUEST and 12 min for YSK. In-house-S was retained only as exploratory context, not as independent kit validation. O-QUEST may be an efficient preliminary threshold-estimation protocol, but larger studies with predefined equivalence margins are required before formal interchangeability can be concluded.

1571314771 — Strategy-Based Behavioral Analytics in a Tablet Memory Game for Interpretable Cognitive Screening in Older Adults

Authors: Warissara Limpornchitwilai and Boonserm Kaewkamnerdpong (King Mongkut's University of Technology Thonburi, Thailand)

Abstract: Digital gameplay logs may reveal subtle cognitive differences that are not captured by final task scores alone. This study investigated whether strategy-based behavioral features derived from a tablet-based memory-matching game could distinguish healthy older adults from individuals with possible mild cognitive impairment (pMCI). Thirty-five older adults were categorized according to Montreal Cognitive Assessment scores into a healthy control group (HC) and a pMCI group. Click sequences and matching behavior were transformed into four strategy features: Memory-Guided, Organized, Perceptual-Cue, and Inefficient/Uncertain. Directional Mann-Whitney U tests were used to examine group differences, and the strategy scores were subsequently evaluated as inputs to seven machine-learning classifiers using a nested validation pipeline across 30 repeated balanced hold-out rounds. The HC group showed significantly greater use of Memory-Guided, Organized, and Perceptual-Cue strategies, whereas the pMCI group exhibited more Inefficient/Uncertain behavior. The linear support vector machine achieved the strongest performance, with a repeated-validation accuracy of 0.801 (0.069) and a test accuracy of 0.833 (0.131). These findings suggest that interpretable, strategy-based gameplay metrics can successfully capture sub-clinical variations in search and working-memory heuristics. The proposed framework holds promise as a transparent, scalable tool for early cognitive screening, though further validation in larger, clinically confirmed groups is required.

1571314776 — A Digital Health Wallet for Verifiable Cross-Border Exchange of HL7 FHIR International Patient Summary

Authors: Wen-Jou Chang and De-Jhen Li (National Taipei University of Nursing and Health Sciences, Taiwan); Yun-Jou Chang (China University of Technology, Taiwan); Chung-Yueh Lien (National Taipei University of Nursing and Health Sciences, Taiwan)

Abstract: Cross-border healthcare encounters require timely access to interoperable patient health records, yet few mechanisms enable patients to securely carry and present an International Patient Summary (IPS) across jurisdictions. This paper presents a prototype digital health wallet architecture that integrates Health Level 7 (HL7) Fast Healthcare Interoperability Resources (FHIR) IPS, JSON Web Signature (JWS) ES256 digital signatures, and the Integrating the Healthcare Enterprise (IHE) Verifiable Health Link (VHL) specification to support patient-mediated IPS exchange. A custom FHIR summary operation was implemented to generate IPS-conformant Bundles from heterogeneous clinical data sources. The signed IPS Bundle is distributed through a wallet pass containing a Quick Response (QR) code with a VHL payload, enabling healthcare providers to retrieve and verify the document using the issuer's public key. OAuth 2.0 and SMART on FHIR patient-scoped authorization are used to protect patient access. Evaluation using five patient records demonstrated successful IPS generation, end-to-end retrieval, signature verification, and tamper detection. The architecture provides a foundation for verifiable, patient-controlled IPS exchange and future integration with the World Health Organization (WHO) Global Digital Health Certification Network (GDHCN).

1571316204 — Personalized Healthcare Platform for Health Assessment and Lifestyle Management

Authors: Warin Suttiron, Khanaphong Inchoo and Rattanan Laorboot (Srinakharinwirot University, Thailand); Chanchai Thaijiam (SWU, Thailand); Theerasak Chanwimalueang (Srinakharinwirot University, Thailand); Saksorn Thaijiam (Patumwan Demonstration School, Thailand); Tanormsak Senakham (Srinakharinwirot University, Thailand)

Abstract: The rising prevalence of non-communicable diseases has increased the demand for preventive healthcare and continuous health monitoring. This paper aims to develop an artificial intelligence-based personalized healthcare recommendation system to reduce inequalities in access to healthcare professionals. The system integrates health-related data points collected from both user inputs through a mobile application and data from smart wearable devices via the internet of things technology, such as heart rate, body composition, and sleep quality metrics. These data are analyzed using a decision tree algorithm to provide exercise and nutrition recommendations tailored to each individual's physical condition. The evaluation results indicate that the system achieved an item objective congruence score ranging from 0.50 to 1.00, as assessed by experts, and produced recommendation error rates of no more than 20% compared with expert judgments, meeting the established acceptance criteria. Therefore, the system can be considered an effective tool for promoting proactive healthcare management and sustainably reducing the workload of medical personnel.

1571318116 — A Microservice-Oriented Cloud PACS for Unified Web and Traditional DICOM Imaging Workflows

Authors: Si-Wei Yang and Chung-Yueh Lien (National Taipei University of Nursing and Health Sciences, Taiwan)

Abstract: Modern picture archiving and communication systems (PACS) must support both DICOMweb and traditional DICOM communication. However, implementing them as separate workflows can lead to inconsistent storage, query, and retrieval behavior. This paper presents a microservice-oriented cloud PACS that unifies both communication methods through shared ingest, query, retrieval, synchronization, application entity, and storage services based on Raccoon, an open-source PACS image archive. The architecture employs stream-oriented object processing, Command Query Responsibility Segregation (CQRS)-based metadata publication, quarantine handling, RPC-based inter-service communication, and structured telemetry. The system was evaluated using a The Cancer Imaging Archive (TCIA)-derived dataset of 25,422 unique DICOM instances. Each instance was submitted through both STOW-RS and C-STORE, resulting in 50,844 protocol submissions, and workflow behavior was compared with Raccoon, Orthanc, and dcm4che. The proposed PACS completed all evaluated workflows without transfer failures, published queryable metadata for every unique instance, and returned complete retrieval responses. These results demonstrate the feasibility of a unified microservice architecture for consistent DICOMweb and traditional DICOM workflows. Future work includes DICOM conformance testing, production security, audit logging, multi-tenant support, and clinical validation.

1571323346 — A Comparative Study of Prompt Engineering Strategies for Generative ASR Error Correction in Low-Resource Bangla Healthcare Speech

Authors: Prajat Paul and Mohamed Mehfoud Bouh (Kyushu University, Japan); Ashir Ahmed (Kyushu University & Grameen Communications, Japan)

Abstract: Automatic speech recognition (ASR) for low-resource languages like Bangla remains error-prone, particularly in clinical settings where manual ground-truth transcription is costly and slow. This paper compares seven prompt engineering strategies across three large language models, GPT-5.5 Pro, Gemini 3.1 Pro, and Claude Opus 4.8, for generative error correction of Bangla doctor-patient ASR transcripts. Using 20 telemedicine consultations transcribed via Wit.ai and evaluated against human- generated ground truth, correction reduced Word Error Rate by up to 45.1% relative to the uncorrected baseline. No single strategy was universally optimal: self-consistency performed best for GPT-5.5 Pro and Gemini 3.1 Pro, while a combined role, example, and reasoning strategy performed best for Claude Opus 4.8. Clinical role framing also outperformed technical NLP framing across all three models, offering practical, model- aware guidance for deploying LLM-based correction in low-resource clinical ASR pipelines.

D2R1AE

Medical Image Processing III

Session Chair: Theekapun Charoenpong

Time	Paper ID	Presenter	Paper Title
10:45–11:00	1571305732	An Ta	ASTCare: a Multi-Modal AI Platform for Dermatological Diagnosis and Intelligent Hospital Triage Using Vision-Language Models
11:00–11:15	1571306251	V. Phanichraksaphong	Deep Learning-Based Multi-Label Classification of Chest X-Ray Images for Thoracic Disease Detection
11:15–11:30	1571306827	P. Amornprasertchai	Slice Matching Method Between CT and MRI for Pelvic Tumor Image using Maximum Bone Structural Dice Similarity Coefficient
11:30–11:45	1571311836	P. Kamonvaranon	Evaluating Input Modalities for Non-Contrast MRI Brain Tumor Segmentation via 3D AIR-UNet
11:45–12:00	1571311914	Yu-Ti Tu	Hippocampal Attention Filtering for Small-Data Alzheimer's Disease Classification from MRI
12:00–12:15	1571312635	Kitiyaporn Takham	WoundSeg: AI-powered analysis for wound healing assay
12:15–12:30	1571313217	P. Paewpolsong	Quantitative OCT Software for Aquatic Tissue Morphometry: A 2,4-D Case Study in Giant Freshwater Prawn

1571305732 — ASTCare: a Multi-Modal AI Platform for Dermatological Diagnosis and Intelligent Hospital Triage Using Vision-Language Models

Authors: An Ta, Tuan Nguyen and Son Nguyen (Ho Chi Minh City University of Technology (HCMUT), Vietnam); Duy Nguyen (Sun.Studio Joint Stock Company, Vietnam); Chau Vo (HCMUT, Vietnam)

Abstract: Medical facilities face mounting pressure from high patient volumes, where overlapping symptoms across skin conditions make manual diagnosis time-consuming and error- prone, leading to diagnostic delays and clinical bottlenecks. Existing Artificial Intelligence (AI) tools remain largely patient-facing and fail to support the professional doctor-patient workflow. To address this, we present ASTCare, an integrated system that automates clinical diagnosis, specialty triaging, and appointment scheduling within a single modular framework. Built on the Dify orchestration platform, ASTCare synergizes two specialized agents: (1) a Two-Phase Vision-Language Model (VLM)- driven Diagnosis Agent combining a DenseNet201-based encoder with a lightweight LLaMA decoder for dermatological diagnosis, and (2) a Gemini 3 Flash-powered LLM (Large Language Model)-based Chatbot Agent for patient consultation and appointment scheduling. The first part of ASTCare is validated on the HAM10000 dataset - 10,015 dermatoscopic images spanning seven diagnostic categories including melanoma. For the second part, the VLM-driven Diagnosis Agent achieves Macro F1-score of 78.2%, while the LLM-based Chatbot Agent scores 25.55/30 under GPT 5 class-based autonomous evaluation, confirming strong reasoning and interaction capability. By offloading pre-diagnosis workload to an automated AI layer, ASTCare reduces manual overhead, alleviates pressure on healthcare teams, and enables dermatological care to scale effectively with growing demand.

1571306251 — Deep Learning-Based Multi-Label Classification of Chest X-Ray Images for Thoracic Disease Detection

Authors: Varinya Phanichraksaphong (King Mongkut's Institute of Technology Ladkrabang, Thailand & School of Engineering, Thailand); Supakorn Suwan (King Mongkut's Institute of Technology Ladkrabang, Thailand); Thamatis Thninvanichkul (School of Engineering, King Mongkut's Institute of Technology Ladkrabang, Thailand); Pongthep Poungthong (King Mongkut's Institute of Technology Ladkrabang, Thailand)

Abstract: Chest radiography is widely used for thoracic disease diagnosis; however, manual interpretation is time-consuming and dependent on radiologist expertise. This study presents a deep learning-based multi-label classification framework for automated thoracic disease detection using 125,928 chest X-ray images covering fifteen diseases and one normal category. Two transfer learning architectures, ResNet50 and DenseNet121, were evaluated using Macro AUC, Micro AUC, and Subset Accuracy. Experimental results showed that ResNet50 outperformed DenseNet121, achieving a Macro AUC of 0.8132, Micro AUC of 0.8668, and Subset Accuracy of 0.5129. Disease- wise analysis demonstrated strong performance for COVID-19, Emphysema, Edema, Cardiomegaly, and Pneumothorax. In addition, a graphical user interface and heatmap visualization module were developed to improve usability and model interpretability. The results demonstrate the potential of deep learning-assisted systems for large-scale chest disease screening and clinical decision support.

1571306827 — Slice Matching Method Between CT and MRI for Pelvic Tumor Image using Maximum Bone Structural Dice Similarity Coefficient

Authors: Pitchaporn Amornprasertchai and Theekapun Charoenpong (Srinakharinwirot University, Thailand)

Abstract: Direct slice-to-slice matching between CT and MRI is an important process for surgical planning in the pelvic tumor diagnosis. A major challenge in existing research is that the two modalities often have different numbers of slices, slice thicknesses, and spatial positions. This study proposes a slice matching method between computed tomography (CT) and magnetic resonance imaging (MRI) for pelvic tumor images using bone structures as anatomical references and maximum Dice Similarity Coefficient. The proposed method consists of four main steps: 1) data preparation, 2) CT-MRI bone segmentation, 3) image rescaling and centroid alignment, and 4) CT- MRI bone structural slice matching. CT and MRI slices are matched based on maximum Dice Similarity Coefficient between bone structure in CT and MRI image. We compare performance of two methods between the maximum bone structure similarity score (MBS) and the proposed method using a maximum bone dice similarity coefficient (MBD). Data from 10 patients with 145 reference slice pairs were used in experiments. The MBS method achieved a mean absolute error (MAE) of 9.92 slices, exact accuracy of 6.90%, accuracy within 1 slice (AR1) of 26.21%, and accuracy within 2 slices (AR2) of 37.24%. The proposed MBD method achieved an MAE of 9.76 slices, exact accuracy of 9.65%, AR1 of 26.21%, and AR2 of 40.69%. The proposed MBD method showed better performance. The results suggest that maximum DSC-based matching is more effective than the combined global Similarity Score in this dataset, although further improvement is still needed.

1571311836 — Evaluating Input Modalities for Non-Contrast MRI Brain Tumor Segmentation via 3D AIR-UNet

Authors: Phurich Kamonvaranon, Sirikarn Kumban, Theerasak Chanwimalueang, Suchada Tantisatirapong, Noramon Dron and Sira Jampa-ngern (Srinakharinwirot University, Thailand)

Abstract: Accurate brain tumor segmentation traditionally relies on contrast-enhanced MRI. However, gadolinium-based contrast agents pose patient health risks and environmental toxicity. To develop a safer alternative, this study evaluates non-contrast multi-modality fusion techniques using a 3D AIR-UNet architecture. Findings reveal that while adding a wavelet fusion channel (4-channel model) slightly improves whole tumor (WT) segmentation, it introduces noise that degrades tumor core (TC) and enhancing tumor (ET) accuracy, inflating the Hausdorff distance (HD95). Thus, an optimized 3-channel non-contrast pipeline (T1, T2, T2-FLAIR) coupled with static thresholding post-processing is advocated to suppress false positives. The proposed model achieves a WT Dice score of 82.29%, comparable to the contrast-enhanced baseline (83.22%), and a competitive 43.81% for the challenging ET sub-region. Ultimately, this framework demonstrates significant potential as a computationally efficient, ecologically responsible, and clinically safer alternative.

1571311914 — Hippocampal Attention Filtering for Small-Data Alzheimer's Disease Classification from MRI

Authors: Yu-Ti Tu (Yuan Ze University, Taiwan); Chun-Yi Lin (National Sun Yat- sen University, Taiwan); Isack Farady (Yuan Ze University, Taiwan)

Abstract: Magnetic resonance imaging (MRI)-based classification of Alzheimer's disease (AD) remains challenging when training data are limited and discriminative anatomical patterns are subtle. In such settings, deep learning models may generate predictions from broad image context without consistently focusing on clinically relevant regions. In this work, we propose a hippocampal region-of-interest (HRI) attention filtering framework to improve small-data AD classification from MRI. The proposed framework adopts a two-stage design. In the first stage, a pre-trained network generates class activation maps to localize discriminative regions associated with AD classification. To encourage anatomically meaningful attention, the resulting heatmaps are screened using an HRI reference, and a Gaussian Mixture Model (GMM) is employed to identify anomalous heatmaps whose activation patterns are inconsistent with the expected hippocampal location. In the second stage, the filtered HRI heatmaps are incorporated into the classification process to improve downstream prediction. We evaluate the proposed approach on 2D MRI slices from the ADNI dataset across axial, coronal, and sagittal views under a limited-data setting. Experimental results show that HRI-based attention filtering improves classification performance over baseline convolutional models, suggesting that anatomically guided attention refinement can be a practical strategy for MRI-based AD classification when training data are scarce.

1571312635 — WoundSeg: AI-powered analysis for wound healing assay

Authors: Kitiyaporn Takham, Traipob Korpanitchkul and Khwandow Kunchana (Chiang Mai University, Thailand); Pagasukon Mekrattanachai (University of Phayao, Thailand); Thatchayut Unjitwattana and Chawan Manaspon (Chiang Mai University, Thailand)

Abstract: Wound-healing or scratch assay is widely used to evaluate cell migration, proliferation, and treatment efficacy, but image analysis often requires substantial manual effort. This work develops WoundSeg, an AI-assisted software platform that integrates publicly available segmentation models for wound-healing assay analysis, providing scale calibration, wound-area segmentation, and preliminary reporting of wound-healing metrics. Compared with conventional ImageJ-based analysis, WoundSeg achieved lower wound-area measurement errors relative to expert annotations while improving usability. These results suggest that WoundSeg provides an efficient and user-friendly approach for wound-healing assay analysis, supporting rapid evaluation of treatment responses in preclinical research.

1571313217 — Quantitative OCT Software for Aquatic Tissue Morphometry: A 2,4-D Case Study in Giant Freshwater Prawn

Authors: Pichapop Paewpolsong, Jadsada Saetiew and Jiraporn Saenjae (Suranaree University of Technology, Thailand); Chutima Thanomsit (Rajamangala University of Technology Isan, Thailand); Panomsak Meemon (Suranaree University of Technology, Thailand)

Abstract: Optical coherence tomography (OCT) enables non-destructive, micrometer-scale imaging of whole aquatic specimens, but quantitative analysis remains challenging because general image-processing tools lack OCT-specific functions and many clinical segmentation methods are unsuitable for irregular specimen geometry. This work presents custom software for quantitative aquatic OCT analysis. The software integrates multi-view visualization, image enhancement, dynamic-programming boundary detection, surface flattening, intensity-based area measurement, and three- dimensional bounding-box morphometry. Its feasibility was demonstrated using juvenile giant freshwater prawns (Macrobrachium rosenbergii) exposed for 24 h to five sublethal concentrations of 2,4-dichlorophenoxyacetic acid dimethylammonium and an untreated control. Three prawns were included per group, and the eye, gill, abdomen, and telson were imaged. Of 72 region-level datasets, 58 produced usable measurements. Eye aspect ratio differed significantly among groups (Kruskal-Wallis $p = 0.020$). However, the pattern was non-monotonic, no control-dose comparison remained significant after correction for multiple testing, and no reliable dose- dependent response was found. Gill, abdomen, and telson metrics also showed no significant group differences or monotonic trends. These findings demonstrate the feasibility of an integrated, operator-assisted workflow for quantitative aquatic OCT morphometry while highlighting the need for larger samples, standardized acquisition, repeatability testing, and validation against manual or histological measurements.

D2R2AE

Biomedical Signal Processing III

Session Chair: Supan Tungjitkusolmun

Time	Paper ID	Presenter	Paper Title
10:45–11:00	1571319745	B. Rung-Ruang	Digital Phenotyping of Non-Motor Symptoms and Risk Factors for Parkinson's Disease Screening
11:00–11:15	1571321715	Cho Nandi Hlaing	EEG-Based Depression Detection: A Comparative Study of ERP and Resting-State Paradigms
11:15–11:30	1571321808	Wulin Xi	Channel-Dependent Controllability of the Spindle Mode in a Thalamocortical Neural Mass Model of Sleep
11:30–11:45	1571321871	Jun Akazawa	Development of a Flexible Multichannel Surface Electrode for Motor Unit Action Potential Measurement Toward a Seamless Muscle Fatigue Assessment System
11:45–12:00	1571321950	Nicha Thachuen	EEG-Based Binary Classification of Alzheimer's Disease and Frontotemporal Dementia Using Spectral and Connectivity Feature Fusion
12:00–12:15	1571322016	N. Jongnimitmongkol	EEG-Based Analysis of Consumer Preference toward Cashew Milk
12:15–12:30	1571322289	Wei Li	Detection and Classification of mVEP Using Multiple Stimuli with Phase Differences

1571319745 — Digital Phenotyping of Non-Motor Symptoms and Risk Factors for Parkinson's Disease Screening

Authors: Busayamas Rung-Ruang, Nicha Thachuen, Pichavee Chantayanee, Theerasak Chanwimalueang, Kulthida Methawasin and Suchada Tantisatirapong (Srinakharinwirot University, Thailand)

Abstract: Parkinson's disease (PD) is a progressive neurodegenerative disorder that primarily affects motor function, while non-motor symptoms (NMS) often emerge years before the onset of motor impairment. Demographic risk factors, including age, sex, and education level, also influence disease susceptibility. This study proposes a machine learning-based screening framework .that integrates demographic risk factors and NMS for early PD detection. Questionnaire data from 59 patients with PD and 61 healthy controls aged 40 years and older were analyzed. Three wrapper-based recursive feature elimination (RFE) configurations using support vector machine (SVM), random forest (RF), and logistic regression (LR) as base estimators were employed to identify informative feature subsets. The selected feature subsets were subsequently evaluated using SVM, RF, decision tree (DT), and LogitBoost classifiers. The best-performing model, combining RFE-RF with a Linear-SVM classifier, achieved an accuracy of 95.00%, a sensitivity of 93.37%, a specificity of 96.57%, and an F1- score of 94.66%. These results demonstrate improved classification performance compared with previous questionnaire-based approaches and highlight the potential of the proposed non-invasive and cost-effective screening framework for early PD detection

1571321715 — EEG-Based Depression Detection: A Comparative Study of ERP and Resting-State Paradigms

Authors: Cho Nandi Hlaing (King Mongkut's Institute of Technology Ladkrabang, Thailand); Don Teachasarin (King Monkut' s Institute of Technology Ladkrabang, Thailand); Suvit Poomrittigul and Treesukon Treebupachatsakul (King Mongkut's Institute of Technology Ladkrabang, Thailand)

Abstract: This study investigates whether the event-related potential (ERP) and resting-state EEG signals are more effective identifying depression, using 52 matched subjects (24 MDD, 28 HC) from the 128-channel MODMA dataset. Nine feature-based classifiers alongside four deep learning architectures were evaluated by using subject-level leave- one-subject-out (LOSO) cross-validation under controlled experimental conditions. For ERP signals, Random forest (RF) achieved the highest accuracy of 86.5% (area under the receiver operating characteristics curve, AUC-ROC = 0.932) outperforming all deep learning models. For resting-state, optimized SVM achieved the highest feature-based accuracy of 76.9% (AUC-ROC = 0.854). Cochran's Q test confirmed significant performance differences among models on ERP ($Q = 30.3$, $p = 0.003$), and McNemar's tests showed that ERP significantly outperformed resting state for SVM, RF, and MLP ($p < 0.05$). The feature-based method consistently outperformed the deep learning on both paradigms, and the ERP paradigm yielded higher classification accuracy across most models.

1571321808 — Channel-Dependent Controllability of the Spindle Mode in a Thalamocortical Neural Mass Model of Sleep

Authors: Wulin Xi (Guangdong Technion-Israel Institute of Technology, China); Yao Lin (Westlake University, China); Jijun Yin (Qualcomm, USA); Zhi-Hong Mao (University of Pittsburgh, USA)

Abstract: Neural mass models are a common tool for studying sleep rhythms, but they are rarely treated as control systems. We ask a control-theoretic question about a thalamocortical model of non-rapid eye movement (NREM) sleep: which input channel can drive the spindle rhythm? Following Costa et al. [1], we model the thalamocortical circuit involved in sleep control as a 30-state nonlinear system, linearize it about an equilibrium point, and compute a modal controllability score for each input channel. The spindle mode near 13.59 Hz has a thalamic score of 1.0 but a cortical score of only 0.006, so the cortical channel has little direct influence on the spindle mode; in other words, the cortical channel is almost "orthogonal" to it. The cortical channel still reaches the slow oscillation near 0.74 Hz, so it is not weak in general; it is near-orthogonal specifically to the spindle mode. Because the modal controllability score does not depend on input strength, a low value of the score implies a structural limit that cannot be resolved by increasing the gain of the input. Simulation of the full nonlinear model confirms the findings from the modal controllability scores computed on the linearized model: at a noise-free operating point, the effect of the cortical channel remains more than an order of magnitude below the effect of the thalamic channel on an independent EEG proxy readout. A single modal controllability score therefore identifies the thalamic channel as the spindle's actuator before any nonlinear simulation.

1571321871 — Development of a Flexible Multichannel Surface Electrode for Motor Unit Action Potential Measurement Toward a Seamless Muscle Fatigue Assessment System

Authors: Jun Akazawa (Meiji University of Oriental Medicine, Japan)

Abstract: Recently, there has been increasing demand for the development of a seamless muscle fatigue assessment system that enables non-invasive and unobtrusive evaluation of muscle activity during daily life. As the first step toward this goal, a flexible multichannel surface electrode was developed for measuring motor unit action potentials (MUAPs), and a multichannel surface electromyography (EMG) measurement system was constructed. Multichannel surface EMG signals were recorded from the biceps brachii, and the MUAP waveform, firing times, and muscle fiber conduction velocity (CV) of the motor unit selected and maintained using visual feedback were analyzed. The results demonstrated that the MUAP waveforms could be identified across all channels and that the firing times and CV of the selected motor unit could be successfully estimated. These findings suggest that the proposed multichannel surface EMG measurement system using the flexible multichannel surface electrode is a promising foundational technology as a first step toward the realization of a seamless muscle fatigue assessment system.

1571321950 — EEG-Based Binary Classification of Alzheimer's Disease and Frontotemporal Dementia Using Spectral and Connectivity Feature Fusion

Authors: Nicha Thachuen, Sira Jampa-ngern, Noramon Dron and Theerasak Chanwimalueang (Srinakharinwirot University, Thailand); Chanchai Thaijiam (SWU, Thailand); Suchada Tantisatirapong (Srinakharinwirot University, Thailand)

Abstract: Alzheimer's disease (AD) and frontotemporal dementia (FTD) are neurodegenerative disorders with overlapping clinical symptoms, making differential classification challenging. Therefore, this work proposes an electroencephalography (EEG)-based feature-fusion framework for distinguishing AD, FTD, and cognitively normal (CN) subjects using an open-access OpenNeuro dataset. This study integrates two complementary EEG representations, namely a Welch power spectral density (PSD) map and a spectral coherence connectivity (SCC) summarized map. The PSD map represents frequency-domain brain activity across EEG channels, whereas the Summarized SCC map represents band-wise channel-level connectivity. A two-branch deep learning framework integrates these representations to evaluate their complementary value for dementia classification. In the binary classification tasks, the proposed framework achieved accuracies of 90.00% for AD versus CN, 81.25% for FTD versus CN, and 72.22% for AD versus FTD. The results suggest that combining PSD-based spectral information with SCC summarized connectivity features may provide a practical and compact alternative for EEG-based AD, FTD, and CN classification.

1571322016 — EEG-Based Analysis of Consumer Preference toward Cashew Milk

Authors: Natcha Jongnimitmongkol, Napassanun Lirujpraphakorn, Suchada Tantisatirapong, Theerasak Chanwimalueang and Prakairung Paksin (Srinakharinwirot University, Thailand); Pennapa Chonpathompikunlert

(Thailand Institute of Scientific and Technological Research, Thailand); Nutthida Phianchana (Thailand)

Abstract: This study investigates consumer preference toward cashew milk by integrating electroencephalography (EEG) signals and biochemical dopamine concentrations as objective evaluation metrics. Data were collected from 32 participants, comprising pre- and post-consumption resting-state EEG recordings, urine dopamine levels measured via competitive enzyme-linked immunosorbent assay (ELISA), and subjective preference scores. EEG signals were preprocessed using independent component analysis (ICA) with ICLabel for robust artifact removal, followed by power spectral density (PSD) estimation using Welch's method to extract relative band power across the delta, theta, alpha, beta, and gamma frequency bands. Statistical analyses were performed to evaluate consumption-induced physiological changes and their relationships with behavioral preference. The results revealed a significant decrease in relative delta and theta power, accompanied by a significant increase in relative alpha power, relative beta power, and dopamine concentration following cashew milk consumption. Furthermore, correlation analyses demonstrated that the difference in relative beta power and the post-consumption relative gamma power were significantly and positively correlated with self-reported consumer preference scores. These findings demonstrate that multi-modal assessments combining EEG relative band power, particularly in higher frequency bands, with dopaminergic responses can provide profound, objective insights into food preference, thereby offering a robust framework for consumer neuroscience and food product development.

1571322289 — Detection and Classification of mVEP Using Multiple Stimuli with Phase Differences

Authors: Wei Li, Eito Tamura, Simon Kojima and Shin'ichiro Kanoh (Shibaura Institute of Technology, Japan)

Abstract: Motion-onset visual evoked potential (mVEP)-based brain-computer interfaces (BCIs) utilize electroencephalogram (EEG) responses elicited by visual motion stimuli. This study proposes a multi-stimulus paradigm in which two motion stimuli are presented with a half-cycle phase difference to improve mVEP discrimination performance in multi-stimulus environments. In the experiment, two visual stimuli consisting of a white bar moving from right to left within a square frame were presented. Five gaze targets were defined within each frame, yielding ten targets in total. EEG signals were recorded from 39 channels in seven subjects. For classification, EEG signals recorded from 17 occipital electrodes were used as input to linear discriminant analysis (LDA), and the classification accuracy was evaluated. The highest classification performance was obtained using features extracted from the 100-200 ms and 300-400 ms intervals after motion onset with a temporal segmentation width of 50 ms. Under this condition, the proposed method achieved mean classification accuracies of 80.3 for the two-class task and 57.4% for the ten-class task, both substantially above the chance level of 10%. These results demonstrate that introducing a half-cycle phase difference improves the separability of mVEP responses and enables stable multi-target gaze discrimination in the presence of multiple non- target stimuli. The findings suggest the feasibility of mVEP-based BCIs for low-burden multi-target interfaces and future flick-input spellers.

D2R3AE

Biosensors II

Session Chair: TadayuKi Akagi

Time	Paper ID	Presenter	Paper Title
10:45–11:00	1571317139	K. Pipatprasert	Electrical Impedance Measurement of Induced Calcium Oxalate Crystals in Microfluidic Chips
11:00–11:15	1571318635	Mahalakshmi Kannan	Temperature-Guided Engineering of Ternary NiCoCe Layered Double Hydroxides Coupled with NiFe Prussian Blue Analogue for Sensitive Electrochemical Sensing of Isoproturon
11:15–11:30	1571320051	Kroekchai Thongtae	Development of a 1,10-Phenanthroline-5,6-dione/f-MWCNT-Modified Electrode for Electrochemical NADH Biosensing
11:30–11:45	1571320836	Ajay Prasanth	Bioactive Curcumin-Loaded Calcium Alginate Dressing for Accelerated Chronic Diabetic Wound Healing
11:45–12:00	1571322364	C. Phiphattanaphiphop	Fabrication and Electrochemical Characterization of Flexible Three- Electrode Microsensors on Glass and Polyimide (Kapton) Substrates for Non-Enzymatic Glucose Detection
12:00–12:15	1571322406	Kitsada Thadson	Investigation of the Interaction between Salmonella Typhimurium Outer Membrane Proteins and Aptamers Using Molecular Docking for In Silico Biosensor Development
12:15–12:30	20260009	Thitipa Rupprom	Integrated PMMA–Paper Hybrid Microfluidics for CRISPR-Cas12a Detection of Mycobacterium tuberculosis

1571317139 — Electrical Impedance Measurement of Induced Calcium Oxalate Crystals in Microfluidic Chips

Authors: Koranit Pipatprasert, Pakpoom Somboon, Chanchai Boonla and Natcha Madared (Chulalongkorn University, Thailand); Thammawit Suwannaphan (King Mongkut's University of Technology North Bangkok Bangkok, Thailand); Alongkorn Pimpin (Chulalongkorn University, Thailand)

Abstract: This study presents a microfluidic platform for impedance measurement of calcium oxalate crystals based on the calcium oxalate crystallization index (COCI) concept. A stereolithography (SLA) fabricated microfluidic chip with integrated copper electrodes was developed to induce calcium oxalate crystal formation and perform electrical impedance measurements. Standard calcium oxalate monohydrate (COM) suspensions (10-50 mg/L) and chemically induced calcium oxalate crystals were evaluated using impedance spectroscopy. Repeated measurements of deionized water demonstrated good system repeatability. Distinct impedance responses were observed for both COM suspensions and induced calcium oxalate crystals compared with the baseline measurement. Optical microscopy and scanning electron microscopy further confirmed successful crystal formation inside the system. Although a clear concentration-dependent trend of the impedance was not observed, the proposed microfluidic platform successfully detected changes associated with calcium oxalate crystal formation, demonstrating its potential as a simple and low-cost approach for future kidney stone screening test.

1571318635 — Temperature-Guided Engineering of Ternary NiCoCe Layered Double Hydroxides Coupled with NiFe Prussian Blue Analogue for Sensitive Electrochemical Sensing of Isoproturon

Authors: Mahalakshmi Kannan (MING CHI University of Technology, Taiwan)

Abstract: The development of temperature-guided multifunctional materials has emerged as an effective strategy for improving electrochemical sensing performance in environmental monitoring. Herein, a temperature-engineered ternary NiCoCe layered double hydroxide (LDH) was synthesized via a hydrothermal route at different temperatures (100, 120, and 140 °C) and integrated with a redox-active cubic NiFe Prussian Blue Analogue (PBA) through a sonochemical approach to construct a highly efficient electrochemical sensing platform. The optimized NiCoCe(120)LDH@NiFe PBA hybrid exhibited enhanced charge-transfer kinetics, abundant electroactive sites, and superior electrocatalytic activity owing to the synergistic interaction between the temperature-regulated LDH architecture and the porous PBA framework. Differential pulse voltammetry (DPV) demonstrated excellent analytical performance toward the herbicide isoproturon (IPU), achieving a wide linear detection range of 0.05-1845.15 µM, a low detection limit of 29.3 nM, and a strong sensitivity of 1.356 µA µM-1 cm-2. The sensor also exhibited excellent selectivity, repeatability, reproducibility, and long- term stability, with relative standard deviation values below 6%. Practical applicability was confirmed through successful quantification of IPU in fish tank, river, paddy, and tap water

samples, yielding recoveries between 93.82% and 106.23%. This temperature-guided material design provides an effective platform for rapid and sensitive monitoring of persistent environmental pollutants, contributing to water quality assessment, protection of aquatic ecosystems, and mitigation of potential risks to human health through sustainable environmental surveillance.

1571320051 — Development of a 1,10-Phenanthroline-5,6-dione/f-MWCNT-Modified Electrode for Electrochemical NADH Biosensing

Authors: Kroekchai Thongtae, Kewarin Phonklam and Tonghathai Phairatana (Department of Biomedical Sciences and Biomedical Engineering, Faculty of Medicine, Prince of Songkla University)

Abstract: Reduced nicotinamide adenine dinucleotide (NADH) is an essential electroactive cofactor widely employed in in dehydrogenase-based electrochemical biosensors. However, its direct electrochemical oxidation is often limited by high overpotential and slow electron-transfer kinetics, resulting in poor analytical performance. In this study, a screen-printed carbon electrode (SPCE) modified with 1,10-phenanthroline-5,6-dione (PD) and carboxyl-functionalized multi-walled carbon nanotubes (f-MWCNT) was developed to enhance the electrochemical response toward NADH oxidation. Three electrode modification configurations, namely PD/SPCE, f-MWCNT-PD/SPCE (composite), and PD/f-MWCNT/SPCE (layer-by-layer), were fabricated and compared by cyclic voltammetry (CV). Among them, the composite electrode exhibited the sharpest redox peaks, the highest peak currents, and the smallest peak-to-peak separation, indicating superior electron-transfer characteristics. The surface morphology of the bare SPCE and the optimized f-MWCNT-PD/SPCE was characterized by scanning electron microscopy, confirming the successful formation of a rough and homogeneous composite coating. The effect of PD concentration (0.5, 1.0, 2.0 and 3.0 mg/mL) in the composite electrode was further evaluated by CV using NADH concentrations ranging from 0 to 1.0 µM. Calibration curves constructed from the change in PD oxidation peak current demonstrated that the electrode modified with 1.0 mg/mL PD achieved the highest sensitivity of 2.7738 µA/µM (R2=0.9537), whereas electrodes prepared with 0.5, 2.0, and 3.0 mg/mL PD exhibited sensitivities of 2.1090, 1.3804, and 1.8866 µA/µM, respectively. These results demonstrated that both the electrode modification strategy and PD loading significantly influence the electrochemical performance of the sensor. The proposed f-MWCNT-PD electrode provides a promising platform for NADH sensing and the future development of dehydrogenase-based electrochemical biosensors.

1571320836 — Bioactive Curcumin-Loaded Calcium Alginate Dressing for Accelerated Chronic Diabetic Wound Healing

Authors: Ajay Prasanth (MING CHI University of Technology, Taiwan); Kuo- Yung Hung (Ming Chi University of Technology, Taiwan); Umamaheswari Rajaji (Research Centre for Intelligent Medical Devices, Taiwan)

Abstract: The present study aims to develop a curcumin-loaded calcium alginate dressing designed to enhance chronic and diabetic wound healing through sustained drug release, antioxidant activity, and antibacterial protection. The prepared dressing was systematically characterized using FTIR, SEM, swelling, and degradation studies to confirm its chemical composition, structural stability, and surface morphology. Results revealed a highly porous, flexible, and biocompatible film with excellent drug retention and gradual diffusion, promoting cell proliferation and tissue regeneration. Overall, the dressing demonstrates strong potential as a promising bioactive material for advanced wound management applications.

1571322364 — Fabrication and Electrochemical Characterization of Flexible Three- Electrode Microsensors on Glass and Polyimide (Kapton) Substrates for Non-Enzymatic Glucose Detection

Authors: Chalinee Phiphattanaphiphop and Kanista Khamprapai (Chiang Mai University, Thailand)

Abstract: The development of wearable biosensors has attracted considerable interest in real- time health diagnostics. However, conventional electrochemical sensors are typically fabricated on rigid substrates, which limits their conformability to human skin. This study presents the design, fabrication, and electrochemical characterization of micro- scale, three-electrode sensing platforms developed on both conventional glass and flexible polyimide (Kapton) substrates using a combined sputtering and photolithography process. Electrochemical characterization via cyclic voltammetry (CV) in a standard redox probe solution confirmed successful micro-patterning, with the glass-based sensor yielding an electrochemically active surface area (ECSA) of 5.1×□10□^(-4) □" cm" □^2. For non-enzymatic glucose sensing under alkaline conditions (0.1 M NaOH in PBS, pH 7.4), the Kapton-based sensor demonstrated a discernible response trend across a glucose concentration range of 20 to 100 mM. Although the Faradaic current amplitude on the flexible substrate was

constrained to the sub-nanoampere range due to the inherent sheet resistance and surface morphology of the polymer, the platform successfully sustained stable electrochemical reactions. This work demonstrates the feasibility of micro-fabricated flexible electrode arrays and establishes a foundational baseline for future signal-amplification strategies in wearable, non-enzymatic continuous glucose monitoring devices.

1571322406 — Investigation of the Interaction between Salmonella Typhimurium Outer Membrane Proteins and Aptamers Using Molecular Docking for In Silico Biosensor Development

Authors: Kitsada Thadson (Rangsit University, Thailand); Thana Sutthibutpong and Phitsini Suvarnaphaet (King Mongkut University of Technology Thonburi, Thailand)

Abstract: Aptamer-based biosensors for the detection of Salmonella Typhimurium have shown considerable potential across a wide range of diagnostic applications. However, identifying high-affinity aptamer candidates requires extensive SELEX experiments, which are costly and time-consuming due to their iterative nature. Recent advances in molecular docking provide valuable insights into atomic-level receptor-aptamer interactions while enabling comparative evaluation of candidate aptamers prior to experimental validation. This study presents a computational workflow for evaluating the binding of several reported aptamers against multiple outer membrane proteins of S. Typhimurium. The docking results indicate that OmpC exhibits the strongest binding affinity among the evaluated receptor proteins for all tested aptamers. Furthermore, interaction analysis identifies the key binding residues and quantitatively characterizes the intermolecular interactions underlying receptor-aptamer complex formation. These findings provide useful insights for the rational design and in silico optimization of aptamer-based biosensors for S. Typhimurium detection.

20260009 — Integrated PMMA–Paper Hybrid Microfluidics for CRISPR-Cas12a Detection of Mycobacterium tuberculosis

Authors: Thitipa Rupprom , Oakar Min, Pattarawan Tangrattanakamolkul , Rinrada Boworntummarat , Jindapa Nampeng and Pimkhuan Hannanta-anan, Department of Biomedical Engineering, School of Engineering, King Mongkut’s Institute of Technology Ladkrabang, Bangkok, Thailand

Abstract: CRISPR-Cas12a-based molecular diagnostics offer high sensitivity and specificity for nucleic acid detection; their point-of-care (POC) utility remains constrained by complex workflows and reliance on centralized laboratory equipment. Here, a PMMA–paper hybrid microfluidic platform was engineered to unify isothermal CRISPR-Cas12a reactions with on chip fluorescence detection for Mycobacterium tuberculosis (TB) DNA identification. Comparative evaluation of cellulose (WF/1) and glass fiber (GF/C, GF/D) substrates established GF/C as the ideal readout pad, characterized by a maximum Signal-to Background Ratio (SBR) (4.52 ± 0.50) and peak fluorescence intensity (107.29 ± 0.89 a.u.). Thermal characterization validated effective internal heat transport, maintaining the target temperature of 39.0 °C needed for CRISPR-Cas12a activity. The platform achieved reliable on-chip detection of target TB DNA, yielding clear signal separation between positive (61.90 ± 1.99) and negative (37.05 ± 1.83) reactions. Despite exhibiting a reduced fluorescence intensity relative to conventional tube-based assays, the hybrid chip retained robust signal contrast for accurate diagnostic interpretation. This hybrid architecture represents an accessible and compact strategy for field-deployable CRISPR molecular testing

D2R4AE

Bio-robotics and biomechanics I

Session Chair: Wongwit Senawong

Time	Paper ID	Presenter	Paper Title
10:45–11:00	1571314260	Peter Berkelman	Motion Control for Magnetic Capsules Using Coil Array and Low Frame Rate Localization
11:00–11:15	1571315319	Itgel Megzer	Impedance-Based Self-sensing of Muscle Contraction Displacement of a Biohybrid Actuator
11:15–11:30	1571319511	Michihiko Fukunaga	Muscle Force Estimation of the Ankle Complex During Traverse Slope Walking Using an Anatomically Constrained Two-Axis Model
11:30–11:45	1571321279	K. Boonyasurat	BRAINIAC: Salience-Gated Sparse Execution for Low-Cost CPU Simulation of the C. elegans Connectome
11:45–12:00	1571321925	S. Nakdhamabhorn	A Parallel Ant-Colony Pheromone-Inspired Path Planner for Assistive and Hospital Service Robot Navigation
12:00–12:15	1571322829	John Minogue	Validation of 2D Markerless Motion Capture Using FreeMoCap
12:15–12:30	1571323450	S. Piyavannakul	A Depth-Camera-Based Interactive Game System for Quantitative Upper-Limb Motion Assessment in Stroke Rehabilitation

1571314260 — Motion Control for Magnetic Capsules Using Coil Array and Low Frame Rate Localization

Authors: Peter Berkelman (University of Hawaii System, USA); Mitsuki Soma (Boston University, USA); Sean Trafford (University of Hawaii, USA)

Abstract: The development of active wireless capsules is highly significant for medical applications, as these offer the possibility of minimally invasive or fully noninvasive access to bodily organs and tissues in the gastrointestinal tract, circulatory system, and other internal cavities for diagnosis and intervention. Wireless capsule endoscopy in particular has become widely adopted for diagnostic visualization of the entire gastrointestinal tract as the capsule advances by peristalsis. If a wireless capsule contains a magnet, then forces can be generated upon it externally to actively control its motion through electromagnetic actuation. If the actuation subsystem is combined with a sensing subsystem so that the internal capsule can be localized with respect to internal anatomy, then closed-loop feedback may be used to control its motion in a stable manner to drive it to desired locations for diagnosis or intervention. The high latency and limited frame rates of localization based on medical imaging methods such as ultrasound, computed tomography, or magnetic resonance imaging, combined with the motion constraints from internal anatomy, pose a challenge to the stability and effectiveness of standard feedback control methods for magnet capsule motion control however. We have investigated and demonstrated motion control for magnet capsules using a 20 Hz frame rate optical localizer to emulate medical imaging localization methods and coil array electromagnetic actuation from a magnetic levitation system. Open-loop feedforward forces produced in response to human interaction are combined with active damping to produce practical stable magnet motion on a planar surface with the unpredictable dynamics of stick-slip friction. Recorded motion results are presented for path-following trajectory motions of cylindrical magnets in both vertical and horizontal orientations.

1571315319 — Impedance-Based Self-sensing of Muscle Contraction Displacement of a Biohybrid Actuator

Authors: Itgel Megzer, Mutsuki Hagiwara and Wataru Hijikata (Institute of Science Tokyo, Japan)

Abstract: Skeletal muscle-based biohybrid actuators are considered promising actuator platforms because they offer unique characteristics such as self-repair and the ability to be driven by biochemical energy sources like blood glucose, which enables novel applications including muscle batteries. To utilize skeletal muscle as an actuator in practical systems, high precision control is essential, and model-based control strategies have therefore been actively investigated. However, due to parameter variations and environmental changes, feedback control is highly beneficial, which in turn requires sensing of the actuator state and complicates miniaturization and in vivo applications. In this study, we address this issue by estimating muscle contraction from electrical impedance measurements, thereby enabling sensor-less displacement estimation and future feedback control without dedicated external sensors.

1571319511 — Muscle Force Estimation of the Ankle Complex During Traverse Slope Walking Using an Anatomically Constrained Two-Axis Model

Authors: Michihiko Fukunaga (Oita University, Japan); Shinya Nakaguchi (TMEIC Corporation, Japan)

Abstract: Traverse slope walking requires complex three-dimensional adaptation of the ankle complex to maintain mediolateral stability. Conventional gait analyses commonly represent the ankle as a single hinge joint, making it difficult to separately evaluate the functional roles of the talocrural joint (TCJ) and subtalar joint (STJ) or to estimate the associated muscle forces during uneven-terrain walking. In this study, an anatomically constrained two-axis ankle model was applied to biomechanical analysis of traverse slope walking. The TCJ and STJ were represented by their primary physiological rotational axes, allowing the three-dimensional ankle motion to be decomposed into joint-specific rotations. By constraining the joint degrees of freedom according to anatomical function, sufficient muscle redundancy was preserved, enabling estimation of individual muscle forces through static optimization. Kinematic and kinetic data were obtained from three-dimensional motion capture and ground reaction force measurements during level walking and traverse slope walking. The results demonstrated that TCJ kinematics remained nearly unchanged across all walking conditions, whereas the STJ exhibited marked condition-dependent adaptations, particularly during lower-side walking on the steeper slope. Muscle-force estimation revealed prolonged activation of the peroneus muscles during lower-side walking and earlier activation of the tibialis posterior during upper-side walking, suggesting complementary muscular strategies for mediolateral stabilization. Furthermore, the estimated joint kinematics and muscle activation timings during level walking agreed well with previously reported radiographic and electromyographic findings, supporting the physiological validity of the proposed framework. These findings demonstrate that the proposed anatomically constrained two-axis model provides a practical framework for simultaneously evaluating ankle joint mechanics and muscular coordination during traverse slope walking. The proposed methodology may contribute to future applications in clinical gait analysis, rehabilitation, and biomechanical evaluation of locomotion on uneven terrain.

1571321279 — BRAINIAC: Salience-Gated Sparse Execution for Low-Cost CPU Simulation of the C. elegans Connectome

Authors: Kongkridakorn Boonyasurat and Chuchart Pintavirooj (King Mongkut's Institute of Technology Ladkrabang, Thailand)

Abstract: Direct simulation of a biological connectome updates every neuron and synapse at each time step, which can be computationally inefficient because only a small fraction of the circuit may be active at a given moment. BRAINIAC is a Python library that reduces this cost by evaluating only sensory, active, or salient(importance) parts of the same connectome on a consumer CPU without requiring neuromorphic hardware. The system was evaluated using a Caenorhabditis elegans connectome model with 302 neurons and 5,149 directed connections in a 2-D environment. A dense full- connectome baseline was compared with BRAINIAC and several runtime-scheduling variants. BRAINIAC reduced the average number of active neurons per step from 302 to approximately 13 and processed roughly 226 synapses per step instead of 5,149. This reduced estimated per-step computation by 88.1% and decreased wall-clock processing time from 13.45 ms to 2.71 ms per step while the simulated worm continued to forage. Budgeted variants achieved up to 89.9% estimated FLOP reduction. These results indicate that salience-gated sparse execution can reduce the computational cost of connectome simulation on commercial CPUs while preserving the underlying biological wiring.

1571321925 — A Parallel Ant-Colony Pheromone-Inspired Path Planner for Assistive and Hospital Service Robot Navigation

Authors: Sakol Nakdhamabhorn (Chulabhorn Royal Academy, Thailand); Dileep Sivaraman (Mahidol University, Thailand)

Abstract: Autonomous service robots in hospitals and care facilities (delivering medication and supplies, disinfecting, and assisting mobility-impaired patients) must reliably reach every commanded location in cluttered, human-shared indoor spaces while moving along smooth, predictable paths. Bio-inspired planners produce such naturalistic paths: Pheromone-Inspired and Path-Integrated (PIPI) planning navigates by following the gradient of a virtual pheromone field while integrating its own motion and reactively avoiding obstacles. In its original form, however, PIPI commits to a single deterministic agent that is easily trapped by concave obstacles and fails to reach some rooms, which is unacceptable for a service robot. This paper recasts PIPI as a parallel ant colony: many stochastic PIPI agents explore concurrently on a shared pheromone field, the successful ones reinforce their trails, and the field evaporates between rounds. Implemented as a nav core global-planner plugin and evaluated on a TurtleBot3 simulation in a cluttered office environment that stands in for a hospital floor, against single-agent PIPI and Dijkstra, the colony raises planning success from

57% to100% and closed-loop navigation from 5=8 to 8=8 goals, reaching full planning and navigation reliability while producing paths smoother than grid-optimal search (total heading change 3:3 vs. 5:3 rad for Dijkstra and 7:2 rad for single-agent PIPI) at a path length statistically indistinguishable from the grid-optimal route. We further show that the colony's reliability comes from parallel stochastic coverage rather than iterative pheromone convergence.

1571322829 — Validation of 2D Markerless Motion Capture Using FreeMoCap

Authors: John P Minogue, Melanie Napierala, Breanna Lowe, Philip Byrne and John F Drazan (Fairfield University, USA)

Abstract: The accurate measurement of human movement is a crucial tool for biomechanics researchers. Marker based tracking approaches, while accurate, are expensive and time consuming, often precluding high throughput data collection in the field. Markerless tracking systems remove many of these constraints, however, they often are either expensive or require significant coding experience or training data sets to be used. FreeMocap is a free-to-download, codeless approach for markerless motion tracking, with the ability to collect data without a connection to the internet. The purpose of this study was to validate the performance of this markerless motion tracking approach on a laptop webcam relative to a gold standard marker-based system. 27 healthy adult subjects performed different body-weight exercises while sagittal plane lower body angles were calculated using both the marker-based and markerless approach. FreeMoCap showed "very strong" correlation with the gold standard during the squat and countermovement jump (CMJ) for all joint angles with correlation values \(geq0.97\). RMSE values for the knee and ankle for these movements were \(leq7.691^\circ\), while higher RMSE values were seen at the hip \(leq10.989^\circ\). As field measurements, whether in the clinic or on the sports field, often do not have stable internet access, the ability to collect markerless kinematic data without internet access is a significant strength of this approach. While this study indicates that FreeMoCap hasn't yet achieved the same accuracy as the marker-based for research- grade data, it's affordability compared to other markerless systems makes it an attractive tool for field based research.

1571323450 — A Depth-Camera-Based Interactive Game System for Quantitative Upper-Limb Motion Assessment in Stroke Rehabilitation

Authors: Sasiphat Piyavannakul and Wongwit Senavongse (Srinakharinwirot University, Thailand)

Abstract: Stroke is a leading cause of long-term disability, with upper limb impairment substantially affecting activities of daily living. This study proposes a markerless, game- based upper limb rehabilitation system integrating the Orbbec Femto Bolt depth camera with a Unity-based interactive game. The system tracks upper limb movements in real time, calculates joint angles, provides visual feedback, and automatically records rehabilitation data for therapist reviews. Measurement accuracy was evaluated against a universal goniometer for both upper limbs. Across the left and right shoulder and elbow evaluations, accuracy remained approximately 97% or higher, while the overall MAE ranged from 0.83° to 1.07°. The system was also evaluated by eight rehabilitation specialists using a five-point Likert-scale questionnaire, achieving an overall satisfaction score of 3.94 out of 5. These results demonstrate high measurement agreement and positive expert acceptance regarding usability and clinical suitability. The proposed system provides an interactive platform combining markerless motion tracking, game-based rehabilitation, and quantitative movement recording, with potential as a complementary tool for upper limb rehabilitation and longitudinal progress monitoring.

D3R1ML

Medical Image Processing IV

Session Chair: Che-Wei Lin

Time	Paper ID	Presenter	Paper Title
10:45–11:00	1571322162	Gad Barash	Region-Specific Infrared Thermography of Task-Related Brain Activity: A Feasibility Study in Healthy Subjects
11:00–11:15	1571322390	Thodsaporn Phansri	Kinematic Beat Envelopes as a Dual-Modality Proxy for Motility Verification and Intensive Morphological Assessment in Automated CASA
11:15–11:30	1571322615	Arthit Buranasing	A Lightweight Deep Learning Model with Explainable AI for Staging Alzheimer's Disease using MRI Scans
11:30–11:45	1571322970	Riku Tanabe	Introducing Node Heterogeneity into Neural and Hemodynamic Response Models for Functional Connectivity Reproduction
11:45–12:00	1571323174	P. Putyuen	AI Assist for Emergency First Responders
12:00–12:15	1571323454	Phichamon Intra	Performance Comparison of Deep Learning Models for Multi-Structure Cardiac Segmentation in Two-Chamber Echocardiography Images
12:15–12:30	1571323459	Phiengfah Upasen	Development of a Robotic Arm for Wound Detection and Analysis via Multispectral Camera with Real-Time Control

1571322162 — Region-Specific Infrared Thermography of Task-Related Brain Activity: A Feasibility Study in Healthy Subjects

Authors: Gad Barash and Ofek Yehuda (Afeka Academic College of Engineering, Israel); Dima Bykhovsky (Shamoon College of Engineering, Israel); Elchanan Azriel and Oshrit Hoffer (Afeka Academic College of Engineering, Israel); Shahar Cohen (Be'erot Mental Health Center, Israel); Ruth Zaks-Ohayon and Doron Todder (Beerot Mental Health Center, Israel)

Abstract: We show that passive thermal imaging of the head and face, combined with structured cognitive activation and a fully automated analysis pipeline, non-invasively reveals task-related brain-activity signatures in healthy subjects. The approach is low-cost, contact-free, and portable, and it advances functional thermography from a whole-face arousal measure to region-specific mapping, with applications from psychophysiological research to portable monitoring of cognitive and affective state. Twenty-four sessions were recorded from four healthy adults across five cognitive protocols using a consumer-grade FLIR One Pro camera. A computer-vision pipeline extracts anatomically anchored regions of interest (ROIs) across three camera views using scale-invariant coordinate systems that automatically track head motion, without manual per-frame calibration. Four temperature features per ROI per frame are reduced to pairwise differences between co-imaged ROIs, which cancel whole-head drift, and correlated with the stimulation reference by normalized cross-covariance with an autocorrelation-corrected Bartlett band. In all five protocols, the pipeline identified strong within-run correlations, reaching |r| up to 0.90 and significant against the Bartlett band at physiologically plausible lags, and the leading feature and region pair differed by task, showing sensitivity to task identity rather than a generic arousal response. These results establish the feasibility of automated, region-specific thermographic brain-activity mapping and provide a reproducible, open-source foundation for larger confirmatory studies.

1571322390 — Kinematic Beat Envelopes as a Dual-Modality Proxy for Motility Verification and Intensive Morphological Assessment in Automated CASA

Authors: Thodsaporn Phansri (Chiang Mai University, Thailand); Komgrit Leksakul (Thailand); Chalinee Phiphattanaphiphop (Chiang Mai University, Thailand); Rungrueang Phatthanakun (Synchrotron Light Research Institution (SLRI), Nakhon Ratchasima, Thailand)

Abstract: Standard computer-assisted sperm analysis (CASA) typically evaluates motility by tracking sperm heads and deriving kinematic indicators such as VCL, VSL, and ALH. When CASA is moved onto low-cost edge hardware, for example a Raspberry Pi 5 paired with ordinary brightfield microscopy, the usual approach becomes unreliable. Lower spatial resolution and low-contrast monochrome imagery often break head-tracking routines that were originally built around specialized dark-field optics. To work around these optical and hardware constraints, this study presents a framework that couples head tracking with tail detection through skeletonization. The combined strategy improves tracking stability while also opening a route to early morphological screening by reading tail-beat dynamics over time. For deeper pattern recognition, the system uses a CNN initialized with MobileNetV3- Large pre-trained weights to classify tail-beating behaviors automatically. By joining these two modes, the method offers a low-cost, high-accuracy alternative to

conventional CASA, aimed at extracting clinically meaningful information in laboratories with limited resources

1571322615 — A Lightweight Deep Learning Model with Explainable AI for Staging Alzheimer's Disease using MRI Scans

Authors: Arthit Buranasing (Srinakharinwirot University, Thailand)

Abstract: The rising global aging population has precipitated a significant increase in Alzheimer's disease (AD) cases, making early and accurate diagnosis a critical priority for effective therapeutic intervention and patient care management. While Deep Learning (DL) models offer highly promising diagnostic capabilities using Magnetic Resonance Imaging (MRI), their transition from laboratory to clinic is frequently hindered by two formidable deployment barriers: extremely high computational costs that prohibit usage in standard, resource-constrained clinical environments, and the inherent "black box" problem of neural networks, which fundamentally hinders clinical trust and regulatory adoption. This paper presents a comprehensive study that intricately integrates a lightweight Convolutional Neural Network (CNN) with Explainable Artificial Intelligence (XAI) to classify AD into four severity stages. Utilizing the Augmented Alzheimer MRI Dataset V2, comprising 33,984 balanced images, we extensively benchmarked advanced lightweight architectures (MobileNetV2, EfficientNetB0, MobileNetV3Small) against traditional heavyweight models (ResNet50, DenseNet121, VGG16). Experimental results unequivocally demonstrate that MobileNetV2 achieved the highest classification accuracy of 81.68%, requiring only 2.92 million parameters and a mere 141.71 ms inference time per image. To directly address the black-box issue, Gradient-weighted Class Activation Mapping (Grad-CAM) was implemented, providing intuitive visual heatmaps that highlight the specific anatomical regions-such as the ventricles and cortical sulci-contributing to the model's decisions. Finally, the optimized diagnostic model was successfully integrated into a production-ready clinical prototype named "ZenPulse," an end-to-end automated MRI analysis system meticulously designed to seamlessly enhance modern healthcare workflows.

1571322970 — Introducing Node Heterogeneity into Neural and Hemodynamic Response Models for Functional Connectivity Reproduction

Authors: Riku Tanabe, Takuto Niinuma, Masato Sugino, Kenta Shimba and Kiyoshi Kotani (The University of Tokyo, Japan)

Abstract: To understand the physiological and physical mechanisms underlying macroscopic brain activity, neural mass models and hemodynamic response models have been widely used to reproduce observed neural data. In neural mass models, the introduction of node heterogeneity-where local parameters are set individually for each region-has improved the reproducibility of functional connectivity (FC), which quantifies functional interactions between regions based on functional Magnetic Resonance Imaging (fMRI) data. On the other hand, although it is known that hemodynamic responses exhibit local variations, they have traditionally been modeled as homogeneous across nodes. In this study, we constructed a cortical model that incorporates node heterogeneity into both the neural mass model and the hemodynamic response model. We then optimized the model to fit FC estimated from empirical fMRI data using a gradient-based optimization framework. Introducing heterogeneity into the neural mass model improved the fit to empirical FC, and the best fit was achieved by further introducing heterogeneity into the hemodynamic response model. Furthermore, although the optimization aimed solely at reproducing FC, the spatial distribution of the estimated parameters of the hemodynamic response model was consistent with physiological findings. These results suggest that node heterogeneity in the hemodynamic response contributes to reproducing empirical FC and can be estimated in a physiologically meaningful way.

1571323174 — AI Assist for Emergency First Responders

Authors: Phatcharapon Putyuen, Chanapatch Chiewsothorn and Pakorn Mekhora (King Mongkut's Institute of Technology Ladkrabang, Thailand); May Phu Paing (School of Engineering, Thailand & King Mongkuts Institute of Technology, Thailand)

Abstract: Timely actions and accurate decision-making are crucial to save lives during emergency situations. This paper uses the Trauma THOMPSON (T3) dataset to create a suite of Artificial Intelligence (AI) based tools that can be used by Emergency First Responders. These tools support five critical emergency response tasks: action recognition, action anticipation, detection of hands, detection of other surgical tools, and Visual Question Answering (VQA). An Action Dictionary-guided (ADG) classifier was applied for both action recognition and anticipation, achieving accuracies of 36.38% and 41.19%, respectively. For the detection tasks the YOLO11m model was employed, achieving an mAP@0.5 of 98.63% for hand detection and 96.96% for the detection of 17 distinct surgical instruments. Finally, for VQA, a frozen version of the BLIP-2 feature extractor, combined with a 16-class Multi-Layer Perceptron (MLP) classifier was applied, providing 86.71%

accuracy.

1571323454 — Performance Comparison of Deep Learning Models for Multi-Structure Cardiac Segmentation in Two-Chamber Echocardiography Images

Authors: Phichamon Intra, Sira Jampa-ngern and Atithep Khaone (Srinakharinwirot University, Thailand)

Abstract: Two-dimensional echocardiography is a widely adopted non-invasive medical imaging modality for the assessment of cardiac structure and function. However, manual delineation of cardiac boundaries remains a time-consuming task requiring substantial clinical expertise. This study presents a comparative evaluation of three deep learning architectures Fully Convolutional Network (FCN), U-Net, and DeepLabV3+ for automated multi-structure cardiac segmentation in Apical Two-Chamber echocardiographic views using the publicly available CAMUS dataset. Model performance was assessed via 10-fold cross-validation, with the Dice Similarity Coefficient (DSC) serving as the primary evaluation metric. Segmentation outputs from the best-performing model were further utilized to estimate Left Ventricular Ejection Fraction (LVEF) for cardiac function assessment. Experimental results demonstrate that DeepLabV3+ achieves superior overall performance, attaining mean DSC values of 0.938 and 0.941 for the End-Systole (ES) and End-Diastole (ED) phases, respectively, outperforming U-Net (0.893, 0.894) and FCN (0.871, 0.888). The performance advantage of DeepLabV3+ is attributed to its Atrous Spatial Pyramid Pooling mechanism, which enables effective multi-scale feature extraction and enhances delineation accuracy across heterogeneous cardiac structures. These findings suggest that DeepLabV3+ holds strong potential for deployment in automated echocardiographic analysis pipelines to support clinical decision-making in cardiac disease diagnosis.

1571323459 — Development of a Robotic Arm for Wound Detection and Analysis via Multispectral Camera with Real-Time Control

Authors: Phiengfah Upasen (Chitralada School, Thailand)

Abstract: This study presents the development of a robotic arm integrated with a multispectral camera and an embedded control system for automated wound inspection. The proposed prototype combines three robotic motion mechanisms-base rotation, vertical translation, and front-structure rotation-with sequential image acquisition under white, red, blue, green, yellow, and UV illumination. The system was implemented using Raspberry Pi and Arduino Mega 2560 platforms and fabricated using 3D-printed ABS and PETG components. Preliminary laboratory testing on normal and wounded simulated skin surfaces showed assembly and motion performance results of 78.00%- 92.00%, a 100.00% success rate for coordinated six-band image acquisition, an 84.00% wound-presence detection result, and an 80.00% multispectral image- acquisition workflow result. These findings demonstrate the feasibility of integrating robotic positioning and multispectral imaging into an automated wound-inspection platform. The current study is limited to preliminary prototype evaluation under simulated conditions and provides a foundation for future wound-image analysis and clinically relevant validation.

D3R2ML

Bioinformatics I

Session Chair: Ming-Long Yeh

Time	Paper ID	Presenter	Paper Title
10:45-11:00	1571314845	Watin Promfiy	Agents Optional, Calibration Essential: Efficient Medical Question Answering with Open Language Models
11:00-11:15	1571322328	Voraphop Vorapasit	Clinical Pattern Analysis of Irregular ICU Laboratory Data Over 4 Days via Canonical Polyadic Decomposition
11:15-11:30	1571322686	Kunthida Srilasak	Analysis of Observation Window and Kernel Functions in Support Vector Machine for Survival and Mortality Classification of Critical Patients using Blood Biomarkers
11:30-11:45	1571322723	P. Kasembunyakorn	Hidden Markov Models for Clinical State Modeling in ICU Mortality Prediction
11:45-12:00	1571323513	Karnpitcha Meekul	Differential Radiomic Signatures Across Brain Regions in Schizophrenia, ADHD, and Bipolar Disorder: A Multi-Model Consensus Framework
12:00-12:15	1571323790	M. Jobayer Chowdhury	Divergence Between WHO Laboratory and Non-Laboratory CVD Risk Charts Across Stepwise Population Survey and Portable Health Clinic Settings in Bangladesh
12:15-12:30	1571322685	Jitpimon Siripanth	Customized 3D Ocular Prosthesis

---

1571314845 — Agents Optional, Calibration Essential: Efficient Medical Question Answering with Open Language Models

Authors: Watin Promfiy and Suvit Poomrittigul (King Mongkut's Institute of Technology Ladkrabang, Thailand)

Abstract: Large language models are increasingly wrapped in retrieval-augmented, multi-agent pipelines for clinical question answering, usually reported with a single strong model and a generation-based accuracy number. We ask whether this scaffolding actually helps, and whether the gains survive a protocol that removes answer-extraction artifacts. Using six open-weight language models (1.5 to 32 billion parameters) and seven open medical question-answering benchmarks (MedQA, MedMCQA, and five medical subsets of MMLU), we run a controlled two-by-two factorial over retrieval and scoring mode (constrained versus generation), together with self-consistency and a four-agent plan-retrieve-answer-verify pipeline. We find that, measured against a trivial parse-free constrained log-probability scorer, the four-agent pipeline is neutral-to- harmful for five of the six models and improves on it for only one; that the popular impression of large agentic gains on weaker models is largely a measurement artifact of generation-based answer extraction, which constrained log-probability scoring removes; and that the verifier accepts almost every answer as supported, with Matthews correlation near zero for biomedical-tuned models. As a constructive remedy, the constrained scorer's own confidence supports calibrated selective prediction, and a confidence-gated cascade with thresholds chosen on a held-out split recovers the best fixed method's accuracy within about one point at up to five-fold lower cost by selecting the cheapest sufficient tier per question. We release all code, prompts, and a fully offline evaluation harness.

1571322328 — Clinical Pattern Analysis of Irregular ICU Laboratory Data Over 4 Days via Canonical Polyadic Decomposition

Authors: Voraphop Vorapasit, Suchada Tantisatirapong, Sira Jampa-ngern and Noramon Dron (Srinakharinwirot University, Thailand)

Abstract: Clinically relevant ICU laboratory trajectories contain early signals of clinical deterioration, but extracting interpretable patterns is challenging due to missingness, irregular sampling, and strong survivor/non-survivor imbalance. We propose an outcome-aware Weighted Non-negative CPD to decompose a three-way tensor \(Labs \times Patients \times Days\) built from 9 clinically relevant laboratory parameters: Potassium, Sodium, Chloride, Creatinine, Blood Urea Nitrogen (BUN), Total CO2, White blood cell (WBC) count, Hematocrit (Hct), and Platelet count (PLTcount) collected over 4 consecutive days in a retrospective cohort from Chonburi Hospital. Bayesian Optimization selected R = 3 and \({\boldsymbol{\lambda }}_{\boldsymbol{L}2}\approx\) 0.0290, achieving a Fit Score of 94.51%, a Weight of 2.00, and a CORCONDIA of 59.92%. The 3 components revealed clinically interpretable patterns with distinct temporal dynamics, specifically capturing Acute Infection and Inflammatory Response, Patient-Specific Renal Impairment, and Fundamental Physiological Homeostasis trajectories. The proposed model provides a compact, interpretable representation of imbalanced ICU laboratory time series for downstream risk stratification and hypothesis generation.

1571322686 — Analysis of Observation Window and Kernel Functions in Support Vector Machine for Survival and Mortality Classification of Critical Patients using Blood Biomarkers

Authors: Kunthida Srilasak, Metee Meelap, Sira Jampa-ngern and Noramon Dron (Srinakharinwirot University, Thailand)

Abstract: Accurate prognostic assessment remains a major challenge in critical care due to the heterogeneity of critically ill patients. Blood biomarkers have been widely used for outcome prediction, while recent advances in machine learning have enabled more effective analysis of complex clinical data. However, the optimal Support Vector Machine (SVM) kernel function and biomarker observation window for prognostic classification in heterogeneous critically ill patients remain unclear. This study compared the performance of different SVM kernel functions for survival and mortality classification over different observation windows using six blood biomarkers: platelet count, white blood cell count, blood urea nitrogen, creatinine, lactate, and pH. Model performance was evaluated using five-fold stratified cross-validation. The results demonstrated that the Polynomial kernel outperformed the Linear and Gaussian radial basis function (RBF) kernels, while the five-day observation window provided the highest predictive performance. These findings suggest that SVM combined with blood biomarkers is a promising approach for survival and mortality prediction and may support clinical decision-making in critically ill patients.

1571322723 — Hidden Markov Models for Clinical State Modeling in ICU Mortality Prediction

Authors: Pongpanoot Kasembunyakorn, Sira Jampa-ngern and Noramon Dron (Srinakharinwirot University, Thailand)

Abstract: Intensive care units (ICUs) rely on laboratory markers to judge how severe patient's condition is, but common severity scores combine these markers into a single value and ignore how each one changes over time. It is therefore unclear how much a single marker's day-to-day trend, on its own, tells us about survival. To address this problem, we evaluated six routine markers: lactate, white blood cell count (WBC), blood pH, platelet count, creatinine, and blood urea nitrogen (BUN). Continuous markers are turned into a simple Stable-Deteriorating-Critical trend and used to predict in-hospital death with its own hidden Markov model (HMM), tested by five-fold cross-validation. Creatinine, BUN, and lactate predicted death best (AUROC is 0.64). Platelet count and WBC classified each day's state accurately but did not separate survivors from non-survivors above chance (AUROC is around 0.54 to 0.55) at predicting the final outcome, and pH carried no useful signal. These results give a clear, marker-by-marker baseline showing which routine markers hold the most survival information, and a starting point toward developing more complex models.

1571323513 — Differential Radiomic Signatures Across Brain Regions in Schizophrenia, ADHD, and Bipolar Disorder: A Multi-Model Consensus Framework

Authors: Karnpitcha Meekul (Satriwithaya School, Thailand); Suejit Pechprasarn (Rangsit University, Thailand); Kwinnat Yuenyongpisit (Satriwithaya School, Thailand)

Abstract: The clinical characteristics of attention-deficit/hyperactivity disorder (ADHD), bipolar disorder, and schizophrenia frequently coincide, making differentiated diagnosis challenging. Each of the three disorders has been linked to structural MRI abnormalities, although it is yet unknown if particular brain regions serve as biomarkers unique to each illness. Using the public ds000030 dataset (n=265), we provide a multi- model consensus approach to detect differential radiomic signatures. We extracted first-order and histogram-based radiomic features from 10 Harvard-Oxford Atlas locations after N4 bias correction and MNI registration. Nine machine learning models were trained using nested cross-validation. We combined their feature importance into a consensus, summarized it, and verified it with SHAP. The precuneus, anterior cingulate, and temporal pole were repeatedly highlighted by the consensus despite the poor four-class classification (balanced accuracy 0.373, over the 0.25 chance threshold), with significant agreement between SHAP and built-in relevance (Spearman's rho = 0.82). Disorder-differential patterns were identified by per-region analysis: the amygdala was most discriminative for ADHD (AUC = 0.64), and the temporal pole was most discriminative for schizophrenia (AUC = 0.75). These areas concurred with known neuroimaging results. Our findings demonstrate that interpretable, disorder-differential radiomic biomarkers that are consistent across models and supported by prior research can be identified through a performance- weighted consensus across multiple models.

1571323790 — Divergence Between WHO Laboratory and Non-Laboratory CVD Risk Charts Across Stepwise Population Survey and Portable Health Clinic

Settings in Bangladesh

Authors: Md Jobayer Hossain Chowdhury and Syed Usama Hussain Shah Bukhari (Kyushu University, Japan); Ashir Ahmed (Kyushu University & Grameen Communications, Japan)

Abstract: The World Health Organization (WHO) 2019 cardiovascular disease (CVD) risk charts exist in a laboratory- based version (using total cholesterol and diabetes status) and a non-laboratory-based version (using body-mass index, BMI) promoted for resource-limited settings. Whether the two charts agree equally well across different clinical settings is unknown. The present analysis compared the Who CVD risk charts across two independent Bangladeshi datasets. The WHO laboratory and non-laboratory charts were applied to (1) the nationally represen- tative STEPS 2018 survey (paired cohort N =3,300) and (2) the Portable Health Clinic (PHC), a portable health care system with an integrated EHR (Electronic Health Record) (paired cohort N =1,762), restricted to adults aged 40-74 years. Agreement was assessed with Bland-Altman analysis, Passing-Bablok regression, Spearman correlation, Cohen's kappa, Lin's concordance correlation coefficient (CCC), and Stuart-Maxwell/Bowker tests of marginal homogeneity; screening performance was evaluated against laboratory thresholds. In STEPS the charts agreed closely (risk gap, lab − non-lab, −0.1 pp; 95% limits of agreement −2.9 to +2.8 pp; CCC 0.896; Passing-Bablok slope 1.00). In PHC the risk gap was far larger (+2.2 pp; limits −4.7 to +9.1 pp; CCC 0.774; Passing-Bablok slope 1.20), widening with risk (Stuart-Maxwell $\chi 2=358.9$, $p<0.001$). At the ≥20% treatment threshold the non-laboratory chart missed 137/177 (77.4%) laboratory-defined high-risk adults in PHC (sensitivity 22.6%). A two-stage protocol (non-laboratory ≥10% triage → laboratory confirmation at ≥20%) recovered sensitivity to 97.7% while sparing 71.7% of blood tests. Agreement between the WHO charts is setting-dependent, driven chiefly by diabetes and cholesterol prevalence. The non-laboratory chart is adequate for low-risk population screening but materially under-detects high- risk patients in the PHC setting; a two-stage protocol resolves this trade-off. The chart's exclusive reliance on smoked-tobacco status is a further, under-recognised blind spot given the high prevalence of smokeless tobacco use in South Asia.

1571322685 - Customized 3D Ocular Prosthesis

Authors: Jitpimon Siripanth, Amakorn Poommoon, Faculty of Dentistry, Thammasat University; Sakchai Vongkittirux, Tanakorn Aurboonsong, Department of Ophthalmology, Faculty of Medicine, Thammasat University; Waraporn Mitsuntisuk, Passsawut Tokeaw, Department of Ophthalmology, Faculty of Medicine, Kasetsart University; Nedchanok Nakham, Jaisai Sampasneetamrong, Pakin Charassathien, Chulabhorn International College of Medicine, Thammasat University

Abstract: Eye loss from various causes significantly impacts patients' quality of life, affecting their psychological and social well-being. Conventional customized ocular prosthesis creation by gypsum molding and hand-painting is a lengthy, manual process with variable quality. To overcome this, a multidisciplinary team developed 3D printed customized ocular prosthesis. This innovative method uses 3D printing to create a customized conformer for direct fitting, improving accuracy and eliminating conventional process. Crucially, patients receive the personalized prosthesis in a single visit, thus, reducing costs, improving their convenience, and dramatically shortening wait times and ultimately enhancing their quality of life.

D3R3ML

Cardiovascular and respiratory systems

Session Chair: Kuo-Yung Hung

Time	Paper ID	Presenter	Paper Title
10:45-11:00	1571303046	Tsubasa Tomii	Heartbeat-Synchronized Motor Speed Modulation Using High Sensitivity Self-Sensing in a Magnetically-Ventricular Assist Device
11:00-11:15	1571314666	P. Naiyanetr	Design and Development of a Total Artificial Heart Using Computational Fluid Dynamics
11:15-11:30	1571315983	Vasit Sirilapanan	A Virtual Flow Blockage Framework for Hemodynamic-Based Thrombosis Modeling
11:30-11:45	1571321186	Chiharu Kutsuzawa	Development of a magnetically levitated shear loading device for evaluating shear endurance of blood
11:45-12:00	1571322223	T. Wisitponchai	An Eulerian Multiphase Framework for Investigating Thrombus Stability and Deformation
12:00-12:15	1571322678	Akkarwin Li	In-Vitro Hemodynamic Evaluation of an Atrial Shunting Device Using a Custom Mock Circulatory System
12:15-12:30	1571315222	Chieru Muta	Development of a Fully Passively Levitated Blood Pump Using Axial Thrust and Passive Magnetic Bearings

1571303046 — Heartbeat-Synchronized Motor Speed Modulation Using High Sensitivity Self-Sensing in a Magnetically-Ventricular Assist Device

Authors: Tsubasa Tomii, □□□ and Wataru Hijikata (Institute of Science Tokyo, Japan)

Abstract: As the number of patients with heart failure continues to increase, the long-term use of ventricular assist devices (VADs) has become increasingly common. However, continuous-flow support may prevent aortic valve opening, which can lead to thrombus formation around the valve. To address this problem, heartbeat-synchronized motor speed modulation has been investigated, in which blood flow assistance by a VAD is synchronized with the pulsation of the diseased heart. Accurate estimation of cardiac pulsation is essential for realizing this control. However, weak pulsations are difficult to estimate because the power spectral density ratio (PSD ratio) of the pulsation component to the non-pulsation component is low. In this study, the impeller support stiffness was shaped in each frequency range using a loop-shaping method based on H-infinity control theory. Compared with the conventional control system, the proposed method improved the PSD ratio of the estimated pump flow rate by about 2.0 times. Furthermore, self-sensing heartbeat-synchronized motor speed modulation was achieved without additional sensors under weak pulsation conditions, while maintaining the phase difference between the pulsation and the reference flow rate within a quarter cycle.

1571314666 — Design and Development of a Total Artificial Heart Using Computational Fluid Dynamics

Authors: Phornphop Naiyanetr, Goragoch Gesprasert, Nontakorn Chatsongjaroen and Pech Chatsirinoppakun (Mahidol University, Thailand)

Abstract: This study presents the design and development of a total artificial heart intended as a bridge to transplantation for patients with end stage heart failure. The blood pump geometry is optimized by varying both housing and impeller parameters. Each design is evaluated using CFD (ANSYS Fluent). From CFD simulation, hydraulic performance, wall shear stress, and normalized index of hemolysis are calculated at multiple flow rates and rotational speeds. From CFD, at 2750 rpm and 5 L/min, the final model can generate both left and right head pressure; 137.946mmHg and 26.647mmHg, respectively. In comparison with the initial model, the final model can increase both left and right head pressure by 3.62 % and 4.45 %, respectively. The normalized index of hemolysis (NIH) was 0.0315 g/100L (reduced by 21.25 % from the initial model). The final model also provided a wider operating range and achieved maximum systemic pressure before reaching the hemolysis threshold. A prototype was then evaluated in a mock circulatory loop using a blood analog (water - glycerin solution). From the experiment, hydraulic parameters of left side pump followed the same trend as the simulation results. In conclusion, both CFD simulation and prototype experiments show that the proposed design process can improve both hemodynamic performance and hemocompatibility of a compact total artificial heart pump. Therefore, this study provides a foundation for future prototype refinement.

1571315983 — A Virtual Flow Blockage Framework for Hemodynamic-Based Thrombosis Modeling

Authors: Vasit Sirilapanan (Kasetsart University, Thailand); Pongnarit Plengsangsri (Thailand); Fida Majdoub (ECAM Lasalle, France); Thunyanoot Prasertsakul and Chanon Ariyaprakai (Navamindradhiraj University, Thailand); Yongmann Chung (University of Warwick, United Kingdom (Great Britain))

Abstract: Thrombosis is a major contributor to stroke and is strongly associated with disturbed hemodynamics. Early identification of thrombosis prone regions, particularly in the deep veins where thrombus formation frequently initiates, is therefore essential for timely intervention but remains challenging. In this study, a virtual flow blockage model (VFBM) has been developed to represent thrombosis through progressive flow obstruction governed by local hemodynamic conditions. The model is calibrated using experimentally measured thrombus volume data by identifying threshold ranges of streamwise velocity and strain rate associated with thrombosed regions. Transient computational fluid dynamics simulations were performed in a backward-facing step geometry which promotes flow recirculation, while the Carreau-Yasuda non Newtonian viscosity model was used to capture the shear thinning behavior of blood flow. Within the VFBM framework, flow resistance gradually increased in computational elements that satisfy the calibrated thrombus risk criteria, enabling simulation of thrombus nucleation and propagation as a flow driven process. The resulting virtual blockage adaptively alters the effective flow domain and influences downstream hemodynamics. This approach provides a computationally efficient framework for simulating thrombosis and performing hemodynamics-based thrombus risk assessment.

1571321186 — Development of a magnetically levitated shear loading device for evaluating shear endurance of blood

Authors: Chiharu Kutsuzawa (Tokyo Institute of Technology, Japan); Wataru Hijikata (Institute of Science Tokyo, Japan)

Abstract: Acquired von Willebrand syndrome (AVWS), which is caused by the degradation of high-molecular-weight multimers of von Willebrand factor (vWF), is induced by the high shear stress generated in ventricular assist devices (VADs). Since the susceptibility of vWF to shear-induced degradation varies among patients, a quantitative and homogeneous shear-loading system for evaluating individual resistance to vWF degradation is required. In this study, we designed and prototyped a magnetically levitated shear loading device, consisting of a levitating and stationary inner cylinder and a rotating outer cylinder. The inner cylinder is supported by magnetic bearings, and a "shear-center system" to compensate for magnetic imbalance and maintain the inner cylinder at the center of the shear field. The device control system were designed based on magnetic field analysis and dynamic modeling. Furthermore, levitation experiments of a prototype device were conducted with the shear loading section filled with tap water. The results demonstrated that the inner cylinder stably reached and maintained the target position even when the outer cylinder was rotated at 2,000 rpm. These findings demonstrate the feasibility of the designed magnetically levitated shear loading device as a platform for shear endurance evaluation of resistance to vWF degradation.

1571322223 — An Eulerian Multiphase Framework for Investigating Thrombus Stability and Deformation

Authors: Tanchanok Wisitponchai, Nutthanan Wanluk, Sarinporn Visitsattapongse and Chuchart Pintavirooj (King Mongkut's Institute of Technology Ladkrabang, Thailand); Asimina Kazakidi (University of Strathclyde, United Kingdom (Great Britain))

Abstract: Thrombosis is a major contributor to cardiovascular and cerebrovascular disease, where thrombus deformation and embolization can lead to severe ischemic events. Existing computational models often represent thrombi as fixed geometries or rely on prescribed constitutive formulations, their ability to investigate thrombus deformation and mechanical stability under hemodynamic loading. In this study, an Eulerian multiphase (EMP) framework was developed to model thrombus as an evolving continuum phase interacting with blood flow. A concentration-dependent momentum sink term was introduced to represent thrombus mechanical resistance. Parametric analyses were performed by varying the resistance coefficient, pseudo-viscosity, and model exponent. Results showed that pseudo-viscosity primarily governed the onset of thrombus mobility, whereas the resistance coefficient controlled the magnitude of deformation. The proposed formulation reproduced stable, transitional, and highly deformable thrombus morphologies and naturally generated heterogeneous core-shell structures. Hemodynamic analysis revealed localized flow acceleration over the thrombus apex, accompanied by elevated wall shear stress, vorticity, and lift forces concentrated along the blood-thrombus interface, indicating regions of greatest hydrodynamic loading. These findings demonstrate the potential of the EMP framework for investigating the coupled interactions between thrombus mechanics and hemodynamics and provide a foundation for future multiphase blood-thrombus simulations.

1571322678 — In-Vitro Hemodynamic Evaluation of an Atrial Shunting Device Using a Custom Mock Circulatory System

Authors: Akkarwin Li and Anak Khantachawana (King Mongkut's University of Technology Thonburi, Thailand)

Abstract: Heart Failure with Preserved Ejection Fraction (HFpEF) remains a critical cardiovascular challenge characterized by elevated left atrial pressure (LAP) and limited pharmacological treatment options. Interatrial shunting has emerged as a promising device-based therapy; however, robust preclinical evaluation is required to ensure safety and efficacy. This study evaluates the hemodynamic performance of an 8-mm Atrial Depressurized Device (ADD) utilizing a custom-developed pulsatile Mock Circulatory System (MCS). Integrated with a patient-specific silicone atrial model, the MCS was configured to simulate four distinct HFpEF congestion scenarios under both resting (60 BPM) and exercise (100 BPM) conditions. Real-time pressure monitoring demonstrated that the system achieved rapid transient stabilization within 8 to 10 seconds post-shunting. Hemodynamic assessments revealed that the ADD significantly reduced LAP (by an average of 2.27 mmHg at rest and 6.15 mmHg during exercise) while moderately increasing right atrial pressure. The intervention successfully alleviated left-side congestion without causing complete interatrial pressure equalization, maintaining the essential systemic-to-pulmonary pressure gradient. These experimental results closely align with established clinical data, validating the therapeutic efficacy of the 8-mm ADD and confirming the reliability of the developed MCS as an advanced in-vitro platform for cardiovascular device evaluation.

1571315222 - Development of a Fully Passively Levitated Blood Pump Using Axial Thrust and Passive Magnetic Bearings

Authors: Chieru Muta and Wataru Hijikata (Institute of Science Tokyo, Japan)

Abstract: Ventricular assist devices (VADs) support blood circulation in patients with heart disease by rotating an impeller. For long-term use, noncontact impeller support is required to improve durability and reduce blood damage. However, conventional support methods have difficulty achieving both passive operation and a large fluid gap. Therefore, this study proposes a new passive levitation system that utilizes axial thrust and magnetic force to enable passive impeller levitation while maintaining a large fluid gap. In the proposed system, permanent magnets support the radial and angular motions, whereas axial thrust generated by the pumping flow supports the axial motion. Although axial thrust is generally reduced in centrifugal pumps, this study deliberately utilizes it as a restoring force. The pump geometry was designed using computational fluid dynamics so that the axial thrust changes with the axial displacement of the impeller. Four shroud dimensions were subsequently optimized using an L9 orthogonal array. The optimized geometry achieved 3.65 times the axial thrust stiffness of the redesigned gap geometry before L9 optimization while maintaining sufficient pump performance. These results demonstrate the feasibility of passive large gap impeller levitation using axial thrust and magnetic force.

D3R4ML

Biomedical Signal Processing IV

Session Chair: Tohru Yaki

Time	Paper ID	Presenter	Paper Title
10:45–11:00	1571299587	Ir. Dr. A. Azhim	AI-Based Vascular Age Regression Using Carotid Doppler Hemodynamic Features
11:00–11:15	1571306249	V. Phanichraksaphong	Wavelet Feature Extraction with Deep Learning Models for Heart Sound Recognition
11:15–11:30	1571306860	Saravanan M	Template Matching-based Detection of Interictal Epileptiform Discharges (IEDs) in Human sEEG data
11:30–11:45	1571306951	Yicong Xiao	Categorization and Spatiotemporal Analysis Reveal Motor Functional Heterogeneity in Utah Array Recordings
11:45–12:00	1571311730	Helen Mao	Entrainment of Alpha Oscillations in a Wilson-Cowan Neural Population
12:00–12:15	1571312939	P. Tangkiatphaibun	Raman Spectroscopy and Machine Learning for Classification of Edible Oils Using an Open-Source Spectral Dataset
12:15–12:30	1571313859	Yuchen Liu	Rapid Detection of BRCA1 Mutation using Gold Nanoparticles and a Portable Optical System

1571299587 — AI-Based Vascular Age Regression Using Carotid Doppler Hemodynamic Features

Authors: Ir. Dr. Azran Azhim (National Institute of Technology Kitakyushu College, Japan); Jun Matsukubo (Information Systems Course, Japan)

Abstract: Vascular aging is closely associated with arterial stiffness and altered hemodynamic characteristics, which are important indicators of cardiovascular risk. This study proposes an AI-based vascular age regression framework using carotid Doppler hemodynamic features for continuous vascular aging assessment. Pulsed-wave Doppler blood flow velocity waveforms were obtained from the common carotid artery of 202 healthy subjects aged between 20 and 69 years. Several physiologically meaningful waveform features, including peak systolic velocity (S1), reflected wave peak (S2), inflection point (I), diastolic peak (D), end-diastolic minimum (d-min), resistive index (RI), velocity reflection index (VRI), and velocity elastic recoil index (VEI), were extracted for machine learning analysis. A Random Forest regression model was employed to estimate vascular age using the extracted hemodynamic features. Experimental results demonstrated a regression performance with a mean absolute error (MAE) of 8.8 years, root mean square error (RMSE) of 10.56 years, and coefficient of determination (R^2) of 0.623. Feature importance analysis revealed that VRI was the dominant predictor associated with vascular aging, followed by S1 and d- min velocity features. The proposed framework provides a non-invasive and physiologically interpretable approach for continuous vascular age estimation using Doppler ultrasound signals and explainable machine learning techniques. The findings suggest the feasibility of AI-assisted vascular aging assessment for future cardiovascular screening applications.

1571306249 — Wavelet Feature Extraction with Deep Learning Models for Heart Sound Recognition

Authors: Varinya Phanichraksaphong (King Mongkut's Institute of Technology Ladkrabang, Thailand & School of Engineering, Thailand); Supakorn Suwan and Pongthep Poungthong (King Mongkut's Institute of Technology Ladkrabang, Thailand)

Abstract: Currently, heart disease has risen significantly in recent years due to demographic changes. Both men and women are showing more cases of abnormalities detectable through phonocardiogram(PCG) signals. These signals are widely used to diagnose for identifying a wide range of cardiovascular conditions, including arrhythmias, valvular heart diseases, congenital heart defects, cardiomyopathies, and heart failure. In this research, we apply wavelet scattering transform(WST) and continuous wavelet transform(CWT) as wavelet analysis techniques. For the Deep learning component, we incorporate three primary architectures a one-dimensional CNN(WaveNet), a two- dimensional CNN(MLNet) and a self-attention Transformer to classify heart sounds from phonocardiogram (PCG). By identifying heart sounds using phonocardiogram(PCG) data, the ensemble technique of our deep learning model achieves better performance than recent studies and is effectively applied to diagnosing and predicting cardiac disorders.

1571306860 — Template Matching-based Detection of Interictal Epileptiform Discharges (IEDs) in Human sEEG data

Authors: Saravanan M (Indian Institute of Science, Bengaluru, India); Krishnakumaran Rajendran (Indian Institute of Science, Bangalore, India); Shabari Girishan Kv (Indian Institute of Science Bangalore, India); Kirteyman Singh Rajput (Indian Institute of Science, Bangalore, India); Kalyani Karkare (Ramaiah Medical College and Memorial Hospital, India); Hardik J. Pandya (Indian Institute of Science Bangalore, India)

Abstract: In drug-resistant epilepsy (DRE), seizure zones are localized by identifying characteristic neural signatures in stereo-electroencephalography (sEEG) recordings. Despite its diagnostic precision, sEEG analysis remains time-intensive because it relies on manual expert review over extended recording durations. Automating this process would reduce neurologists' workload and improve diagnostic efficiency. Interictal epileptiform discharges (IEDs) serve as continuous, spatially informative surrogate markers of the epileptogenic zone, making them the primary target for automated long-term sEEG monitoring. Four significant IED signatures were identified, including interictal spikes, sharp discharges, slow-wave discharges, and High Frequency Oscillations (HFOs). A hybrid signal-processing and feature-fusion framework was developed to detect, organize, and analyze IEDs, accounting for patient-specific variability. The algorithm processes raw sEEG signals through a multi- stage pipeline. Temporally segmented epochs are transformed into Gabor-filter-based feature matrices, multiplicatively fused to suppress noise, and then refined through adaptive modulation and normalization. The resulting features pass through a competitive weighted decision pipeline to minimize false detections, yielding a unified output of detected IED events or quantitative metrics for clinical interpretation. The spatiotemporal analyses are verified by an epileptologist, and the results are reported.

1571306951 — Categorization and Spatiotemporal Analysis Reveal Motor Functional Heterogeneity in Utah Array Recordings

Authors: Yicong Xiao and Juan Pablo Botero Torres (University of Utah, USA); Spencer Kellis (Blackrock Neurotech, USA); Florian Solzbacher (University of Utah, USA)

Abstract: The Utah Electrode Array (UEA) is widely used to record neural signals from motor- related cortical areas, but differences in electrode location and implantation depth can cause differences in recorded neural signals, introducing motor functional heterogeneity within the array. This study analyzed neural signals recorded from the UEAs implanted in the frontal motor cortex of two monkeys. Electrodes were categorized into early- and late-response types based on their temporal firing characteristics. While each UEA exhibited a dominant response type, a subset of electrodes showed another type. The analysis revealed functional heterogeneity in neural signals recorded from the UEAs and suggests that the coexistence of different response types within a single UEA may result from uneven implantation depths or proximity to functional boundaries. These findings provide a reference for understanding functional heterogeneity and suggest the need to account for such functional heterogeneity when interpreting chronic intracortical recordings.

1571311730 — Entrainment of Alpha Oscillations in a Wilson-Cowan Neural Population

Authors: Helen X Mao (Yale University, USA); Yao Lin (Westlake University, China); Jijun Yin (Qualcomm, USA); Meir H Kryger (Yale University, USA)

Abstract: Alpha band oscillations (8-12 Hz) play a key role in sleep regulation and onset. The goal of this paper is to analyze the influence of external electrical stimulation on alpha waves in the brain; such influence could potentially lead to more effective sleep-aid technologies that utilize targeted stimulation. Recent studies have shown that electrical stimulation can guide brain waves and modulate neural rhythms. However, population-level dynamics are difficult to study through physical experiments. This paper utilizes the Wilson-Cowan equations, which describe the dynamics between excitatory and inhibitory neuron populations, to model alpha wave generation. We mathematically analyze the equations to describe and predict the behavior of alpha oscillators, including linearizing the nonlinear system about a fixed point to take advantage of frequency analysis from linear systems. This allows analysis of the resonant frequencies of alpha oscillations. We also use simulation to demonstrate that the model's self-sustained oscillations can be guided by stimulations near the natural resonant frequency of the system, implying that transient alpha waves in the brain may be influenced by external electrical stimulation. We conclude that alpha-band waves can be guided by targeted stimulation, which provides a theoretical foundation for the development of personalized technologies designed to improve relaxation and sleep quality.

1571312939 — Raman Spectroscopy and Machine Learning for Classification of Edible Oils Using an Open-Source Spectral Dataset

Authors: Parawee Tangkiatphaibun (King Mongkut's Institute of Technology Ladkrabang & AIRC Advanced Imaging Research Centre, Thailand); Pasin Kuncharin (KMITL, Thailand); Angélique Roux (Polytech Marseille Aix-Marseille Universit, France); Wibool Piyawattanametha (KMITL and Chulalongkorn University, Thailand)

Abstract: The authentication of edible oil is currently significant for adulteration prevention and food quality control. Eight classes of edible oil were analyzed using machine learning techniques in this study. The dataset consisted of 560 spectra collected from olive, canola, coconut, grape seed, sesame, peanut, sunflower seed, and linseed oils. Before the classification, a Principal Component Analysis (PCA) was applied to reduce spectral dimensionality. Several machine learning algorithms, including Support Vector Machine (SVM), Linear Discriminant Analysis (LDA), K-Nearest Neighbor (KNN), and Random Forest (RF), were trained. The best classification accuracy of 77.1% was acquired using PCA-SVM models, while Random Forest achieved 62.1%. The findings suggest that Raman spectroscopy combined with machine learning can be used for automated edible oil classification. This may support future food authentication applications.

1571313859 — Rapid Detection of BRCA1 Mutation using Gold Nanoparticles and a Portable Optical System

Authors: Yuchen Liu (Shanghai University, China)

Abstract: To address the limitations of long turnaround time and high equipment cost in existing methods for detecting pathogenic BRCA1 mutations, this study developed a photodiode-transimpedance amplifier (TIA) current detection platform based on the selective crosslinking-induced aggregation of gold nanoparticles (AuNPs). In the presence of complementary targets, AuNP aggregation causes solution discoloration, and the resulting change in transmittance can be quantitatively reflected by the photocurrent magnitude. Using an 8 bp deletion mutation in the BRCA1 gene as a model, wild-type and mutant samples exhibited significantly different photocurrent responses over the range of 1-100 nM, with a detection limit of 1 nM. The platform is simple to operate, completes detection within approximately 40 min, and provides a cost-effective and sensitive new strategy for the rapid screening of BRCA1 mutations.

D3R1AE

Biomedical Signal Processing V

Session Chair: Shin'ichiro Kanoh

Time	Paper ID	Presenter	Paper Title
10:45–11:00	1571322290	Honoka Funatsuki	Spatiotemporal Properties and Classification of Estimated Cortical Current Responses Evoked by Vibrotactile Stimulation of Finger Segments
11:00–11:15	1571322638	N. Siribunyaphat	Continuous Sequential Command Generation in SSVEP-Based Brain-Computer Interfaces Using Multi-Level Time-Varying Frequency Visual Stimuli
11:15–11:30	1571322719	Arthit Buranasing	Context-Aware Mental Stress Detection in Free-Living Conditions: Mitigating Confounding Variables via Multi-Modal Wearable Data Fusion
11:30–11:45	1571322804	P. Panyachuai	Low-Latency Sleep Stage Classification from Single Channel EEG for Adaptive Sleep Apnea Alarm Systems
11:45–12:00	1571322873	Yuki Jono	The Effects of Different Smartphone Notification Sounds on Sustained Attention: Behavioral and Electroencephalographic Measures
12:00–12:15	1571322900	Togi Kurata	A Feasibility Study of Feature Extraction Methods to Improve Finger Movement Classification from Cortical Currents
12:15–12:30	1571322912	Masato Kudo	Neural Signature of Motor Imagery for Wings: A Pilot Study on Supernumerary Limbs Without Human Anatomical Counterparts

1571322290 — Spatiotemporal Properties and Classification of Estimated Cortical Current Responses Evoked by Vibrotactile Stimulation of Finger Segments

Authors: Honoka Funatsuki, Simon Kojima and Shin'ichiro Kanoh (Shibaura Institute of Technology, Japan)

Abstract: Somatosensory imagery-based BCI (SI-BCI) enables users to control external devices by imagining sensations on specific body locations. However, the low spatial resolution of electroencephalography (EEG) makes it difficult to distinguish between closely spaced body locations, such as individual fingers. To address this, our previous study employed cortical current estimation and demonstrated different spatial distributions in cortical responses evoked by vibrotactile stimulation to different fingers, thereby revealing the feasibility of their classification. In this study, the possibility of discriminating between the proximal and distal phalanges within the same finger was investigated. Oscillatory EEG responses evoked by vibrotactile stimulation were analyzed, and estimated cortical currents and their spatial distributions were evaluated and compared. The results showed differences in the spatial distributions between the proximal and distal phalanges of the same finger. Furthermore, the grand average classification accuracy across subjects was approximately 95\%, showing the feasibility of discriminating different finger segments using SI-BCI.

1571322638 — Continuous Sequential Command Generation in SSVEP-Based Brain-Computer Interfaces Using Multi-Level Time-Varying Frequency Visual Stimuli

Authors: Nannaphat Siribunyaphat, Natjamee Tohkhwan, Yunyong Punsawad, Danaya Tongpradit, Soraya Tohhad and Chutima Choochot (Walailak University, Thailand)

Abstract: This research presents the analysis and evaluation of a continuous command generation system from a steady-state visual evoked potential (SSVEP) signal using a multi-level flickering square visual stimulus with time-varying frequency. Three signal analysis methods were used: Dynamic Power Spectral Density (Dynamic PSD), Short- Time Fourier Transform (STFT), and Continuous Wavelet Transform (CWT), to compare the frequency component tracking ability and signal classification accuracy under analysis time intervals of 1 second and 2 seconds. The results showed that CWT performed best under all conditions, achieving 95.2% accuracy for 1 seconds and 99.6% for 2 seconds. Furthermore, classification under increasing and decreasing frequency stimulus modes showed CWT achieving the highest accuracy of 99.2% and 100%, respectively. For continuous command generation evaluation, the system achieved an average accuracy of 98% in increasing frequency mode and 100% in decreasing frequency mode under 3, 4, and 5 command cycles. These results demonstrate that the CWT method is suitable for feature extraction of time-varying frequency SSVEP signals. The proposed system has the potential for application in brain-signal control systems that require a sequential sequence of commands.

1571322719 — Context-Aware Mental Stress Detection in Free-Living Conditions: Mitigating Confounding Variables via Multi-Modal Wearable Data Fusion

Authors: Arthit Buranasing (Srinakharinwirot University, Thailand)

Abstract: Continuous mental stress monitoring in free-living conditions using consumer-grade wearables remains a significant challenge due to high levels of biological noise. Models relying solely on Heart Rate Variability (HRV) often suffer from high False Positive Rates (FPR), as they struggle to differentiate psychological stress from physiological responses to physical exertion or accumulated fatigue. This study proposes a Context- Aware Architecture (Model C) that fuses dynamic short-term physiological history (Rolling RMSSD) with cyclical temporal context (circadian rhythm) and recovery context (sleep efficiency). Utilizing the highly unconstrained MMASH dataset, the framework was evaluated using a rigorous Leave-One-Subject-Out Cross-Validation (LOSO-CV) scheme. The proposed model, powered by the eXtreme Gradient Boosting (XGBoost) algorithm, demonstrated robust performance in a highly noisy environment. The ablation study and subsequent threshold optimization revealed that integrating contextual data reduced the FPR from 45.45% (HRV-only baseline) to 41.14%, while maintaining a high F1-Score of 92.88% and an overall accuracy of 88.24%. The findings substantiate that multi-modal data fusion effectively mitigates confounding variables, making wearable stress detection significantly more reliable for real-world ambulatory applications by suppressing disruptive false alarms.

1571322804 — Low-Latency Sleep Stage Classification from Single Channel EEG for Adaptive Sleep Apnea Alarm Systems

Authors: Phanthakarn Panyachuai, Pakpum Somboon and Naricha Chirakalwasan (Chulalongkorn University, Thailand)

Abstract: Sleep stage classification is vital for sleep monitoring and the management of disorders such as obstructive sleep apnea (OSA). However, reliable classification from single- channel electroencephalography (EEG) remains challenging because of the complex temporal dynamics of sleep and the severe class imbalance inherent in sleep data. This study proposes an automatic sleep stage classification system for sleep apnea monitoring based on single-channel EEG and a dual-branch CNN-BiLSTM architecture. EEG signals from the Sleep-EDF Cassette dataset (100 Hz) are segmented into 5-second epochs and processed through parallel short-term and long- term convolutional branches, followed by Squeeze-and-Excitation attention and a Bidirectional LSTM. A Weighted Cross-Entropy objective addresses class imbalance, while an HMM with Viterbi decoding is applied as a post-processing stage to enforce physiologically plausible sleep stage transitions. To strengthen temporal modeling, a Context Window formulation incorporating multiple consecutive epochs is introduced. The HMM post-processing stage improves overall accuracy from 75.44% to 84.07%, while the eight-epoch Context Window ensemble further achieves the best overall accuracy of 85.21% and a macro F1-score of 79.76%, improving the F1-score of the transitional N1 stage from 35.1% to 46.5%. These findings demonstrate that incorporating multi-epoch temporal context substantially improves light-sleep stage detection and provides a promising foundation for future real-time adaptive alarm systems for sleep apnea, in which stimulus intensity is modulated according to the estimated sleep depth

1571322873 — The Effects of Different Smartphone Notification Sounds on Sustained Attention: Behavioral and Electroencephalographic Measures

Authors: Yuki Jono, Miki Kaneko and Keiji Iramina (Kyushu University, Japan)

Abstract: This study examined behavioral and exploratory EEG responses to smartphone- related notification sounds during a sustained arithmetic task. Fifty-one participants performed a 15-min continuous one-digit addition task while BeReal, Rebound, and Vibration sounds were presented twice each. EEG was recorded from a subset of 8 participants, and frontal log-transformed theta/beta ratio (TBR) was analyzed. Reaction time significantly increased in the 0-4 trials after all three sounds. The magnitude of slowing did not significantly differ among sound types. However, BeReal non-users showed a larger reaction time increase than users after the BeReal sound, suggesting that application experience may modulate behavioral responses to notification sounds. Frontal TBR did not show a consistent group-level pre-post change. However, exploratory EEG analysis may suggest sound-dependent tendencies and a moderate non-significant association with the Smartphone Addiction Proneness Scale score. These findings indicate that smartphone-related notification sounds can automatically capture attention and produce measurable, short-lived interference during sustained cognitive work. Exploratory behavioral and EEG results further suggest that application experience and problematic smartphone use may modulate individual responses to notification sounds

1571322900 — A Feasibility Study of Feature Extraction Methods to Improve Finger Movement Classification from Cortical Currents

Authors: Togi Kurata, Shunnosuke Okada, Honoka Funatsuki, Simon Kojima and Shin'ichiro Kanoh (Shibaura Institute of Technology, Japan)

Abstract: Motor imagery-based brain-computer interface (MI-BCI) utilizing electroencephalogram (EEG) enables to classify motor cortex activity associated with mental imagery of specific body part movements e.g. left and right hand or feet. However, classifying smaller body parts, such as individual fingers, remains challenging due to the low spatial resolution of EEG signals. In this study, as a pilot study towards the detection of motor imagery of five individual fingers, feature extraction method from EEG signals during the execution of finger movement was investigated. We estimated cortical currents from EEG signals recorded during actual finger movements and evaluated both the spatial distribution of brain activity and classification performance to optimize data processing methods. Features were extracted from both raw EEG and estimated cortical currents using event-related desynchronization (ERD) within specific frequency bands and common spatial patterns (CSP). A support vector machine (SVM) classifier was then used to decode the five-finger movement patterns, and its performance was evaluated via 3-block cross-validation. The results showed that features derived from the estimated cortical currents consistently outperformed those from scalp EEG. Specifically, applying CSP to the cortical currents achieved an average classification accuracy of 88.0% across five subjects (reaching up to 96.3% in the best subject), significantly higher than the 24.3% obtained when applying CSP to the EEG signals. Furthermore, analysis of the CSP activation patterns confirmed that this approach effectively captured the subtle spatial differences in cortical activity corresponding to individual finger movements.

1571322912 — Neural Signature of Motor Imagery for Wings: A Pilot Study on Supernumerary Limbs Without Human Anatomical Counterparts

Authors: Masato Kudo (Kyushu University, Japan); Miki Kaneko (Osaka University, Japan); Keiji Iramina (Kyushu University, Japan)

Abstract: Recently, the field of supernumerary limbs (SLs), which aims to enhance human capabilities, has attracted increasing attention. In particular, many researchers have focused on how SLs controlled by electroencephalogram (EEG) affect brain activity and body ownership. However, many studies on the SLs have been limited to the duplication of existing body parts such as the third arm and the sixth finger. In this study, we focused on virtual wings as counterpart-free supernumerary limbs (CFSLs), which have no anatomical counterpart in the human body. We investigated how cortical representations are formed by motor imagery (MI) of the CFSLs by comparing them with MI of the hands as existing limbs. As a result, similar to hand MI, wing MI, for which no dedicated anatomical representation exists in the human motor cortex, evoked movement-related cortical potentials and a contralateral power decrease in the alpha band. Furthermore, by classifying MI of the hands and wings using a machine learning model, an average accuracy of 67% and an average AUC of 74% were achieved. These results suggest that MI of CFSLs, at least MI of the wings, has similar properties to MI of existing limbs, and forms a relatively independent cortical representation while recruiting cortical regions associated with existing body parts as functional substitutes for the CFSLs.

D3R2AE

Medical Image Processing V / Bio-robotics and biomechanics II

Session Chair: Manuel Lique Casaneve

Time	Paper ID	Presenter	Paper Title
10:45–11:00	1571323738	P. Pathomnop	Performance Comparison Between Multi-Class and Sequential Binary Deep Learning Frameworks for Osteoporosis and Osteopenia X-Ray
11:00–11:15	1571323766	Md Walid Hassan	Effect of Separation between ARF Excitation Pulses and Inclusion Size on Portable Viscoelastic Response Ultrasound Imaging Platform
11:15–11:30	1571323767	S. Mannan Trisha	Acoustic Parameter Sensitivity of VESTA for On-Axis ARFI Viscoelastic Ratio Estimation
11:30–11:45	1571325061	Diego Aedo	Exploring Explainability and Confidence for Pseudo-Label Selection in Biomedical Image Classification
11:45–12:00	1571312150	Kodai Ochi	Verification of Pressure Redistribution Capability in Plant-Incorporated Materials
12:00–12:15	1571312534	Yin Qing Tan	Gender Differences and Biomechanical Insights into Vertical Jump Performance in Young Adulthood
12:15–12:30	1571313825	Mutsuki Hagiwara	Model-based control of biohybrid actuators incorporating online parameter identification

1571323738 — Performance Comparison Between Multi-Class and Sequential Binary Deep Learning Frameworks for Osteoporosis and Osteopenia X-Ray

Authors: Puntharik Pathomnop (Satriwithaya School, Thailand); Piraya Waraporn (Satriwithaya School); Kitsada Thadson and Suejit Pechprasarn (Rangsit University, Thailand)

Abstract: Osteoporosis and osteopenia are progressive bone disorders characterized by reduced bone density and structural deterioration, increasing the risk of fractures and highlighting the importance of early diagnosis. Existing deep learning approaches for knee osteoporosis screening often evaluate only a limited number of convolutional neural network (CNN) architectures, providing limited insight into how network design influences classification performance. Therefore, this study systematically compares multiple CNN architectures using both multi-class and sequential binary classification frameworks for automated knee X-ray classification of normal, osteopenia, and osteoporosis cases. The dataset consisted of balanced knee X-ray images from three classes and was randomly split into 80% for training and 20% for validation. Image preprocessing included resizing all images to 224 × 224 pixels, applying random horizontal flipping and random rotation to the training images, and normalizing the input data using ImageNet statistics. Eleven CNN architectures, including GoogLeNet, ResNet18, ResNet50, ResNet101, EfficientNet-B0, DarkNet19, DarkNet53, ShuffleNet, DenseNet201, VGG16, and MobileNetV2, were initialized with ImageNet pre-trained weights and evaluated using two classification frameworks: sequential binary classification (normal-versus-abnormal followed by osteopenia-versus- osteoporosis) and direct multi-class classification. Among the evaluated architectures, ShuffleNet achieved the highest performance for the normal-versus-abnormal classification task, with an accuracy of 94.76%, precision of 95.04%, recall of 94.73%, and F1-score of 94.74%. For the osteopenia-versus-osteoporosis classification task, DarkNet19 achieved the best performance, with an accuracy of 87.76%, precision of 88.44%, recall of 88.22%, and F1-score of 87.76%. In the direct multi-class classification framework, VGG16 achieved the highest performance, with an accuracy of 79.53%, precision of 80.17%, recall of 79.62%, and F1-score of 79.59%. Overall, the sequential binary classification framework outperformed the direct multi-class classification approach, demonstrating the effectiveness of decomposing the three- class classification task into two binary classification stages.

1571323766 — Effect of Separation between ARF Excitation Pulses and Inclusion Size on Portable Viscoelastic Response Ultrasound Imaging Platform

Authors: Md Walid Hassan (University of Hawaii at Manoa, USA); Damian Cacko and Ziemowit Klimonda (Polish Academy of Sciences, Poland); Md Murad Hossain (University of Hawaii at Manoa, USA)

Abstract: Viscoelastic response (VisR) ultrasound is an on-axis acoustic radiation force (ARF)- based elastography method that qualitatively assesses tissue viscoelasticity by fitting ARF-induced displacement within the excitation region to a one-dimensional mass- spring-damper (MSD) model, yielding peak displacement (PD), relative elasticity (RE), and relative viscosity (RV). On-axis methods offer finer spatial resolution and depth sensitivity than off-axis shear-wave approaches but depend strongly on displacement SNR and model-fit stability, especially challenging on portable hardware. Extending our prior feasibility study

on the portable us4R-lite+ platform, we characterize how three factors affect inclusion detectability: the separation between the two co-localized ARF push pulses, set by the number of tracking pulses (Ntp) between them; the percentage of the displacement recovery profile used for MSD fitting; and inclusion diameter. Using an L7-4 array, inclusions of 4.7, 8.6, 34.0, and 70.9 kPa in a 16.7 kPa background were imaged in a CIRS 049A phantom, with Ntp varied from 4-10 at 10.4-mm diameter, and diameter varied from 2.5-16.7 mm at Ntp = 7. Detectability was quantified by contrast-to-noise ratio (CNR) of PD, RE, and RV at the CNR-optimal recovery-profile percentage for each condition. PD remained robust across the tested Ntp range, whereas the fit- derived RE and RV were more sensitive to push separation and to the recovery-profile percentage, with the tightest and highest CNR obtained at short push separation (Ntp = 4-5). CNR for all three parameters increased with inclusion diameter up to 10.4 mm. These results inform acquisition-timing and target-size design for portable point-of-care viscoelastic imaging.

1571323767 — Acoustic Parameter Sensitivity of VESTA for On-Axis ARFI Viscoelastic Ratio Estimation

Authors: Simina Mannan Trisha (University of Hawaii System, USA); Md Murad Hossain (University of Hawaii at Manoa, USA)

Abstract: Viscoelastic tissue characterization is increasingly recognized as a diagnostic biomarker in oncology, as tumor progression alters both tissue elasticity and viscosity in ways that neither property alone can fully capture. We recently developed VESTA, a two-stage machine learning pipeline that estimates elasticity ratio (ER) and viscosity ratio (VR) directly from normalized ARFI displacement features at the A-line level, without per-A-line model fitting. However, VESTA was trained on simulations with fixed acoustic parameters, and its robustness to acoustic acquisition conditions encountered in clinical settings such as variations in focal depth, F-number, attenuation, and sound speed has not been evaluated. To address this limitation, we investigate the acoustic parameter sensitivity of VESTA by applying each perturbation independently to two spherical inclusion test materials representing distinct ER-VR contrast regimes. For each condition, FEM (LS-DYNA) and acoustic (Field II) simulations were performed and the trained VESTA pipeline was applied without retraining. Results show that ER and VR predictions remained stable across all four perturbations, with changes in MPE of no more than +5.75% for ER and +3.0% for VR relative to baseline. The largest deviation was observed under F-number variation for the high-contrast material (ER MPE: 14.25% to 20.0%), while VR estimation remained robust across all conditions (MPE ≤ 7%). These findings demonstrate that VESTA generalizes to realistic acoustic parameter variation without retraining, supporting its feasibility for deployment across a range of clinical acquisition configurations.

1571325061 — Exploring Explainability and Confidence for Pseudo-Label Selection in Biomedical Image Classification

Authors: Diego Aedo and Christopher Flores (Universidad del Bío-Bío, Chile)

Abstract: Recent advances in biomedical image classification have been driven by deep neural networks and transfer learning, yet the scarcity of expert annotations remains a significant obstacle. Semi-supervised learning (SSL) addresses this challenge by leveraging unlabeled data via pseudo-labeling, though inaccurate pseudo-labels can introduce confirmation bias and degrade model performance. This study examines whether explanation-based signals, such as SHAP-derived relevance, offer complementary information to traditional prediction confidence for pseudo-label selection. SHAP is used to estimate the relevance of image regions, and progressive masking quantifies the impact on classification performance when the most relevant regions are progressively masked. The explanation-based score is then combined with prediction confidence to inform pseudo-label selection. Experiments on kidney and COVID-19 image classification tasks utilized SigLIP 2 with generic pretraining, together with generic and medical-domain variants of BiomedCLIP and RadImageNet. Supervised experiments demonstrate competitive classification performance across datasets and backbones, while the masking experiments confirm that progressively obscuring highly relevant regions consistently degrades predictive performance. In the semi-supervised setting, incorporating SHAP-derived information into confidence- based pseudo-label selection improves performance in certain configurations, particularly for SigLIP 2 and BiomedCLIP on the kidney task, and for BiomedCLIP on the COVID-19 task. However, confidence-only selection remains optimal for other cases, including RadImageNet and COVID-19 SigLIP 2. These findings suggest that explanation-based signals can serve as a valuable complementary criterion for pseudo-label selection in SSL, although their benefit depends on the dataset and visual backbone.

1571312150 — Verification of Pressure Redistribution Capability in Plant-Incorporated Materials

Authors: Kodai Ochi and Mitsuharu Matsumoto (The University of Electro- Communications, Japan)

Abstract: In recent years, research on biohybrid technology inspired by living organisms has been developing. However, development using living organisms is still limited, meaning the growth capabilities of living organisms cannot be fully utilized. Therefore, in this study, we propose a plant-incorporated material that utilizes the increase in volume due to the growth of living plants. In this paper, experiments were conducted to verify the potential of the stems and leaves that plants develop by growth to function as a cushioning material that disperses external forces inward. As a result, the pressure redistribution capability of the proposed method was confirmed through comparison experiments on the developed plant-incorporated materials depending on whether they contained plants.

1571312534 — Gender Differences and Biomechanical Insights into Vertical Jump Performance in Young Adulthood

Authors: Yin Qing Tan (Universiti Tunku Abdul Rahman, Malaysia); Siow Cheng Chan (University Tunku Abdul Rahman, Malaysia); Tan Wen Chin (Universiti Tunku Abdul Rahman, Malaysia)

Abstract: Vertical jump (VJ) performance is widely used to assess lower-limb power, neuromuscular coordination, and athletic capability. This study investigated gender differences and biomechanical characteristics across three types of VJ: squat jump (SJ), countermovement jump (CMJ), and countermovement jump with arm thrust (CMJAT) in healthy young adults. A total of 61 healthy participants (27 males and 34 females) were recruited. Jump height, take-off force, impact force, maximum concentric power, peak speed, and take-off speed were recorded using a G-walk sensor. Independent t-tests were used to compare performance between genders, while one-way ANOVA was conducted to evaluate the differences among jump conditions. Results showed that male participants achieved significantly greater jump height, take-off force, concentric power, peak speed, and take-off speed than females across all jump conditions ($p < 0.05$). Among the three jump conditions, CMJAT consistently produced the highest performance outcomes in both genders, with significant improvements in jump height, power output, and movement speed compared with SJ and CMJ. The enhanced performance observed in CMJAT is attributed to the additional contribution of arm swing, which facilitates greater utilization of the stretch-shortening cycle and increases mechanical work during take-off. These findings highlight the influence of gender and jump techniques on vertical jump performance. The incorporation of arm swing substantially enhances jumping ability. The study provides biomechanical insights that may contribute to the optimization of performance evaluation, conditioning strategies, and injury prevention in young adults.

1571313825 — Model-based control of biohybrid actuators incorporating online parameter identification

Authors: Mutsuki Hagiwara and Wataru Hijikata (Institute of Science Tokyo, Japan)

Abstract: Biohybrid actuators driven by skeletal muscle have attracted considerable attention as soft actuators because of their self-repair capability and ability to directly utilize adenosine triphosphate (ATP) as an energy source. For the practical application of biohybrid actuators, accurate force control is essential. In our previous works, a model- based control method was developed based on a mathematical model describing the contraction process of skeletal muscle. However, changes in muscle characteristics over time can cause discrepancies between the model output and the actual actuator behavior, resulting in degraded control performance. In this study, an online parameter identification method was integrated with the model-based controller to compensate for variations in muscle characteristics. The proposed method updates selected model parameters in real-time based on the difference between the model output and the measured contraction force. To evaluate its effectiveness, control experiments were conducted using a biohybrid actuator driven by the gastrocnemius muscle of Xenopus laevis. The results demonstrated that the online parameter identification method successfully adapted the model to changes in muscle behavior and improved force- tracking accuracy without reducing responsiveness. These findings indicate the potential of adaptive model-based control for the application of biohybrid actuators.

D3R3AE

Biomaterials I

Session Chair: Nobuhiko Kojima

Time	Paper ID	Presenter	Paper Title
10:45–11:00	1571312342	Chawan Manaspon	Cellular Immune Interactions of Nitriding Titanium Substrates Under Pro-Inflammatory Challenge
11:00–11:15	1571314446	Patipat Kamdenlek	Formulation and Characterization of Carbomer/Pluronic F127 Hydrogel with Tunable Temperature-Dependent Viscosity and Cytocompatibility
11:15–11:30	1571315027	Princess Joy Naig	Functionally Stable Electrospun PVP/Collagen/Hyaluronic Acid Nanofibrous Biomaterials Loaded with Curcumin and Gallic Acid for Skin Interface Applications
11:30–11:45	1571315412	Chonticha Annanon	Characterization of Vancomycin-Loaded PLGA Nanoparticles for Targeted Drug Delivery
11:45–12:00	1571315574	Laphas Wijitpanya	A Preliminary Study of In Vivo Degradation Test of Biodegradable Polyhydroxyalkanoate Materials for Tissue Engineering in a Wistar Rat
12:00–12:15	1571317637	T. Korpanitchkul	Effect of Laser Surface Texturing on RAW264.7 Cells Inflammatory Responses
12:15–12:30	1571319535	Arissara Suksap	Surface Properties of the Electropolished 316L Stainless Steels under Simulated Biological Conditions: A Proof-of-Concept Study

1571312342 — Cellular Immune Interactions of Nitriding Titanium Substrates Under Pro-Inflammatory Challenge

Authors: Chawan Manaspon and Phakpoom Jeeauy (Chiang Mai University, Thailand); Patipat Kamdenlek (Thaksin University, Thailand); Suninad Kaewnisai and Artit Chingsungnoen (Mahasarakham University, Thailand); Komgrit Eawsakul (Walailak University, Thailand); Chavin Jongwannasiri (Chulabhorn Royal Academy, Thailand)

Abstract: Developing advanced biomaterials for regenerative medicine is essential to minimize implant rejection, reduce associated inflammatory diseases, and ultimately expand patient access to care through more reliable medical interventions. This study investigated the surface modification of Ti-6Al-4V (Ti64) via plasma nitriding to evaluate how titanium nitride (TiN) surfaces influence time-dependent immunomodulation. Here, a hydrophobic TiN layer with a water contact angle of 91.8o±1.0 and a nanoscale roughness (Ra) of 20.5±1.4 nm was used and evaluated. The immunomodulatory profiling was methodically evaluated using RAW264.7 macrophages cultured under both basal (LPS-) and pro-inflammatory (LPS+) conditions over 7 days. At 24 hours, the hydrophobic TiN surface exerted minimal anti-inflammatory action on early chemical mediators, with nitric oxide (NO) concentrations remaining elevated at 5.4±0.5 nM. The real-time qPCR demonstrated a temporally dynamic gene response under endotoxin challenge. At 24 hours, the TiN surface successfully mitigated acute inflammatory pathways by drastically attenuating Il-6 gene transcription. However, extended culture to day 7 uncovered a distinct delayed upregulation of Tnf-α, with expression levels significantly surging to approximately 5.8-fold, vastly overshooting the Control LPS+ group thresholds. The TiN temporarily showed acute Il-6 signaling, it triggers a delayed pro-inflammatory Tnf-α response over time, highlighting the necessity of long-term immunomodulatory evaluations to patient health.

1571314446 — Formulation and Characterization of Carbomer/Pluronic F127 Hydrogel with Tunable Temperature-Dependent Viscosity and Cytocompatibility

Authors: Patipat Kamdenlek (Thaksin University, Thailand); Komgrit Eawsakul (Walailak University, Thailand); Traipob Korpanitchkul (Chiang Mai University, Thailand); Wiwat Suhren (Thaksin University, Thailand); Chawan Manaspon (Chiang Mai University, Thailand)

Abstract: Hydrogels with temperature-responsive properties are widely used in biomedical and healthcare applications, particularly for wound dressing, wound healing, and tissue engineering. In this study, a hydrogel composed of Carbomer (Carbopol) and Pluronic F127 (Poloxamer 407) was developed through a formulation approach. Carbomer solutions at different concentrations were prepared and adjusted to pH 7 prior to hydrogel formulation. Hydrogels containing different concentrations of Pluronic F127 were subsequently prepared to investigate the influence of polymer composition on rheological behavior. The rheological properties of the formulations were evaluated by measuring viscosity as a function of temperature, while cytocompatibility was assessed using L929 fibroblast cells. One formulation with higher Pluronic F127 content exhibited a clear thermogelling transition, characterized by a sharp increase in viscosity above approximately 27°C and pronounced hysteresis effect during the cooling cycle. In contrast, formulations with higher

carbomer content exhibited more stable viscosity profiles with reduced temperature sensitivity, indicating the dominant effect of the carbomer network. Cytocompatibility testing demonstrated that all formulations-maintained cell viability above 70%, indicating non-cytotoxic behavior. In conclusion, the developed hydrogel system demonstrated tunable temperature-responsive behavior, favorable cytocompatibility. The findings suggest its potential for wound dressing and wound healing applications, supporting the development of advanced biomaterials for healthcare applications.

1571315027 — Functionally Stable Electrospun PVP/Collagen/Hyaluronic Acid Nanofibrous Biomaterials Loaded with Curcumin and Gallic Acid for Skin Interface Applications

Authors: Princess Joy Naig (MING CHI University of Technology, Taiwan); Kuo-Yung Hung (Ming Chi University of Technology, Taiwan)

Abstract: Facial sheet masks made from synthetic sheet fabrics commonly rely on nutrient-rich liquid serums to saturate the mask and deliver bioactive ingredients to the skin. However, this wet-serum approach is prone to oxidative degradation, particularly when the formulation contains antioxidant compounds that are sensitive to oxidation. To address this limitation, this study fabricated electrospun polyvinylpyrrolidone (PVP)/collagen/hyaluronic acid (HA) nanofiber membranes co-loaded with curcumin (Cur) and gallic acid (GA), both individually and in combination. The membranes were evaluated in terms of morphology, chemical structure, tensile strength, antioxidant activity, antibacterial efficacy, elastase inhibition, cytocompatibility and stability. Among the formulations, the combined Cur-GA membrane (experimental group NF4) produced the smallest bead-free fibers and demonstrated synergistic functional enhancement, demonstrating synergistic rather than purely additive enhancement. NF4 exhibited markedly improved antioxidant activity (71.0% compared with 9.1% for the unloaded control), antibacterial reduction exceeding 97% against Escherichia coli and Staphylococcus aureus, and elastase inhibition of 76.6%, while promoting fibroblast proliferation exceeding 100% relative to the untreated control, indicating cytocompatibility with pro-proliferative effects. Although a decrease in antioxidant activity was observed after 14 days, the electrospun membrane retained antioxidant activity more effectively than a commercial serum-based facial sheet mask evaluated under the same conditions. Additionally, bioactive loading reduced tensile strength, indicating a trade-off between functional performance and mechanical integrity. Overall, these findings suggest that Cur-GA co-loaded PVP/collagen/HA nanofiber membranes are promising multifunctional materials for advanced facial sheet mask applications.

1571315412 — Characterization of Vancomycin-Loaded PLGA Nanoparticles for Targeted Drug Delivery

Authors: Chonticha Annanon and Julinthip Puttawong (Department of Biomedical Sciences and Biomedical Engineering, Faculty of Medicine, Prince of Songkla University); Suchera Loyprasert (Molecular Biotechnology and Bioinformatics, Division of Biological Science, Faculty of Science, Prince of Songkla Univer); Tonghathai Phairatana (Department of Biomedical Sciences and Biomedical Engineering, Faculty of Medicine, Prince of Songkla University)

Abstract: Vancomycin (VCM) remains a primary treatment for Methicillin-resistant Staphylococcus aureus (MRSA) infections; however, conventional systemic administration often suffers from limited localized distribution and high dose-dependent toxicities, particularly nephrotoxicity. Nanotechnology has emerged as a promising approach for drug delivery by enhancing drug stability and enabling localized drug delivery. This study aimed to develop vancomycin-loaded poly (lactic-co-glycolic acid) nanoparticles (PLGA-VCM) via a double-emulsion solvent evaporation (W/O/W) technique and assess their potential as an antimicrobial drug delivery system for the treatment of the MRSA infections. The physicochemical properties of the PLGA-VCM nanoparticles were characterized in terms of particle size, polydispersity index (PDI), zeta potential, and encapsulation efficiency. The developed nanoparticles exhibited an average particle size of 258.07 ± 11.59 nm, a PDI of 0.26 ± 0.02, and a zeta potential of −43.93 ± 1.75 mV. Furthermore, the nanoparticles achieved an encapsulation efficiency of 62.05 ± 2.35%. These results indicate the successful incorporation of VCM into the PLGA matrix, yielding a relatively uniform size distribution and good colloidal stability. In vitro antimicrobial assays demonstrated a robust concentration-dependent inhibition against MRSA, proving that the encapsulated VCM retained its full therapeutic potency. The PLGA-VCM nanoparticles showed concentration dependent antibacterial activity, with a MIC value of 7.04 µg/mL and approximately 96% growth inhibition at the inhibitory concentration. The findings indicate that the synthesized PLGA-VCM nanoparticles exhibit desirable physicochemical characteristics and represent a promising platform for antimicrobial drug delivery in prospective biomedical engineering.

1571315574 — A Preliminary Study of In Vivo Degradation Test of Biodegradable Polyhydroxyalkanoate Materials for Tissue Engineering in a Wistar Rat

Authors: Laphas Wijitpanya (Rangsit university, Thailand); Sani Boonyagul, Anuchan Panaksri and Nuttapol Tanadchangsaeng (Rangsit University, Thailand); Kasem Rattanapinyopituk (Chulalongkorn University, Thailand); Tulyapruek Tawonsawatruk and Rudee Hemstapat (Mahidol University, Thailand)

Abstract: A preliminary study evaluated the long-term in vivo biodegradation kinetics and biocompatibility of various polyhydroxyalkanoate (PHA) materials to determine their potential as scaffolds for tendon tissue engineering. Three PHA configurations, short- chain-length PHA (SCL-PHA), medium-chain-length PHA (MCL-PHA), and a copolymer of poly(3-hydroxybutyrate-co-3-hydroxyhexanoate) at (PHBHHx-10%), were fabricated and subcutaneously implanted into the dorsal area of Wistar rats for up to 6 months, using medical-grade silicone as a non-biodegradable control. Gravimetric analysis at 24 weeks revealed distinct degradation trajectories dictated by the polymers' molecular structure: SCL-PHA exhibited the highest mass loss, retaining ~80% of its initial weight, whereas PHBHHx-10% showed moderate degradation (~11% mass loss). Conversely, MCL-PHA demonstrated superior dimensional stability, retaining ~95% of its mass, matching the silicone control profile. Size-exclusion chromatography (SEC) of MCL-PHA at day 60 revealed a 13.0% reduction in weight- average molecular weight (MW), confirming an internal bulk erosion degradation mechanism despite low bulk mass loss. Histopathological evaluation under ISO 10993- 6:2016 demonstrated excellent tissue tolerance across all PHA groups. Minimal scores (<1.0) were recorded for hemorrhage, inflammation, and foreign body response at both 3 and 6 months, indicating the successful resolution of acute surgical trauma. Fibrosis scores progressively increased from moderate (1.3-2.0) at 3 months to a stable maturation level (3.0-3.2) at 6 months, signifying normative fibrous encapsulation similar to the silicone control. In conclusion, the structural diversity of the PHA family allows for precise tuning of degradation kinetics. Due to its elastomeric resilience, minimal immunogenicity, and slow bulk mass loss, MCL-PHA serves as a promising candidate scaffold capable of sustaining long-term mechanical support during the tendon regeneration phase before being safely resorbed by the host.

1571317637 — Effect of Laser Surface Texturing on RAW264.7 Cells Inflammatory Responses

Authors: Traipob Korpanitchkul and Chawan Manaspon (Chiang Mai University, Thailand); Viboon Saetang (King Mongkut's University of Technology Thonburi, Thailand); Witthaya Daodon (Rajamangala University of Technology Isan, Thailand); Komgrit Eawsakul (Walailak University, Thailand); Chavin Jongwannasiri (Chulabhorn Royal Academy, Thailand)

Abstract: Ti-6Al-4V is commonly used for biomedical implants, but its biological performance is strongly affected by surface-cell interactions. This study evaluated the cytocompatibility and inflammatory response of RAW264.7 macrophage-like cells on unmodified and laser-textured Ti-6Al-4V surfaces. Two laser-textured surfaces, designated as L70 and L140, were tested under non-stimulated (LPS−) and lipopolysaccharide-stimulated (LPS+) conditions. LDH release assay was used to assess injury that caused by the surface, live/dead fluorescence staining was used to observe cell viability and attachment, and ELISA was used to evaluate inflammatory response based on the TNF-α/IL-10 ratio. The LDH assay showed low LDH release in all experimental groups compared with the positive control, indicating no severe membrane damage after 24 h. Live/dead staining confirmed that most attached cells remained viable and showed that cells on L70 and L140 tended to align along the laser-induced grooves. The TNF- α/IL-10 ratio showed no clear inflammatory imbalance on the laser-textured surfaces compared with unmodified Ti64. These findings suggest that laser-textured Ti-6Al-4V surfaces maintained acceptable cytocompatibility and did not induce an obvious excessive inflammatory response in RAW264.7 cells.

1571319535 — Surface Properties of the Electropolished 316L Stainless Steels under Simulated Biological Conditions: A Proof-of-Concept Study

Authors: Arissara Suksap (School of Engineering, King Mongkut's Institute of Technology Ladkrabang (KMITL), Thailand); Neeraphat Kunbuala (Tohoku University, Japan); Kasama Srirussamee and Phacharaphon Tunthawiroon (School of Engineering, King Mongkut's Institute of Technology Ladkrabang (KMITL), Thailand)

Abstract: An increase in aging population has raised the demand for biomedical materials to treat the diseases of the elderly, including the use of biomedical alloys. In order to improve the clinical efficacy, a number of surface modification techniques have been employed, e.g. electropolishing (EP). Owing to the advantage that it does not introduce foreign materials on to the original substrate, this study investigates the changes in surface properties influenced by EP, including roughness, wettability, and corrosion resistance, with the aims to further apply for tailoring the surface of biomedical alloys. The results show that EP has

reduced the average surface roughness and increased wettability. Moreover, an increase in open circuit potential was also observed from the EP samples in artificial saliva, artificial plasma, and simulated body fluid, indicating higher stability when exposed to the simulated biological conditions than those without EP. This study demonstrates the potential use of EP to tailor the surface of properties of biomedical alloys.

D3R4AE

Biomaterials II / Bioinformatics II

Session Chair: Surapong Chatpun

Time	Paper ID	Presenter	Paper Title
10:45–11:00	1571322129	P. Reddy Budipalli	Design of a Bioresorbable, Conforming Intramedullary Device for Graft Support in Critical-Sized Bone Defects with Multimodal Validation
11:00–11:15	1571322606	C. Rattanapongvanich	Platinum-Functionalized Polymersomes as H2O2-Driven Nanomotors
11:15–11:30	1571323153	Pitcha Plaiplerd	Characterization of Soy Protein-Sodium Alginate-PVA Hydrogels under Transglutaminase-Crosslinked
11:30–11:45	1571323500	A. Puengprasert	Development and Characterization of Natural Rubber-Based Compliant Foam Pads for Sensory Interaction and Postural Balance Assessment
11:45–12:00	1571323563	S. Limpijumnong	Optimization of Acid-Mediated Sonochemical Synthesis of Folate- Targeted GaOOH Nanoparticles for HNSCC Therapy
12:00–12:15	1571283038	S. Chokphoemphun	Toward Efficient and Interpretable Preterm Birth Prediction: A Comparison of ML and DL Models with SHAP Analysis
12:15–12:30	1571310706	Vera Sa-ing	Alzheimer's Disease Risk Prediction Using Machine Learning Model

1571322129 — Design of a Bioresorbable, Conforming Intramedullary Device for Graft Support in Critical-Sized Bone Defects with Multimodal Validation

Authors: Pranav Reddy Budipalli (Central Academy of Technology and Arts, USA)

Abstract: Critical-sized bone defects exceed the natural regenerative capacity of bone and require surgical stabilization, which today relies on metallic intramedullary devices that are permanent, are far stiffer than bone, often require reaming of the medullary canal, and must frequently be removed in a second operation. This work presents a fully bioresorbable, conforming, 3D-printable intramedullary device made of polycaprolactone, a slowly degrading polyester whose resorption time is well matched to bone healing, as an alternative to permanent bone-intrusive hardware. The device was evaluated computationally using finite element analysis and biologically by a four- week in vitro culture of rat mesenchymal cells, benchmarked against an open culture dish and a titanium plate (modeling traditional metal devices), with five replicates per group. Under physiological axial, bending, and torsional loading, the device showed safety factors of 7.024-8.045, and under a simulated 8.5× body-weight jump-landing load, it retained a safety factor of 1.983; peak cyclic gait stress (1.0678 MPa) remained 40.59 percent below the estimated fatigue endurance limit (6.400 MPa), predicting infinite life. A first-order degradation model ($k = 0.05270$ month^{-1}) indicated the device retains sufficient strength across the bone-healing window before fragmenting. In culture, cells on the device showed 43.50-fold proliferation over four weeks and 93.58 ± 6.87 percent osteogenic mineralization, statistically indistinguishable from open-dish controls (group $p = 0.959$) and far superior to titanium ($d = 5.37$).

1571322606 — Platinum-Functionalized Polymersomes as H2O2-Driven Nanomotors

Authors: Chuthamas Rattanapongvanich, Natwakorn Meesaeng, Patcharapol Thanomjit, Yannapat Rattanaumnuaishai, Norased Nasongkla and Chalaisorn Thanapongpibul (Mahidol University, Thailand)

Abstract: Self-propelled nanomotors have emerged as promising drug delivery systems because their active motion can enhance nanoparticle transport beyond passive diffusion. Here, platinum-functionalized polymersomes (Pt-PSomes) were fabricated by depositing platinum nanoparticles onto polymersomes synthesized via photoinitiated polymerization-induced self-assembly (Photo-PISA), providing a simple and scalable route for nanomotor fabrication. The effect of platinum precursor feed ratio on platinum loading, catalytic activity, and motility was investigated. Microwave plasma atomic emission spectroscopy confirmed that platinum loading increased with increasing platinum precursor feed ratio, accompanied by enhanced hydrogen peroxide (H2O2) catalytic decomposition. The 1:10 Pt precursor formulation exhibited the highest platinum loading and catalytic activity. Dynamic light scattering demonstrated the greatest increase in translational diffusion for this formulation in the presence of H2O2. Single-particle tracking by nanoparticle tracking analysis (NTA) further confirmed enhanced fuel-responsive motility through more dispersed particle trajectories, increased mean squared displacement, and higher particle velocity. These results demonstrate that Photo-PISA enables the scalable fabrication of Pt-functionalized polymersome nanomotors with

H2O2-responsive propulsion, highlighting their potential as reactive oxygen species (ROS)-responsive platforms for self-propelled drug delivery.

1571323153 — Characterization of Soy Protein-Sodium Alginate-PVA Hydrogels under Transglutaminase-Crosslinked

Authors: Pitcha Plaiplerd and Treesukon Treebupachatsakul (King Mongkut's Institute of Technology Ladkrabang, Thailand)

Abstract: Soy protein isolate (SPI) offers a highly sustainable, biocompatible, and cost-effective plant-based platform for biomaterial development. Safe, eco-friendly, and accessible soy protein hydrogel systems were fabricated by non-toxic enzymatic crosslinking using transglutaminase (TGase). Additional materials, polyvinyl alcohol (PVA) and sodium alginate (SA), were varied and combined with SPI to characterize the soy protein hydrogel. Free thiol group quantification confirmed progressive isopeptide bond formation during incubation across all formulations. The SPI control, SA-containing, and PVA-containing networks displayed time-dependent crosslinking kinetics. All composite hydrogels retain equilibrium moisture content above 80%. The condition of combining 0.5% (w/v) SA and 15% (w/v) PVA to 10% (w/v) soy protein showed a stable water holding capability of over 80% with a high ability to withstand mass loss of only 4.81% when incubated for 24 h by degradation testing in phosphate-buffered saline (PBS). Macroscopic area analysis via ImageJ across various conditions revealed that the addition of 15% (w/v) PVA and 0.5% (w/v) SA with 15% PVA composite provided higher dimensional stability and geometric shape formation compared with only soy protein hydrogel. By combining these results, the cost-effective plant-based hydrogels serve as attractive candidates for many biomedical applications, such as moist wound dressings and localized drug delivery systems.

1571323500 — Development and Characterization of Natural Rubber-Based Compliant Foam Pads for Sensory Interaction and Postural Balance Assessment

Authors: Athiwat Puengprasert, Suwicha Lekjam, Watchara Liewrian, Phitsini Suvarnaphaet and Yeampon Nakaramontri (King Mongkut University of Technology Thonburi, Thailand); Benjarat Saengthong (Rangsit University, Thailand)

Abstract: The modified Clinical Test of Sensory Interaction and Balance (CTSIB-M) evaluates postural control by disrupting somatosensory input using a compliant foam pad. The mechanical properties of the foam directly influence the level of sensory perturbation and, consequently, the assessment outcome. This study developed a natural rubber (NR)-based compliant foam pad and investigated its mechanical properties for potential application in postural balance assessment. NR foam pads were fabricated with foaming times of 30 s, 45 s, and 3 min. Mechanical characterization was performed using test parameters adapted from ASTM D3574-25, including density, indentation force deflection (IFD), compressive Young's modulus, and pore morphology. Increasing the foaming time promoted bubble growth and coalescence, increasing the average pore size from 20.85 ± 9.62 μm to 66.85 ± 33.66 μm, while reducing the foam density from 208.97 to 192.15 kg/m³. These microstructural changes resulted in distinct compressive responses, demonstrating clear relationships among pore morphology, density, IFD, and compressive stiffness. The results demonstrate that the mechanical properties of NR foam can be tailored by controlling the foaming process, providing promising compliant material and a quantitative framework for the design of foam pads for sensory interaction and postural balance assessment.

1571323563 — Optimization of Acid-Mediated Sonochemical Synthesis of Folate- Targeted GaOOH Nanoparticles for HNSCC Therapy

Authors: Sarunputt Limpijumnong, Waratchaya Chimphlee, Panjaphong Lertsathitphong, Pornnapat Tungtrakarnku, Thanyarat Chaibun, Pornsiri Suwannapaporn, Chatchai Muanprasat and Norased Nasongkla (Mahidol University, Thailand); Soracha Thamphiwatana Dechaumphai (Chulalongkorn University, Thailand); Benchaporn Lertanantawong (Mahidol University, Thailand)

Abstract: Conventional therapies for head and neck squamous cell carcinoma (HNSCC) often suffer from severe systemic toxicity and lack precise tumor targeting. Metal oxide nanoparticles, specifically gallium oxyhydroxide (GaOOH), present a promising theranostic alternative due to their inherent biocompatibility, structural stability, and photoluminescent properties. This study introduces an optimized, room-temperature sonochemical synthesis of uniform GaOOH nanostructures directly from bulk liquid gallium. By utilizing acetic acid (AcOH) as a dynamic chemical reagent to lower interfacial surface tension, acoustic cavitation efficiency was significantly enhanced. Optimal morphological uniformity was achieved at a 1.0 M acetic acid concentration with 40 minutes of sonication. To enable active biological targeting, the bare GaOOH nanoparticles underwent sequential surface functionalization with beta-cyclodextrin (beta-CD) for colloidal stabilization and folic acid (FA) to target the folate receptors frequently overexpressed in metastatic HNSCC.

The complete transformation into crystalline GaOOH was verified through XRD, Raman spectroscopy, FESEM, and EDS. Subsequently, ATR-FTIR confirmed the successful integration of the organic ligands onto the nanoparticle surface. The synthesized GaOOH-CD-FA complex demonstrates high structural uniformity and precise ligand integration, establishing a foundation for future targeted nanotherapeutics in precision oncology.

1571283038 — Toward Efficient and Interpretable Preterm Birth Prediction: A Comparison of ML and DL Models with SHAP Analysis

Authors: Susama Chokphoemphun (Kasetsart University Chalermphkiat Sakonnakhon Province Campus, Thailand); Tharatep Poommhee and Apirak Ketrueng (Chalermphrakiat Sakon Nakhon Province Campus, Kasetsart University, Thailand); Napat Boonsong (Naresuan University, Thailand); Natapon Phairin (Chiang Mai University, Thailand); Nitipon Pongphaw (Kasetsart University Chalermphrakiat Sakon Nakhon Province Campus, Thailand)

Abstract: This study proposes a machine learning approach for predicting preterm birth (PTB) using socio-demographic and clinical data, evaluated with stratified 5× cross- validation. The results show that XGBoost achieved the highest AUC, while Random Forest provided the most balanced performance. Logistic Regression offered competitive results with low computational cost, making it suitable for real-time applications. In contrast, Linear SVM and ANN showed lower or less stable performance. SHAP analysis further enhanced interpretability by identifying key risk factors, highlighting the effectiveness of tree-based models for PTB prediction.

1571310706 — Alzheimer's Disease Risk Prediction Using Machine Learning Model

Authors: Vera Sa-ing (King Mongkut's University of Technology North Bangkok, Thailand); Porapat Yeeheng and Sirikalaya Thanasupsin (SCiUS, KMUTT (Darunsikkhalai School) Engineering - Science College, Thailand); Jintana Wongta (King Mongkut's University of Technology Thonburi, Thailand)

Abstract: Alzheimer's disease is a progressive neurodegenerative disorder that poses a critical challenge to global healthcare systems, with early and accurate detection being essential for timely clinical intervention and improved patient outcomes. However, identifying reliable diagnostic patterns from high-dimensional clinical data remains a persistent challenge. This study presents a systematic comparative evaluation of five supervised machine learning algorithms that consist of Random Forest, Gradient Boosting, Neural Network, Logistic Regression, and Support Vector Machine for classification Alzheimer's disease. Experiments were conducted on a large-scale clinical dataset comprising 74,283 instances and 24 feature attributes, utilizing the Orange Data Mining platform through a ten-fold stratified cross-validation framework. Models were assessed across multiple performance metrics, including accuracy, precision, recall, F1-score, Matthews Correlation Coefficient, and Area Under the ROC Curve (AUC). Results indicate that ensemble-based methods demonstrated superior and consistent performance, with both Random Forest and Gradient Boosting achieving the highest AUC of 0.794, while Gradient Boosting attained the best overall accuracy (72.6%) and F1-score (0.728). These findings underscore the effectiveness of ensemble learning for clinical diagnostic tasks and demonstrate the practicality of visual programming-based data mining tools in supporting accessible and reproducible medical data analysis workflows.

D3R1AL

Human machine/computer interface I

Session Chair: Boonserm Kaewkamnerdpong

Time	Paper ID	Presenter	Paper Title
16:00–16:15	1571321520	Muhammad Asif	Evaluating the Effects of Verbal, Non-verbal, and Emotional Interaction Using an Unreal Engine-Based Virtual Framework for Human Robot Interaction
16:15–16:30	1571322020	K. Kaewkamnerdpong	Person-Level Autism Severity Classification Using Multi-Task Motor Biomarkers from a Tablet-Based Activities of Daily Living Game
16:30–16:45	1571322444	P. Orankichalearn	A Real-Time Adaptive Multi-Sensor Monitoring System for Pressure Injury Prevention
16:45–17:00	1571322850	Kiyotaka Fujii	A Basic Study on a Usability Evaluation Method for Medical Devices Using Curvature Analysis of Human Pose Trajectories
17:00–17:15	1571322872	Alexander Woo	Advanced Ride-on Car Design Program for Children with Cerebral Palsy
17:15–17:30	1571322882	Konemany Kanlaya	Development of a Robotic Prosthetic Eye for Blinking Rehabilitation Using an EOG Interface

1571321520 — Evaluating the Effects of Verbal, Non-verbal, and Emotional Interaction Using an Unreal Engine-Based Virtual Framework for Human Robot Interaction

Authors: Muhammad Hassaan Asif (National University of Sciences and Technology, Pakistan); Sara Ali (Monash University, Australia); Anum Jaffar (National University of Sciences and Technology (NUST), Pakistan); Khawaja Fahad Iqbal (School of Mechanical and Manufacturing Engineering (SMME) NUST, Pakistan); Syed Hamza Gilani (National University of Sciences and Technology (NUST), Pakistan); Yasar Ayaz (National University of Science and Technology, Pakistan); Muhammad Baber Sial (National University of Sciences and Technology, Pakistan)

Abstract: Rapid development in the field of robotics has led to an increased amount of research being carried out in Human Robot Interaction (HRI). This paper aims at the development of a real-time testing platform for verbal, non-verbal, and emotional interactions between a human and a robot prior to implementation on hardware. Currently, the available virtual frameworks are lacking in terms of features required for creating these interactions. To address this, the proposed research developed a Human- Robot Interaction (HRI) framework based on Unreal Engine with the ability to choose a robot along with virtual/real humans to carry out verbal, non-verbal, and emotional interactions through Virtual Reality (VR). The robot's response to an interaction with a human is programmed using Python, which communicates with Unreal Engine C++ in real time. To evaluate the effectiveness of the proposed framework, the experiments related to verbal interaction, non-verbal interaction, and emotional interaction were performed and were compared with real-world experiments. The confidence range achieved for the emotions detected in both the virtual and real worlds was comparable, with mean values within 10%, demonstrating the feasibility of the study. Moreover, experiments involving Reinforcement Learning (RL) were performed with the robot successfully demonstrating its ability to learn within the framework by exploring its action space.

1571322020 — Person-Level Autism Severity Classification Using Multi-Task Motor Biomarkers from a Tablet-Based Activities of Daily Living Game

Authors: Kongkidakorn Kaewkamnerdpong (Chulalongkorn University, Thailand); Chatchai Paengkumhag, Warissara Limpornchitwilai and Boonserm Kaewkamnerdpong (King Mongkut's University of Technology Thonburi, Thailand)

Abstract: Motor impairments are highly prevalent in children with Autism Spectrum Disorder and have recently emerged as promising digital biomarkers for autism assessment. While previous tablet-based studies have demonstrated high accuracy in distinguishing autistic from typically developing children, stratifying intra-spectrum severity levels remains a significant clinical challenge. This study introduces an extensible, person- level multi-task framework that classifies ASD severity using fine-grained motor kinematics collected from a tablet-based Activities of Daily Living (ADL) serious game. The framework integrates two complementary motor tasks-a zigzag dragging task and a circular scrubbing task-within an independently optimized detector voting cascade, aggregating cross-session gameplay to generate a single severity prediction per child. Evaluated on a group of 16 children with ASD (aged 6-13 years) via leave-one-person- out cross-validation, the framework achieved a 72.50% three-class classification accuracy, dramatically outperforming single-task session-level baselines (51.56%). Kinematic profiling revealed that complex zigzag trajectories are highly discriminative for mild ASD, whereas continuous circular scrubbing better isolates

moderate and severe tiers. These findings demonstrate that multi-task interaction paradigms capture complementary dimensions of neurodevelopmental motor signatures, providing a scalable, objective tool for personalized autism assessment, severity monitoring, and longitudinal intervention tracking.

1571322444 — A Real-Time Adaptive Multi-Sensor Monitoring System for Pressure Injury Prevention

Authors: Pimpattra Orankichalearn, Jittapat Orankichalearn, Boonpipob Leelarleardsuriya and Kamonchanok Yulaor (Patumwan Demonstration School, Thailand); Chanchai Thaijiam (SWU, Thailand); Namkhun Srisanit (Srinakharinwirot University, Thailand)

Abstract: Pressure injuries remain a significant healthcare concern among bedridden patients, particularly in long-term care environments where continuous monitoring and timely repositioning are difficult to achieve. Conventional repositioning schedules are generally based on fixed time intervals and may not adequately reflect patient-specific risk conditions. This study presents a real-time adaptive system with multi-sensor monitor for pressure injury prevention. The proposed system integrates five Force Sensitive Resistor (FSR) sensors, a DS18B20 temperature sensor, and a DHT22 temperature-humidity sensor with an ESP32-based Internet of Things (IoT) platform. An Individual Sensor Delta Sum (ISDS) algorithm was implemented to monitor sustained pressure exposure, while temperature and humidity measurements were incorporated to support adaptive repositioning reminders under conditions associated with increased pressure injury risk. When the repositioning threshold was reached, the system generated alerts through a buzzer alarm, LCD display, and LINE notification service until patient repositioning was verified through pressure redistribution analysis. The developed prototype was evaluated under simulated bedridden patient care conditions using five healthy volunteers. Experimental results demonstrated 100% alert generation accuracy, 100% repositioning detection accuracy, 100% successful alert cancellation rate, and an average LINE notification delay of 2.0 s. The results indicate that the proposed system can provide reliable repositioning reminders and near real- time caregiver notifications, supporting pressure injury prevention and enhancing patient safety in long-term care settings.

1571322850 — A Basic Study on a Usability Evaluation Method for Medical Devices Using Curvature Analysis of Human Pose Trajectories

Authors: Kiyotaka Fujii (Kitasato University, Japan); Kazumasa Kishimoto (Kyoto University Hospital, Japan); Masami Fujii and Satoshi Kohira (Kitasato University, Japan)

Abstract: Usability evaluation is essential for improving the safety of medical devices. However, conventional methods mainly rely on expert observation and verbal protocol analysis, making objective detection of usability-related problems difficult. This study proposes a simple usability evaluation method based on curvature analysis of human pose trajectories. Video data from a syringe pump usability test were analyzed using MediaPipe Pose to estimate skeletal coordinates. Curvature values of the NOSE and RIGHT_WRIST trajectories were calculated, and frames exceeding a predefined threshold were extracted as microslip candidates. The detected events were compared with expert-based motion and behavioral analyses. Curvature events tended to occur more frequently during movement-related exploratory behavior, whereas the temporal correspondence with expert-based behavioral labels was limited. These findings suggest that curvature analysis is useful for detecting movement-related exploratory behavior but is insufficient to identify all usability-related situations. Combining curvature analysis with stagnation-related metrics may improve usability evaluation.

1571322872 — Advanced Ride-on Car Design Program for Children with Cerebral Palsy

Authors: Alexander Woo (Harvard University, USA); Liam Snyder (USA); Lisa Doran (Kapiolani Medical Center for Women and Children, USA); Scott Miller (University of Hawaii System, USA)

Abstract: Background/Objectives: In this research, a student-led high school program was established in collaboration with a state university and children's hospital for customized fabrication of Modified Ride-On Cars that meet the needs of specific participants in Hawai‘i. Methods: Five cars were developed in series by students with increasing functionality for specific special-needs children cared for at a pediatric rehabilitation center. Different microcontroller-based control techniques with a joystick, buttons, and proximity sensors were experimented with, depending on the capability of the patient. Results: New features were incorporated to improve safety and ease of use, such as maximum speed dials, easy-to-access stop switches, and proximity collision sensors. Conclusions: The program made contributions in community service, education, and technical advancement. It was found that the patient experience could be improved by iterative, patient-centric design. This work also resulted in meaningful and exciting projects that integrated principles of

engineering design, microprocessor control, and new sensor integration. This program is a model for advanced robotics club activities and education.

1571322882 — Development of a Robotic Prosthetic Eye for Blinking Rehabilitation Using an EOG Interface

Authors: Konemany Kanlaya (Institute of Science Tokyo, Japan)

Abstract: Current orbital maxillofacial prostheses for patients with unilateral eye loss are primarily cosmetic and lack active eyelid motion, resulting in an unnatural appearance and limited rehabilitative function. This study presents the development of a wearable robotic orbital prosthetic system that enables natural blinking synchronized with the contralateral healthy eye. The proposed design incorporates a compact mechanical eyelid mechanism driven by solenoid and tension spring to achieve rapid, smooth, and human-like blinking while satisfying wearable size and weight constraints. An electrooculography (EOG)-based eyeglass interface is employed as a non-invasive control method to detect blink intention and trigger prosthetic eyelid motion. The proposed system aims to provide a low-cost, lightweight, and functional wearable prototype that enhances facial symmetry and supports active rehabilitation for individuals with unilateral eye loss.

D3R2AL

Therapeutic and diagnostics systems

Session Chair: Arthon Sunpanich

Time	Paper ID	Presenter	Paper Title
16:00–16:15	1571311812	Takeshi Joyashiki	Evaluation of the Distance-Dependent Frequency Response of a Body-Conducted Sound Sensor
16:15–16:30	1571314696	P. Sangong	Investigation of Factors Influencing the Primary Ultrasound Power Calibration System
16:30–16:45	1571322550	Annika Harnack	In vitro feasibility study of E. coli biofilm reduction on transurethral catheters using optical fiber based blue and violet laser irradiation
16:45–17:00	1571323384	Geunho Shim	Cross-Validation of Hybrid Angular Spectrum and Full-Wave Simulation with a 3D-Printed Skull Phantom for Transcranial Focused Ultrasound
17:00–17:15	1571323749	T. Sopithikul	Toward a Portable Magnetofluidic Diagnostic Platform for Rapid Acinetobacter baumannii Detection Using RPA-CRISPR-Cas13a
17:15–17:30	1571323805	Shriya Thakur	Explainable Survival Prediction and Biomarker Discovery in Hepatocellular Carcinoma

1571311812 — Evaluation of the Distance-Dependent Frequency Response of a Body-Conducted Sound Sensor

Authors: Takeshi Joyashiki (Tokai University, Japan); Chikamune Wada (Kyushu Institute of Technology, Japan)

Abstract: In this study we investigated a diagnostic method for assessing arteriovenous fistula (AVF) function using shunt sounds generated by surgically created vascular access vessels for extracorporeal circulation during blood purification therapy in hemodialysis patients. First, an experimental evaluation system was developed assuming implementation of a body-conducted sound sensor (BCS) on the dorsal aspect of the wrist. Measurements were then performed using this system under conditions designed to simulate the human wrist and forearm. The aim of this study was to evaluate the distance-dependent frequency-response characteristics of a BCS and to compare these characteristics with those of an air-conducted microphone. The results demonstrated that low-frequency components below approximately 400 Hz were preserved in the BCS increasing propagation distance. In addition, frequency components remained detectable up to approximately 900 Hz at a horizontal distance of 10 cm. This finding supports the potential feasibility of employing wrist-mounted wearable sensing systems for AVF assessment.

1571314696 — Investigation of Factors Influencing the Primary Ultrasound Power Calibration System

Authors: Pratchyanon Sangong (National Institute of Metrology Thailand, Thailand); Anijsorn Samart (National Institute of metrology Thailand, Thailand); Pinpinut Nitirojtanakul (National Institute of Metrology Thailand, Thailand)

Abstract: The Radiation Force Balance (RFB) is widely used as a primary method for ultrasound power calibration of ultrasonic transducers, as defined in IEC 61161. However, its measurement accuracy is influenced by several factors that contribute to uncertainty. This study investigates two key parameters affecting RFB performance: water temperature fluctuations and ultrasound emission time intervals (on-off cycling). The influence of temperature was evaluated by comparing measurements under stable- temperature and temperature-varying conditions. The effect of emission timing was examined by systematically varying the ultrasound on-off cycling intervals. For each condition, the radiation force was recorded and analyzed to assess its impact on measurement stability. The results show that water temperature variation has a negligible effect on the calculated acoustic power and radiation conductance, with differences of less than 0.6%, but increases the variability of acoustic power measurements at low power levels due to baseline apparent mass drift. The effect of the emission time interval was power dependent. Increasing the ON time produced negligible changes in radiation conductance but slightly increased measurement variability at 0.5 W, whereas at 10 W, increasing the ON time from 10 s to 25 s reduced radiation conductance by approximately 3.2% and increased measurement variability. Extending the OFF time had little effect at 0.5 W but improved measurement stability at 10 W. These findings provide guidance for selecting appropriate measurement conditions to improve the repeatability and reliability of RFB-based ultrasound power calibration.

1571322550 — In vitro feasibility study of E. coli biofilm reduction on transurethral catheters using optical fiber based blue and violet laser irradiation

Authors: Annika Harnack, Klea Lila, Ben Sicks and Katharina Pruehs (Technische Hochschule Ulm (Ulm University of Applied Sciences), Germany); Martin Hessling (Technische Hochschule Ulm - University of Applied Sciences, Germany)

Abstract: The application of urinary catheters can lead to catheter-associated urinary tract infections (CAUTI). These are among the most common nosocomial infections, which may not only lead to severe complications and increased mortality. but also place a significant financial burden on the healthcare system. A key factor here is the formation of biofilms on the catheter surface, as these biofilms protect pathogens from antibiotics and disinfection measures, and also enable new infections to occur repeatedly. In the last few years, it has become more widely known that visible violet and blue light has antimicrobial properties and is effective even against antibiotic-resistant pathogens. Therefore, in this study, E. coli biofilms were cultured for up to 72 hours on commercial urinary catheters in a simple urinary tract model, and the feasibility of biofilm reduction by irradiation with violet and blue laser light via optical fibers was investigated. As early as 24 hours, biofilms with high bacterial concentrations were observed both with and without irradiation, although biofilm growth subsequently slowed. After 72 hours, the irradiated catheters exhibited at least significantly reduced bacterial concentrations despite a brownish catheter discoloration. This bacterial reduction was particularly true for violet irradiation. The use of optical fibers in combination with violet light therefore appears promising for future CAUTI reduction. However, it remains to be determined what irradiation intensities and durations are appropriate, especially given that human tissue should be exposed to as little radiation as possible, since the effects of violet and blue light on the human urethra have not yet been studied.

1571323384 — Cross-Validation of Hybrid Angular Spectrum and Full-Wave Simulation with a 3D-Printed Skull Phantom for Transcranial Focused Ultrasound

Authors: Geunho Shim, Hyuntae Ju, Doyoon Lee, Seongdong Park and Kisoo Kim (Kyung Hee University, Korea (South))

Abstract: Treatment planning for transcranial focused ultrasound (tFUS) increasingly relies on acoustic simulation to predict the pressure delivered through the skull. Two solver families dominate practice: fast one-way angular-spectrum methods such as the Hybrid Angular Spectrum (HAS), and slower full-wave methods such as the pseudospectral k-Wave. Because these solvers are usually compared only to each other, the field lacks an experimental arbiter of when the fast one-way approximation is adequate. We cross-validate HAS and k-Wave at 250 kHz against two independent ground truths: the O'Neil analytical solution in free water, and water-tank insertion-loss (IL) measurements of twelve three-layer 3D-printed skull phantoms. Because the phantom source paper reports porosity and transmitted pressure but not sound speed, the cortical and porous sound speeds were measured directly by time-of-flight in the same tank and are reported here. In free water the two solvers and the analytical solution agree to within 1 percent in peak pressure and 0.14 mm in focal position (shape correlation 0.9925), confirming that the propagation kernels are equivalent when reflection is negligible. In the phantoms, the one-way solver produces a nearly flat insertion loss that varies by only about 1 dB across all twelve phantoms against a measured span of about 11 dB, because, retaining only a first-order interface reflection, it is largely insensitive to layer arrangement. The full-wave solver, with a single literature-referenced absorption per material (two parameters for twelve phantoms), instead captures the reflection-driven variation of insertion loss across the six reliably-measured non-resonant phantoms (RMSE about 0.7 dB). The strongest resonances, in the phantoms with 2-mm cortical layers (the 2/6/2 configurations), are under-predicted by both solvers within a fluid model and coincide with the least reliable measurements. We conclude that one-way solvers are adequate only where reflection is weak (free water), whereas full-wave modelling is needed to capture the reflection-driven insertion loss of layered structures such as the skull at 250 kHz; the extreme thin-layer resonances require elastic, finer- grid modelling. These results delineate the regime in which each solver class is valid for tFUS planning.

1571323749 — Toward a Portable Magnetofluidic Diagnostic Platform for Rapid Acinetobacter baumannii Detection Using RPA-CRISPR-Cas13a

Authors: Tharathon Sopithikul and Pornpat Athamanolap (Mahidol University, Thailand)

Abstract: Acinetobacter baumannii is a major nosocomial pathogen associated with multidrug resistance and increasing healthcare burden worldwide. Rapid identification of A. baumannii is critical for timely treatment and infection control; however, conventional diagnostic methods often require specialized laboratory equipment and prolonged turnaround times. This study presents the optimization of a magnetic bead-based

DNA purification workflow coupled with an RPA-CRISPR-Cas13a assay for rapid detection of A. baumannii. The purification process was designed to minimize complex sample preparation steps and improve compatibility with future implementation in a portable magnetofluidic point-of-care platform. The workflow combines heat lysis, magnetic bead-based nucleic acid capture, simplified PEG/Tween washing, and one-pot RPA-CRISPR-Cas13a fluorescence detection under isothermal conditions. Experimental results demonstrated successful discrimination between A. baumannii-positive samples and non-target carbapenem-resistant Enterobacteriaceae controls, with positive samples becoming distinguishable from negative controls at approximately 20 minutes during a 40-minute assay. In addition, direct transfer of DNA-bound magnetic beads into the reaction mixture generated target-dependent fluorescence, supporting the feasibility of simplified sample processing for point-of-care use. These findings provide a foundation for integrating DNA purification and CRISPR-based detection into a portable magnetofluidic diagnostic platform for rapid A. baumannii detection.

1571323805 — Explainable Survival Prediction and Biomarker Discovery in Hepatocellular Carcinoma

Authors: Shriya Thakur (AIClub, India); Smriti H Bhandari (India)

Abstract: Accurate survival prediction in hepatocellular cancer remains challenging due to the complex interactions among clinical characteristics, tumor heterogeneity, treatment factors, and genomic alterations. Although machine learning has shown promising performance in improving prognostic prediction, the limited interpretability of many survival models reduces their clinical applicability and biological utility. This study proposes an explainability-driven survival learning framework that integrates clinical variables, tumor characteristics, somatic mutation profiles, and copy number alteration features from the HCC MSK 2024 cohort available through cBioPortal. The framework employs a leakage-aware pipeline with survival-driven univariate Cox feature selection, followed by matched Cox proportional hazards (CoxPH) and DeepSurv models in an effort to enable a fair comparison between statistical and neural survival learning. Model performance is assessed using Concordance Index (C-Index), integrated Brier score (IBS), time-dependent area under the curve (AUC), Kaplan-Meier survival analysis, and log-rank test. To improve model transparency, the proposed framework combines the intrinsic interpretability of CoxPH with three complementary explainable artificial intelligence techniques- DeepLiftShap, Integrated Gradients, and GradientSHAP-followed by consensus gene ranking to identify robust candidate prognostic biomarkers. Expermental results demonstrate that explainability-driven survival learning can improve the interpretability of prognostic models without sacrificing competitive predictive performance, and offer a practical framework for clinically meaningful survival prediction and biomarker discovery in hepatocellular cancer.

D3R3AL

Other Biomedical Engineering / Telemedicine

Session Chair: Chanchai Thaijiam

Time	Paper ID	Presenter	Paper Title
16:00–16:15	1571323495	Bao Nguyen	TechCare: A Smart Healthcare Management System with Integrated LLM-Based Clinical Decision Support
16:15–16:30	1571323503	Chau Vo	Mortality Prediction for ICU Patients at Admission by Layer-frozen BioClinical BERT and Rebalancing
16:30–16:45	1571323324	T. Kraisarin	Development and Optimization of HRM-Based Primers Targeting GSTP1 and RASSF1 DNA Methylation Markers for Prostate Cancer Detection
16:45–17:00	20260001	K. Piphounnok S. Usama Hussain	Analysis of Bioimpedance Response on Thigh Muscles During Knee Extension and Flexion
17:00–17:15	20260002	Shah Bukhari	Reconstructing WHO Cardiovascular Risk-Chart Inputs from Structured and Unstructured MIMIC-IV Data: A Multi-Cohort
17:15-17:30	20260010	Somchat Taertulakarn	Digital Image Analysis for Point-of-Care Urinalysis: Comparison of Grayscale, RGB and Hue-Based Approaches

1571323495 — TechCare: A Smart Healthcare Management System with Integrated LLM-Based Clinical Decision Support

Authors: Bao Nguyen, An Le and Dat Nguyen (Ho Chi Minh City University of Technology (HCMUT) VNUHCM, Vietnam); Duy Nguyen (Sun.Studio Joint Stock Company, Vietnam); Chau Vo (HCMUT, Vietnam)

Abstract: Healthcare systems in many resource-constrained regions face severe hospital overcrowding, high patient-to-clinician ratios, and limited adoption of robust digital clinical decision-support tools despite ongoing digitization efforts. While open-source healthcare management systems such as OpenMRS and OpenEMR successfully digitize administrative and clinical records, they typically lack natively integrated artificial intelligence for clinical decision support. To address this gap, we present TechCare, a layered-architecture smart healthcare management system that integrates an LLM-based chatbot and a dedicated symptom-triage module directly into outpatient clinical workflows. Using Vietnam's public healthcare system as a representative case study, we comparatively evaluated two open-weight Large Language Models-LLaMA 3.1 8B and Meditron-7B-across extensive medical question- answering and symptom triage tasks. Results demonstrate that LLaMA 3.1 8B outperforms Meditron-7B across most evaluation axes; however, system-level analysis confirms neither model is currently deployment-ready without stronger clinical safety controls. These findings offer broader lessons for embedding LLM-based decision support into hospital management systems across similarly constrained health-care settings. Future work will focus on integrating rigorous safety guardrails and localized fine-tuning to enable reliable, real-world deployment.

1571323503 — Mortality Prediction for ICU Patients at Admission by Layer-frozen BioClinical BERT and Rebalancing

Authors: Chau Vo (HCMUT, Vietnam)

Abstract: Early prediction of ICU patient's mortality state is significant for many stakeholders in treatment, care, and hospital resource management activities. However, it gets more challenging as prediction time occurs at patient's admission due to data shortage. At that moment, only a few aspects can be observed for each patient. On the other hand, mortality prediction is well known for its data imbalance challenge, which has not yet been handled comprehensively well in the literature. Therefore, in this work, we resolve this task more practically with both challenges for ICU patients at admission. In such a context, our novel method is proposed by turning this task into text sequence classification by BioClinical BERT fine-tuned with layer freezing for tackling data shortage and rebalancing with Random Undersampling for handling data imbalance. The experimental results on MIMIC-III database show that our resulting model achieved the highest Sensitivity in comparison with others. This achievement is promising as our solution can correctly identify more true at-risk patients for more proper timely treatment and care planning.

1571323324 — Development and Optimization of HRM-Based Primers Targeting GSTP1 and RASSF1 DNA Methylation Markers for Prostate Cancer Detection

Authors: Theerisara Kraisarin and Pornpat Athamanolap (Mahidol University, Thailand)

Abstract: DNA methylation is a promising biomarker for the non-invasive detection of prostate cancer, with promoter hypermethylation of GSTP1 and RASSF1 being among the most frequently reported epigenetic

alterations. This study aimed to develop and analytically optimize high-resolution melting (HRM) assays targeting promoter methylation of GSTP1 and RASSF1. Candidate primer pairs were designed using bioinformatics tools and evaluated using synthetic methylated and unmethylated DNA controls. Assay performance was characterized through initial HRM discrimination, annealing temperature optimization, analytical sensitivity using serial dilution, detection of methylated DNA in an excess unmethylated background, discrimination of different methylation levels, and spike-in experiments using urine-derived cell-free DNA (cfDNA). The optimized assays successfully distinguished methylated from unmethylated DNA, detected low-copy methylated targets, discriminated multiple methylation levels, and retained performance in urine cfDNA following spike-in of methylated DNA. These findings demonstrate the analytical feasibility of the proposed HRM assays and provide a foundation for future clinical validation of urine-based methylation detection for non-invasive prostate cancer screening.

20260001 — Analysis of Bioimpedance Response on Thigh Muscles During Knee Extension and Flexion

Authors: Kungwankai Piphounnok , Promporn Poonsup , Taweechai Ouypornkochagorn , Onpriya Hengjang , Dept. of Biomedical Engineering Faculty of Engineering, Srinakharinwirot University Nakhon Nayok, Thailand; Yandan Jiang Hangzhou International Innovation Institute of Beihang University, Hangzhou

Abstract: During the rehabilitation process, tracking muscle activation is essential for assessing patient conditions and monitoring recovery. While surface electromyography (sEMG) is the conventional method for this purpose, its signals are highly susceptible to interference due to their low response amplitude. Bioimpedance has emerged as an effective alternative capable of probing muscle conditions even in deeper tissues, where it yields a significantly stronger response. However, surface-measured bioimpedance is rarely isolated to the target muscle directly beneath the electrodes; instead, it often captures signals from surrounding muscles and unrelated physiological changes, which can confound the interpretation of the results. In this preliminary study, thigh muscle bioimpedance during knee extension and flexion was measured from four thigh muscles, including the rectus femoris (RF), vastus lateralis (VL), biceps femoris (BF), and semitendinosus (ST) on a healthy participant The protocol was repeated over three trials to investigate changes in impedance relative to the baseline. The results demonstrated that the VL and ST exhibited reliable decreases and increases in impedance, respectively. While the RF showed a desirable decrease, its signal was affected by isometric contractions at both the onset and termination of the movement. Conversely, the BF was the least reliable, largely due to signal crosstalk from the dominant VL muscle and interference from isometric contractions. Ultimately, muscles with a larger cross-sectional area demonstrated higher reliability and were less susceptible to the confounding effects of isometric contractions.

20260002 — Reconstructing WHO Cardiovascular Risk-Chart Inputs from Structured and Unstructured MIMIC-IV Data: A Multi-Cohort Feasibility and Input-Availability Study

Authors: Syed Usama Hussain Shah Bukhari, Md Jobayer Hossain Chowdhury,Manan Vinod Shah, and Ashir Ahmed Faculty of Information Science and Electrical Engineering, Kyushu University

Abstract: To evaluate whether World Health Organization (WHO) cardiovascular disease (CVD) risk-chart inputscan be reconstructed from structured and unstructured MIMIC IV data and whether their availability differs across hospitalderived cohorts. Methods: We analyzed MIMIC-IV v3.1 andMIMIC-IV-Note. A deterministic hierarchy assigned 124,359adults without an acute CVD index event to mutually exclusive cohorts: non- ICU, non-emergency-origin survivors (A1,n = 105,728), a non-ICU, non-ED-origin residual cohort (A2,n = 11,844), and a brief-ICU cohort (A3, n = 6,787). The earliest eligible admission anchored all extraction windows. Eachinput retained its source, timestamp, admission, and evidencegrade. Scoreability was evaluated using strict current-encounter evidence (G0–G1), reconstructed longitudinal evidence (G0– G2),and assumption-enabled evidence that included deterministic numerical substitutions (G0–G3). Automated local-model classification of smoking-status conflicts was assessed separately.Results: Among 67,440 patients aged 40–74 years, no patient met the strict complete-input requirements for either chart under the prespecified G0–G1 definition. Assumption-enabled non laboratory scoreability was 24.47%, 19.69%, and 14.88% in A1, A2, and A3, respectively, whereas assumption- enabled laboratory scoreability was 7.00%, 6.69%, and 6.58%. Compared with A1, non-laboratory scoreability was lower by 4.77 percentage points in A2 and 9.59 percentage points in A3; adjusted odds ratios were 0.73 and 0.45. Deterministic integration of structured and note derived smoking evidence increased known smoking status by 2.01–2.56 percentage points. The local-model sensitivity analysis changed completeness classifications for 86 non-laboratory and seven laboratory records but did not satisfy the prespecified reliability criteria. Conclusion: Provenance-aware reconstruction identified complete WHO CVD risk-chart input sets for a limited, care- selected subset of MIMIC-IV patients, with variation across hospital-derived cohorts. Patient-disjoint cohort definitions, fixed

index admissions, evidence grading, and explicit reporting of non-scoreability improve the transparency of EHR-based risk chart reconstruction. These findings show limited reconstruction feasibility and cross-cohort variation in input availability, but not WHO-chart validation or clinical deployment readiness.

20260010 - Digital Image Analysis for Point-of-Care Urinalysis: Comparison of Grayscale, RGB and Hue-Based Approaches

Authors: Somchat Taertulakarn and Hiranya Sritart, Department of Medical Technology Faculty of Allied Health Sciences Thammasat University Pathum Thani, Thailand

Abstract:

Urine reagent strips are widely used for point-of-care testing (POCT) because they provide rapid and convenient screening of several biochemical parameters. However, conventional visual interpretation can be affected by lighting conditions, color perception, and observer experience. Digital image analysis using smartphones offers a potential approach for improving the consistency of urine dipstick interpretation. This study aimed to compare grayscale, RGB, and hue-based image analysis approaches for the semiquantitative interpretation of urine reagent strips. A total of 80 urine samples were analyzed for protein, glucose, and ketone using commercial urine reagent strips. Digital images were acquired under controlled imaging conditions and analyzed using grayscale intensity, RGB color values, and hue features. The image-derived results were compared with interpretations provided by three experienced medical technologists. Spearman's rank correlation coefficient was used to evaluate the association between image-derived features and expert interpretations, while Cohen's kappa coefficient was used to assess agreement. Hue-based analysis demonstrated the strongest association with expert interpretations, with values ranging from 0.95 to 0.97, and the highest agreement, with values ranging from 0.93 to 0.95, across the three urine parameters. RGB-based analysis showed intermediate performance, while grayscale analysis showed the lowest association and agreement. These findings suggest that hue-based image features may provide a more consistent approach for semiquantitative interpretation of urine reagent strips. Further validation under varied imaging and clinical conditions is required before application in routine POCT settings.

D3R4AL

Medical device design / Human machine-computer interface I

Session Chair: Jeerawan Thanarat

Time	Paper ID	Presenter	Paper Title
16:00-16:15	1571316301	Jeerawan Thanarak	Optimizing the Silicone/Rubber Base Material for Intravenous Injection Practice
16:15-16:30	1571314406	Pasin Thansuwat	Low-Cost Tendon-Driven Hand Exoskeleton for Stroke Rehabilitation Based on Thai Hand Anthropometry
16:30-16:45	1571314367	Sakurako Yamamura	Performance Enhancement of a Passively Levitated Ventricular Assist Device Using Combined Thrust and Magnetic Forces
16:45-17:00	1571319436	P. Chantayanee	An IoT-Based Automatic Medication Dispensing System with Image-Based Pill Verification and Error Prevention for Elderly Care
17:00-17:15	1571323758	Mathew Fujikami	Rapid Fabrication of Polystyrene Microfluidic Channels Using 3D- Printed Resin Molds
17:15-17:30	1571323146	Hiroki Ishii	Partial-Class Transfer Learning for Zero-Shot Multi-Class Motor Imagery BCI

1571316301 — Optimizing the Silicone/Rubber Base Material for Intravenous Injection Practice

Authors: Jeerawan Thanarak, Reshawat Bunyasingh, Purinpras Sriduangmaneechai and Phitchanan Suphalawut (King Mongkut's Institute of Technology Ladkrabang, Thailand)

Abstract: Silicone-based skin models have been used and implemented as part of nursing curricula to allow students to practice injection procedures. Unfortunately, current models are typically very expensive and generally do not mimic the mechanical properties of human skin. To develop a new model, a series of silicone-based composite materials were developed by mixing two different types of silicones together. Five different concentrations of these materials were created by varying the ratio of Silicone SH805 to Platinum-Cured Silicone RA-20 (100: 0, 75: 25, 50: 50, 25: 75, and 0: 100). The resulting dog-bone shaped specimens were then manufactured according to the standards outlined by ASTM E8/E8M. Tensile testing was conducted on the specimens to measure the mechanical properties of each formulation. Young's Modulus was calculated from the data obtained during the tensile testing and the results were compared against the published mechanical properties of human dermal tissue. Statistical analysis using a One-Way Analysis of Variance (ANOVA) and a One Sample t-Test were performed to compare the mean Young's Moduli of the five formulations to determine if there existed statistically significant differences among them. Results of the study indicate that the 0:100 (w/w, SH805: RA-20) composition (i.e., the formulation containing only RA-20) has a Young's Modulus which does not differ significantly ($p > 0.05$) from that of the dermal value. This finding suggests that modifying the composition of the silicones can result in increased tactile realism while providing an economical alternative to traditional nursing training simulations.

1571314406 - Low-Cost Tendon-Driven Hand Exoskeleton for Stroke Rehabilitation Based on Thai Hand Anthropometry

Authors: Pasin Thansuwat, Taksaporn Paphun, Passavorn Mongkolwattanakul, Pichaporn Chersakul, Saruta Vittayakul, Rittikorn Kasemvong, Jeerawan Thanarak and Nutthanan Wanluk (King Mongkut's Institute of Technology Ladkrabang, Thailand)

Abstract: Upper limb dysfunction caused by neurological conditions, particularly stroke, remains a significant global health challenge. The hand, as the most distal and functionally complex segment of the upper limb, is essential for performing daily activities. Impairment of hand function substantially reduces independence and quality of life, affecting tasks such as grasping, writing, and self-care. Various rehabilitation devices, including conventional tools, rigid exoskeletons, and soft robotic gloves, have been developed to support motor recovery. Among these, tendon-driven systems show promise for enabling controlled and repetitive training. However, many existing devices remain limited by high cost, bulky structures, complex mechanisms, and poor adaptability to different hand sizes, particularly in home-based settings. This study presents a low-cost, tendon-driven hand exoskeleton designed for ease of use and fabricated using 3D printing. The design incorporates Thai hand anthropometric data to address sizing mismatches common in commercially available devices. Four fingers were accommodated in the design, with finger segment lengths referenced from a Thai hand anthropometric database. Performance evaluation demonstrated a mean Relative Standard Deviation (RSD%) of 28.11%, indicating fair repeatability across repeated trials under controlled conditions.

1571314367 — Performance Enhancement of a Passively Levitated Ventricular Assist Device Using Combined Thrust and Magnetic Forces

Authors: Sakurako Yamamura and Wataru Hijikata (Institute of Science Tokyo, Japan)

Abstract: Hydrodynamic bearings and magnetic bearings are currently used in ventricular assist devices. However, hydrodynamic bearings have a risk of blood damage due to the narrow fluid gaps, while magnetic bearings have a risk of malfunctioning the active control system. Therefore, a levitation mechanism that combines the thrust force generated as a reaction force when the impeller pumps blood with the magnetic force of permanent magnets has been proposed to achieve a large fluid gap without any active control system. In this study, a double-structured hubless impeller, in which the inflow rate changes in response to the axial displacement, was used. Although previous studies have achieved omnidirectional passive levitation with a fluid gap of several hundred micrometers, the flow rate of 5 L/min and pump head of 100 mmHg required in clinical settings have not yet been achieved. Therefore, this study aims to improve the performance of the ventricular assist device through impeller geometry and magnetic circuit design. As a result of optimizing the inner-to-outer diameter ratio of the double-structured hubless impeller using computational fluid dynamics (CFD) analysis, the maximum pump head of 23 mmHg was achieved while maintaining positive thrust stiffness. In addition, electromagnetic field analysis was used to redesign the magnetic circuit and form a closed magnetic circuit using back yokes, resulting in a 30% improvement in motor torque. These results demonstrate the effectiveness of both fluid and magnetic design in improving the performance of a passive levitation mechanism while maintaining a large fluid gap.

1571319436 — An IoT-Based Automatic Medication Dispensing System with Image- Based Pill Verification and Error Prevention for Elderly Care

Authors: Pichavee Chantayanee, Vasita Wispaphaew, Piyakorn Aswanapakeat, Watcharee Suriyakong and Kangwankai Pipuannok (Srinakharinwirot University, Thailand); Chanchai Thaijiam (SWU, Thailand); Namkhun Srisanit (Srinakharinwirot University, Thailand)

Abstract: The rapid growth of the elderly population and the increasing number of individuals living independently have created significant challenges in medication management, particularly for patients requiring multiple medications. This paper proposes an Internet of Things (IoT)-based automatic medication dispensing system that integrates medication sorting, automated dispensing, image-based pill verification, reminder notifications, and monitoring into a unified platform. The system employs a Raspberry Pi 4 Model B, an ESP32-based controller, a motor-driven dispensing mechanism, and a mobile application for scheduling and monitoring. A prototype was developed and evaluated under controlled laboratory conditions using four types of round-shaped medications. Experimental results show that the proposed pill verification module achieved an overall medication classification accuracy of 88.33%. In addition, the iterative error detection mechanism successfully prevented incorrect medication delivery for three medication types, achieving a success rate of 100%. The results demonstrate that the proposed system can effectively reduce medication errors through image-based verification and iterative validation before dispensing. The proposed system shows promising potential for improving medication safety and supporting independent medication management among elderly individuals.

1571323758 — Rapid Fabrication of Polystyrene Microfluidic Channels Using 3D-Printed Resin Molds

Authors: Mathew Fujikami and Jordan Fujita (University of Hawaii at Manoa, USA); Oscar Tio (University of Hawaii at Manoa); Mathew Matsuo (University of Hawaii at Manoa, USA); Aaron T. Ohta (University of Hawaii, USA)

Abstract: This paper presents a rapid and cost effective method of producing polystyrene microfluidic channels using resin molds produced by a consumer-grade 3D printer. Moving from a design file to a fabricated microfluidic device can be completed within two hours, and without cleanroom facilities. Channels with features down to approximately 100 µm can be reliably produced using this method. This combination of high resolution, low cost, and rapid turnaround makes this fabrication method a promising alternative for prototyping and small scale fabrication of customized microfluidic devices.

1571323146 — Partial-Class Transfer Learning for Zero-Shot Multi-Class Motor Imagery BCI

Authors: Hiroki Ishii, Ayaka Choki, Masato Sugino, Kenta Shimba and Kiyoshi Kotani (The University of Tokyo, Japan)

Abstract: Brain-computer interfaces enable control of external devices through neural activity alone, and motor-imagery based systems are a promising approach for people with motor impairment. Recent systems are expanding from simple two-class control toward many discriminable classes for naturalistic interaction in

three-dimensional and mixed- reality settings. Such systems require subject-specific calibration in which the user performs every target task, and because electroencephalography varies across sessions and subjects, this calibration must be repeated frequently. As the number of classes grows, calibration becomes longer and more fatiguing, creating a trade-off between calibration effort and classification accuracy. We address this trade-off through a transfer learning approach that enables zero-shot decoding of untrained classes. A target subject is aligned to previously recorded subjects using only a measured subset of classes, such that the remaining classes are decoded in a zero- shot manner, without ever being recorded from the target subject. The alignment is a single congruence transformation estimated on the Riemannian manifold of covariance matrices, and because it acts on the whole covariance structure, it also transfers to align the unmeasured, zero-shot classes. On a public four-class dataset under a leave- one-subject-out protocol, this partial-class transfer learning approach, recentering on two of the four classes, recovers accuracy close to full calibration and exceeds conventional resting-state alignment, whereas a single reference class is less reliable. Measuring only half of the classes therefore halved calibration effort while retaining accuracy comparable to full calibration.

Author Index

Author Index

Author Index

Author Index

Author Index

Author Index

Author Index

Author Index